

**NATURAL BIOACTIVE COMPOUNDS AS
INHIBITORS OF CANCER TARGETS**

WILSON MALDONADO ROJAS MSc.

**NATURAL BIOACTIVE COMPOUNDS AS INHIBITORS OF CANCER
TARGETS**

WILSON MALDONADO ROJAS MSc.



**UNIVERSITY OF CARTAGENA
SCHOOL OF PHARMACEUTICAL SCIENCES
Ph.D. PROGRAM IN ENVIRONMENTAL TOXICOLOGY
CARTAGENA DE INDIAS**

2016

**NATURAL BIOACTIVE COMPOUNDS AS INHIBITORS OF CANCER
TARGETS**

WILSON MALDONADO ROJAS MSc.

This work is a document submitted as a requirement for obtain Ph.D. In
Environmental Toxicology

Prof. JESÚS OLIVERO VERBEL. Ph.D.

Director

Environmental and Computational Chemistry Group

University of Cartagena



**UNIVERSITY OF CARTAGENA
SCHOOL OF PHARMACEUTICAL SCIENCES
Ph.D. PROGRAM IN ENVIRONMENTAL TOXICOLOGY
CARTAGENA DE INDIAS**

2016

CAUTIONARY NOTE

The University is not responsible for the items issued by students in their thesis work. Only ensure that nothing contrary is published to dogma and Catholic morals and because the theses do not contain personal attacks against someone, rather look in them the desire to seek truth and justice. "Article 23 of Resolution 13, July 1946

ACCEPTANCE NOTE

Jury President

Jury

Jury

Jury

Cartagena de Indias, 04th August 2016

DEDICATION

To God who created the universe, manager and participant in each of my plans and dreams, by which it was possible to reach this achievement...

To my mother Emilse Rojas Blanco and my father Antonio Maldonado Rodriguez for being my motivation to excel at all times, teaching me the real value of things, the perseverance to achieve the proposed goals, and even when they are not with me right now, I remember them at all times and dedicatethis triumph from the bottom of my heart...

To Liliana Amaya, mother of my three beautiful daughters Carolina, Paula Andrea, and my little Valeria, who are my main motivation, my most precious treasures, and constant source of warmth, tenderness and love...

To my brothers Oscar, Antonio, Luis Alfonso and Luz Marina, and my whole family for the unconditional support given in all these years of hard work and dedication despite the adversities...

To All my friends and colleagues for their help...

This is for you all.

ACKNOWLEDGMENTS

Firstly, I would like to express my gratitude to God for giving me the strength and the ability to move forward in every step of my personal training, for his immense compassion and incomparable love, to him be glory and honor forever.

Besides God, I would also like to thank my family for their support, motivation, confidence and time, many thanks indeed have been each of you builders of this achievement.

My sincere thanks to Professor Jesus Olivero Verbel, my advisor and friend, for his teachings, advices, patience, unconditional support in good and bad times, and the opportunity provided to know and let me be part of his workgroup, and to grow professionally and personally taught by knowledge and high regard, thank you for everything. To all members of the Environmental and Computational Chemistry Group, an excellent group of people and professionals thanks to all without exception, for its immense collaboration. To undergraduate students María Isabel Olivero, Juan Carlos Salinas, Jessica Cerón, Joyce Ramírez, young researchers Karen Rivera, Nadia Coronado, Juan David Sierra, Alejandra Manjarres, Angela Bertel Sevilla and Ricardo Hernandez.

To all my professors from the Ph.D program in Environmental Toxicology, especially Prof. Boris Johnson Restrepo, for all his knowledge and advice during the project, and Prof. Yovanni Marrero Ponce, for his valuable support throughout my training in the DTA, the confidence, advices and knowledge transmitted. To all personnel at the School of Pharmaceutical Sciences, administratives and all staff in general. To the University of Cartagena, alma mater, thank you very much for giving me the opportunity to continue my training process.

I also want to thank Professor Enrique Melendez, an extraordinary scientist and a great person, for giving me the opportunity to work with his research group at the University of Puerto Rico, Mayaguez, as well as, his team of researchers, Xiomara Narvaez, José Carmona and Moralba Dominguez, for their great disposition and patience to train me, and give me part of their knowledge to achieve some of the results presented in this thesis. I would also like to thank people from other research groups who helped me with the activities of my project in my international internship in Puerto Rico, some of them are Carlos Ortega, Leonardo Pacheco, Jorge Guette,

Jose Luis Ruiz and Andres Roman. And to all those who supported and believed in me, thanks a lot.

Finally, I wish to thank to the University of Cartagena, Cartagena (Colombia); as well as as the program for supporting research groups, third call for mobility of students from research groups at the University of Cartagena, 2014 sponsored by the Vice-Rectorcy for Research of the University of Cartagena (2013–2016), CENIVAM (RC-0572-7-2012) and the National Program for Doctoral Studies in Colombia (Colciencias, 528-2011).

CONTENTS

ABSTRACT	15
RESUMEN	17
CHAPTER 1. THESIS OVERVIEW	22
1.1 RATIONALE	22
1.2. HYPOTHESIS	25
1.3. PERTINENCE	25
1.4. OBJECTIVES AND THESIS STRUCTURE	27
1.5. REFERENCES	28
CHAPTER 2. INTRODUCTION TO THE CANCER	35
2.1. CANCER OVERVIEW	35
2.2. DNA METHYLATION IN SKIN CANCER	37
2.3. MOLECULAR PROTEIN-LIGAND DOCKING	38
2.4. NATURALLY OCCURRING COMPOUNDS AND THEIR APPLICATION IN MEDICINE	39
2.5. MOLECULAR BIOLOGY ASSAYS (PCR/RFLP)	40
2.6. CELL VIABILITY ASSAYS	41
2.7. SPECTROSCOPIC METHODS USED TO EVALUATE PROTEIN-LIGAND INTERACTIONS	41
2.8. REFERENCES	42
CHAPTER 3. POTENTIAL INTERACTION OF NATURAL DIETARY BIOACTIVE COMPOUNDS WITH COX-2	49
3.1. ABSTRACT	49
3.2. INTRODUCTION	50
3.3. MATERIALS AND METHODS	50
3.4. RESULTS AND DISCUSSION	54
3.5. CONCLUSIONS	67
3.6. REFERENCES	67
CHAPTER 4. FOOD-RELATED COMPOUNDS THAT MODULATE EXPRESSION OF INDUCIBLE NITRIC OXIDE SYNTHASE MAY ACT AS ITS INHIBITORS	77
4.1. ABSTRACT	77
4.2. INTRODUCTION	78

4.3. MATERIALS AND METHODS	79
4.4. RESULTS AND DISCUSSION	82
4.5. CONCLUSIONS	90
4.6. REFERENCES	91
CHAPTER 5. COMPUTATIONAL FISHING OF NEW DNA METHYLTRANSFERASE INHIBITORS FROM NATURAL PRODUCTS	99
5.1. ABSTRACT	99
5.2. INTRODUCTION	100
5.3. MATERIALS AND METHODS	103
5.4. <i>Molecular Docking with AutoDock Vina and Surflex-Dock</i>	105
5.5. RESULTS AND DISCUSSION	109
5.6. <i>Final Selection of NPs as New DNMTis by Cluster Analysis, Contact Patterns and Biological Information Reported So Far</i>	115
5.7. CONCLUSIONS	121
5.8. REFERENCES	122
CHAPTER 6. ANTICANCER ACTIVITY OF NATURAL DNA METHYLTRANSFERASE INHIBITORS AND INTERACTION WITH HUMAN SERUM ALBUMIN	133
6.1. ABSTRACT	133
6.2. INTRODUCTION	134
6.3. MATERIALS AND METHODS	136
6.4. RESULTS AND DISCUSSION	139
6.5. CONCLUSIONS	148
6.6. REFERENCES	148
CHAPTER 7. CONCLUSIONS AND FINAL REMARKS	155
GLOSSARY	158

TABLES

Table 3.1. Evaluated natural products and their sources.	51
Table 3.2. Docking results for natural bioactive compound on three COX-2 structures.....	56
Table 3.3. Calculated affinities (AutoDock Vina), binding scores values (GOLD and SYBYL) and median inhibitory concentrations [IC ₅₀] for selected COX-2 inhibitors.	61
Table 3.4. Binding affinity (AutoDock Vina) and binding score values (GOLD and Surflex-Dock) for curcumin (keto and enol forms) and celecoxib (inhibitor) on different predicted binding sites (1, 2, and 3) on COX-2.....	66
Table 4.1. AutoDock Vina-calculated affinities obtained for docking of natural bioactive compounds on iNOS.	83
Table 4.2. AutoDock Vina-calculated affinities of selected inhibitors for iNOS and theirs half maximal inhibitory concentrations (IC ₅₀).	88
Table 5.1. Compounds tested against DNMTs used for Building (training set) and Validating (test set) the LDA-based Discriminant Model.	104
Table 5.2. Prediction performance of LDA-based QSAR model for classifying molecules as active or inactive against DNMTs.	110
Table 5.3. Compounds selected from NatProd collection as DNMT inhibitors using QSAR and molecular docking criteria.	112
Table 6.1. Thermodynamic parameters for HSA–natural compounds interactions...146.	

FIGURES

- Figure 2.1.** Reported deaths from Cancer worldwide, 2012..... 36
- Figure 2.2.** A basic mechanism of cancer development. Rad54B instead inactivates the mechanism of cell cycle arrest and promotes cell cycle progression.37
- Figure 2.3.** Schematic representation for molecular docking protocols. Computational chemistry tools combined with statistical methods streamline, facilitate and increase the probability of success in the selection of promising compounds... 38
- Figure 2.4.** Some bioactive compounds and their natural sources. 40
- Figure 3.1.** 3D-Superposition of COX-2 structures (1CVU, 1PXX and 1CX2), showing sequence identity and RMSD values..... 55
- Figure 3.2.** 3D structure of COX-2(1CVU)-ligand complexes..... 58
- Figure 3.3.** Docking conformation of curcumin and arachidonic acid (experimental) on the active site of COX-2 (1CVU)..... 59
- Figure 3.4.** Correlation between docking theoretical data for inhibitors on COX-2 structures (1CX2, 1PXX and 1CVU) and their half maximal inhibitory concentration (Log IC50). 63
- Figure 3.5.** Celecoxib (A) and curcumin (keto, C; enol E) binding sites on COX-2, and ligand binding site preferences for each one of them (B, D, and F, respectively). 65
- Figure 4.1.** Superposition of iNOS structures (3E7G and 1NSI), showing sequence identity and RMSD values..... 79
- Figure 4.2.** Chemical groups for food-related natural compounds used to perform docking studies on iNOS. 80
- Figure 4.3.** 3D view and interacting residues present in the 3E7G/silibinin (A,B) and 1NSI/cyanidin-3-rutinoside (C,D) complexes..... 85
- Figure 4.4.** Correlation between the mean affinities calculated by AutoDock Vina in 3E7G and 1NSI for iNOS inhibitors and their half maximal inhibitory concentration [LogIC50]..... 90
- Figure 5.1.** Mechanism of cytosine DNA methylation catalyzed by DNMTs..... 100
- Figure 5.2.** Chemical structure of representative known nucleoside analogues and non-nucleoside DNMTis, classified as synthetic and natural products. 102

Figure 5.3. Pipeline of virtual screening for DNMTis discovery.....	109
Figure 5.4. Molecular superposition between predicted (yellow) and co-crystalized pose (purple) for sinefungin (3SWR) and SAH (2QRV) with AutoDock Vina (A,B) and Surflex-Dock (C,D) protocols, showing interacting residues on experimental complexes with DNMTs.	111
Figure 5.5. Correlation between binding affinities calculated by AutoDock Vina (A) and Total score by Surflex-Dock (B) and their half maximal inhibitory concentration for forty-five DNMT1 inhibitors; μM (LogIC50).	114
Figure 5.6. Six NPs selected as promissory DNMTis.....	116
Figure 5.7. DNMT1-NPs (9,10-dihydro-12-hydroxygambogic acid and 2',4'-dihydroxychalcone 4'-glucoside) complexes.	119
Figure 5.8. DNMT3A-NPs (9,10-dihydro-12-hydroxygambogic acid and 2',4'-dihydroxychalcone 4'-glucoside) complex.	120
Figure 6.1. Proposed catalytic mechanism for DNA methylation by DNMTs.....	135
Figure 6.2. Human DNMT1-natural compounds complex binding site (A), and main residues involved in the interaction for gambogic acid (yellow), digoxin (blue) and phloridzin (purple) (B) predicted by LigandScout 3.1.....	140
Figure 6.3. <i>In vitro</i> inhibition of DNA methylation for natural compounds.....	141
Figure 6.4. Cytotoxic properties of evaluated natural compounds. Dose-response curves of gambogic acid againsts HT-29 (A) and MCF-7 (C). Dose-response curves of digoxin into HT-29 (B) and MCF-7 (D).....	142
Figure 6.5. UV/VIS spectra for titration of HSA with NPs. The intensity of absorption directly increase with the concentration of gambogic acid for peaks in 280 and 365 nm (A). However, for digoxin not were observed significant variations (B), the used concentration of HSA for this assay was 2.5×10^{-5} M.	143
Figure 6.6. Fluorescence quenching spectra of titration of HSA with gambogic acid (A) and digoxin (B).	144
Figure 6.7. Van't Hoff plot for titrations of HSA with gambogic acid (A) and digoxin (B).....	145
Figure 6.8. HSA-natural compounds complex binding site (A), and main residues involved in the interaction for gambogic acid (yellow) and digoxin (blue) (B) Predicted by LigandScout 3.1.....	147

Figure 6.9. UV-CD Spectral overlay for Titration of HSA with gambogic acid (A). Relationship for concentrations of gambogic acid (0 to 1.25 μM) vs mean residue molar ellipticity at 209.6 nm (B), and 222,0 nm (C). 148

Figure 7.1. Natural Compound Databank from Colombia (NCDC), some screenshot of database are visualized. 1577

ABSTRACT

Cancer is the term for all diseases related with the mutation of normal cells to abnormal uncontrolled cell growth. This disease is the second leading cause of death worldwide. In all cancers, some of the body's cells begin dividing without stopping and spread to the surrounding tissues, causing serious organ damage and death in the final stage. Cancer has a great impact on society, being the main cause of morbidity and mortality worldwide; in 2012 were reported about 14 million new cases and 8.2 million cancer-related deaths. Statistics indicate that in 2016, estimated 1.685.210 new cases of cancer will be diagnosed in the US and 595.690 people are expected to die from this disease. The development of this complex disease, comprise different biological capabilities tumors acquired during development multistage. These characteristics constitute an organizing principle for the rationalization of the complexities of this neoplastic disease. Each step involves multiple cellular mechanisms that are not yet fully understood. So far, there is not a cure for cancer, and there is great concern about the increase in the number of reported cases and deaths from it. Despite this, there are many treatments to prevent premature death by it, but mostly with remarkable side effects such as heart, pulmonary, endocrine and nervous system problems, including development of secondary cancers, due to chemotherapy or radiation treatments, with deterioration of quality of life of patients.

The identification of molecules with the ability to inhibit the activity of target enzymes in cancer processes arises as a promising alternative for the treatment of this disease. Natural products (NPs), have been widely reported as a promising source for the discovery of new drugs because of its large molecular diversity and low toxicity. It is known that 50% of the compounds used to treat cancer are derived from natural compounds, however, the mechanisms responsible for their activity so far not been elucidated clearly, and this information is useful for the rational design of more effective drugs with fewer side effects than treatments used so far.

For all these reasons, it is important to find natural compounds capable of modulating the activity of proteins that support the processes of formation and maintenance of cancer. In this thesis are presented the results of a multidisciplinary methodological strategy that included powerful computational tools such as molecular docking (AutoDock Vina, GOLD and Surflex-Dock, SYBYL), pharmacophore mapping (LigandScout 3.0) combined with statistical methods (cluster analysis, linear discriminant analysis, linear regression, among others) to the search for natural compounds with anticancer activity by inhibition of cancer targets such as, COX-2, iNOS and DNMT1. Additionally, in this work was evaluated the ability of these compounds to bind to human serum albumin (HSA).

The *in vitro* evaluation of anti-methylating activity was evaluated for promisory compounds gambogic acid, digoxin and phloridzin showing that are active against Enzyme DNMT1 (M.Sssl). Being the gambogic acid the one that presented the more potent inhibitory effect, the inhibitory activity was classified in the following order of potency: gambogic acid > digoxin > phloridzin. Digoxin and gambogic acid showed potent cytotoxic activities against human HT-29 and MCF-7 cancer cell lines, with very low IC₅₀ values (in nM and μM order). On the other hand, cytotoxic effects were not significant for phloridzin. Additionally, spectroscopic methods were employed to evaluate the interaction of HSA, drug transporter, with gambogic acid and digoxin. The data obtained from the measures titrations by spectroscopic methods UV-VIS, fluorescence quenching and circular dichroism revealed the possible interaction of HSA with gambogic acid and digoxin, being more favorable to gambogic acid. Thermodynamic parameters were calculated for HSA-gambogic acid and HSA-digoxin complexes, interacting residues in the binding site were predicted, showing static interactions. The results revealed that digoxin and gambogic acid could be a scaffold for the discovery of new anticancer compounds with greater potency, selectivity and fewer side effects, via inhibition of DNA methyltransferases.

RESUMEN

“Compuestos naturales como inhibidores de proteínas blanco en cáncer”

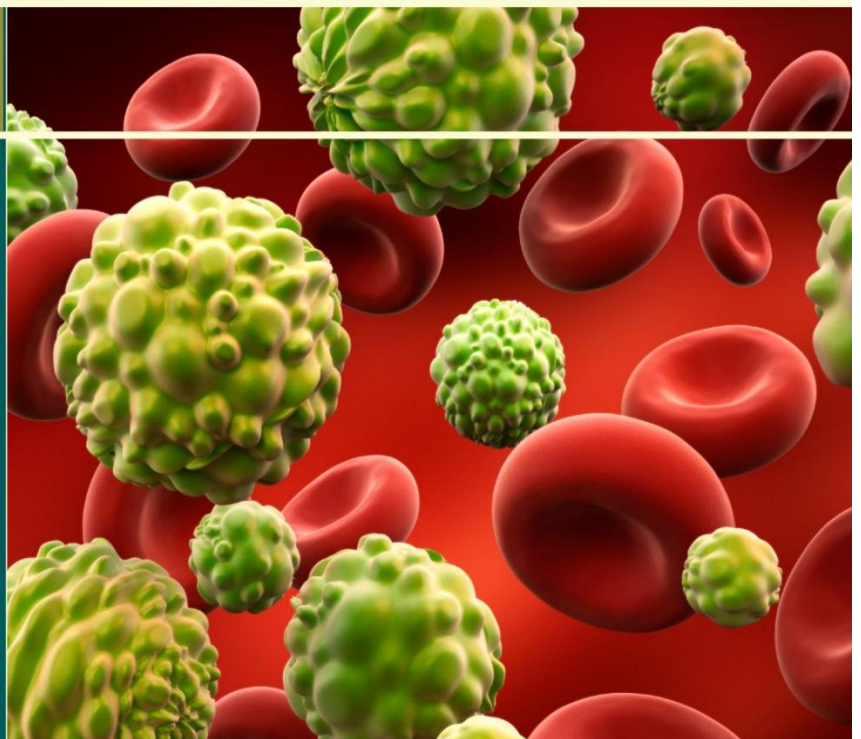
El cáncer, es el término para el conjunto de enfermedades relacionadas con la mutación de células normales a células anómalas de crecimiento no controlado. Esta enfermedad es la segunda causa de muerte en el mundo. En todos los tipos de cáncer, algunas de las células del cuerpo comienzan a dividirse sin parar y esparciéndose a los tejidos circundantes, causando graves daños en los órganos y en la etapa final la muerte. El cáncer tiene un gran impacto en la sociedad, siendo la principal causa de morbilidad y mortalidad en todo el mundo; en 2012 había alrededor de 14 millones de nuevos casos y 8.2 millones de muertes relacionadas con el cáncer. Las estadísticas indican que en el 2016, que alrededor de 1.685.210 de nuevos casos de cáncer serán diagnosticados en los EE.UU. y se estima que 595.690 personas mueran por causa de esta enfermedad. El desarrollo de esta compleja enfermedad, comprende diferentes capacidades biológicas de los tumores adquiridas durante el desarrollo de múltiples etapas. Estas características constituyen un principio de organización para la racionalización de las complejidades de la enfermedad neoplásica. Estas etapas involucran múltiples mecanismos celulares que aún no son del todo entendidos. Hasta ahora, no se cuenta con una cura contra el cáncer y existe una gran preocupación por el aumento en el número de casos reportados y defunciones por la misma. A pesar de esto, existen muchos tratamientos para evitar la muerte temprana por la misma, aunque en su mayoría con efectos secundarios remarcables, tales como problemas cardiacos, pulmonares, endocrinos, del sistema nervioso, incluso generación de canceres secundarios como es el caso de los tratamientos con quimioterapia o radioterapia, que en muchos casos deterioran la calidad de vida de los pacientes.

La identificación de moléculas con la capacidad de inhibir la actividad de enzimas blanco en cáncer se plantea como una alternativa prometedora para el tratamiento de esta enfermedad. Los productos naturales (PNs), los cuales han sido ampliamente reportados como una fuente promisoría para el descubrimiento de nuevos fármacos debido a su gran diversidad molecular y baja toxicidad. Se conoce que el 50% de los compuestos utilizados para el tratamiento de cáncer son derivados de compuestos naturales. Sin embargo, los mecanismos responsables de su actividad hasta ahora no han sido elucidados con claridad, siendo esta información útil para el diseño racional de fármacos más efectivos y con menores efectos secundarios que los tratamientos utilizados hasta ahora.

Por todo lo anterior, es imperante la búsqueda de compuestos naturales con capacidad de modular la actividad de proteínas que soportan los procesos de formación y mantenimiento del cáncer. En este trabajo son presentados los resultados de una estrategia metodológica multidisciplinaria, que incluyo poderosas herramientas computacionales tales como acoplamiento molecular (AutoDock Vina, Surflex-Dock, SYBYL), mapeo farmacofórico (LigandScout 3.0) combinadas con métodos estadísticos (análisis clúster, análisis discriminante lineal, regresión lineal, entre otros) para la búsqueda de compuestos naturales con actividad contra el cáncer. Diferentes ensayos de biología molecular fueron empleados para evaluar la interacción de compuestos naturales seleccionados como promisorios por métodos computacionales, con proteínas reportadas como blancos de cáncer tales como COX-2, iNOS y DNMT1. Adicionalmente fue evaluada la capacidad estos compuestos para unirse a albumina de suero humana (HSA).

La evaluación *in vitro* de la actividad anti-metilante fue evaluada para los compuestos promisorios ácido gambógico, digoxina y flordizina mostrando que son activos contra la enzima DNMT1 (M.Sssl). Siendo el ácido gambógico presentó un efecto inhibitorio más potente, la actividad inhibitoria fue obtenida en el siguiente orden de potencia: ácido gambógico > digoxina > flordizina. La digoxina y el ácido gambógico presentaron potentes actividades citotóxicas contra las líneas celulares de cáncer humano HT-29 y MCF-7, con valores bajos de IC₅₀ (en el orden nM y µM). Por otro lado, efectos citotóxicos no fueron considerables para flordizina. Adicionalmente, métodos espectroscópicos fueron empleados para evaluar la interacción de HSA, conocido transportador de fármacos, con el gambógico y la digoxina. Los datos obtenidos de las titulaciones medidas por métodos espectroscópicos UV-VIS, extinción de fluorescencia y dicroísmo circular revelaron la posible interacción de HSA con ácido gambógico y digoxina, siendo más favorable con ácido gambógico. Los parámetros termodinámicos fueron calculados para los complejos HSA-ácido gambógico, y HSA-digoxina, residuos de interacción en el sitio de unión fueron predichos, mostrando interacciones estáticas. Los protocolos de acoplamiento molecular proteína-ligando soportaron la información obtenida de los parámetros termodinámicos. Los resultados revelaron que el ácido gambógico y digoxina podrían ser una plataforma para el descubrimiento de nuevos compuestos contra el cáncer, con mayor potencia, selectividad y con menores efectos secundarios, por vía de la inhibición de ADN metiltransferasas.

Chapter 1



CHAPTER 1. THESIS OVERVIEW

Cancer is the leading cause of morbidity and mortality worldwide, multiple factors can cause this disease, such as environmental pollutants, UV radiation, heavy metals, endocrine disruptors, polycyclic aromatic hydrocarbons, among others. The searching for more effective cancer treatments counteracting the effects of these agents on cancer apparition is of concern and of great global interest. There is a high demand for natural compounds with chemo-preventive activities that may modulate biochemical mechanisms involved in the development of this disease. In this work, computational tools, were used to search natural compounds with modulatory effect on recognized protein targets in the signaling cascades of cancer formation, such as cyclooxygenase-2 (COX-2), inducible nitric oxide synthase (iNOS) [1], and DNA methyltransferases (DNMTs) [2]. Protocols in molecular biological, cytotoxic assays and spectroscopic methods, were utilized for evaluation of natural compounds identified as promissory anticancer natural-drug.

1.1 RATIONALE

Cancer is a generic term covering a broad group of diseases which can affect any part of the body, also known as malignant tumors or malignancies [3-5]. One of its features is the rapid growth of abnormal cells that extend beyond its boundaries and metastasize invading adjacent parts of the body or spreading to other organs [3, 4]. Statistics data attributed 8.2 million deaths occurring worldwide in 2012. Lung cancer is the one with a higher number of deaths due to smoking. The main types of cancer and deaths are presented as following: lung (1.590.000); liver (745.000); Gastric (723.000); colorectal (694.000); breast (521.000); esophageal cancer (400.000) [6].

Cancer formation can be defined as the result of interaction between patient genetic factors and three categories of external agents, namely: physical carcinogens, such as ultraviolet and ionizing radiation; chemical carcinogens, such as asbestos, components of snuff, aflatoxin or heavy metals [7]; biological carcinogens such as viruses, bacteria or parasites [8]. Ageing have been classified as another fundamental factor in the development of cancer. The incidence of cancer increases greatly with age, most related with accumulate risk factors for certain cancers [9].

The developing of cancer depend on many factors, being smoking, alcohol, unhealthy diet and physical inactivity the main risk factors for cancer worldwide. Some chronic infections are also risk factors, and are more important in middle income and low income countries. The hepatitis B virus (HBV), hepatitis C (HCV) and some types of human papillomavirus (HPV) increase the risk of liver cancer and uterine neck cancer [10]. HIV infection also significantly increases the risk of some cancers, such as cervical [11]. The age-standardized rate for all cancers in the world (excluding non-melanoma skin cancer) for men and women was 182 per 100.000 people in 2012. The rate was higher for men (205 per 100.000) than women (165 per 100.000). The highest cancer rate for men and women together was found in Denmark with 338 people per 100.000 being diagnosed in 2012. The age-Standardized rate was 300 per 100.000 at Least for nine countries (Denmark, France, Australia, Belgium, Norway, United States of America, Ireland, Republic of Korea and The Netherlands) [12]. The countries in the top ten come from Europe, Oceania, Northern America and Asia. All cancers involve the malfunction of genes that control cell growth, division, and death. However, most of the genetic abnormalities that affect cancer risk are not hereditary (inherited from parents), but instead result from damage to genes (mutations) that occur throughout a person's lifetime [13]. Genetic damage may be due to internal factors, such as hormones or the metabolism of nutrients within cells, or external factors, such as tobacco, chemicals, and sunlight [14]. These nonhereditary mutations are called somatic mutations. It is estimated that about 5% of all cancers are strongly hereditary. Most cancers evolve through multiple changes that result from a combination of hereditary and environmental factors [13].

Cancer diseases could be prevented through known interventions, including vaccines, antibiotics, improved sanitation, or education. Some cancers (colorectal and cervix) can be avoided by detection and removal of precancerous lesions through regular screening examinations by a health care professional [15, 16]. Early detection of cancer is important because it provides a greater chance that treatment will be successful. Cancers that can be detected at an early stage through screening

include breast, cervix, colorectal, prostate, oral cavity, and skin [17]. However, screening has been proven to be effective in reducing the mortality for only breast, cervical, and colorectal cancers [18]. Screening and treatment services for most of these cancers are not available in developing countries because of limited resources.

Cancer present a great complexity, cancer cells exhibit distinct attributes by tumors grow and metastasize to distant organs. Logical framework to identify the 8 hallmark features that distinguish a tumor cell from its nonmalignant counterpart have been defined [19], these hallmarks have helped the oncology community appreciate the underlying biological principles operating in a tumor cell. This hallmark including, activating invasion and metastasis, enabling replicative immortality, evading growth suppressors and immune destruction, genome instability and mutation, inducing angiogenesis, reprogramming energy metabolism, evading cell death, sustaining proliferative signaling and tumor-promoting inflammation [19-21].

Natural products have been reported to have important role in the discovery and development of drugs for cancer disease treatment. About 50% of current cancer therapeutics are derived from natural sources [22]. However, the efficacy of natural extracts in treating cancer has not been explored extensively. Scientific research into the validity and mechanism of action of these products is needed to develop natural health drugs for cancer therapy. Several studies have reported the introduction of new natural compounds from traditional medicine to the forefront of modern medicine, in order to provide safer and cheaper complementary treatments for cancer therapy; as well as, possible improvement of quality of life for patients with cancer [23].

New researches aimed at finding innovative treatments are required in order to reduce high indices of morbidity and mortality of this disease [24, 25]. Understanding the cellular and molecular mechanisms regulated by cancer targets provide more opportunities for finding new therapies for cancer [26]. Recent studies have evidenced that inactivation of tumor suppressors via methylation of DNA is an important process in cancer malignance [27, 28], also activation eukaryotic transcription factors, such as nuclear factor-kappa (NF- κ B), activator protein-1 (AP-1) and signal transducer and activator of transcription 3 (STAT3) [1, 29, 30]. Pharmacological targets involved in carcinogenesis, such as cicloxygenase-2 (COX-2), inducible nitric oxide synthase (iNOS) [1, 29], and DNA methyltransferases, have been extensively reported.

The identification of new molecules with the ability to inhibit the activity of these enzymes is a promising solution. Being natural products qualified as a promising source of drugs because their large molecular diversity and low toxicity [31]. Recent

studies conducted using polymers and polymeric natural products reveal new technology perspectives for cancer treatment, these compounds include quercetin [30, 32], doxorubicin [33], curcumin [34, 35], kaempferol [36], 5-aminolevulinic acid [37], among others [38], although their mechanisms of action are not fully known. Searching of bioactive compounds for cancer treatment has become a priority. New approaches based on computational chemistry have been applied in the field of drug discovery in recent decades [39-41], where protein-ligand molecular docking has been widely accepted, being widely used for virtual screening of databases on a specific receptor [42-44]. In this work virtual screening on several databases from natural compounds was performed in order to identify new natural products capable of interacting with three important proteins involved in cancer signaling processes (COX-2, iNOS and DNMT1), with subsequent *in vitro* evaluation as anticancer and interacting with human albumin. These results could be a new window for the design of more potent and specific compounds in the treatment of UV-induced cancer.

1.2. HYPOTHESIS

Natural bioactive compounds may inhibit the activity of cancer related proteins such as COX-2, iNOS and DNMTs.

1.3. PERTINENCE

Cancer is a disease that has a major impact on society, being the major cause of morbidity and mortality worldwide; in 2012 there were about 14 million new cases and 8.200.000 cancer-related deaths [12]. In 2016, an estimated 1.685.210 new cases will be diagnosed cancer in the US and it is expected that 595.690 people die from this disease. Statistical records show that the most common cancers in 2016 will be breast, lung and bronchus, prostate, rectal, colon, bladder, melanoma of skin, non-Hodgkin lymphoma, thyroid, kidney and renal pelvis, leukemia, endometrial and pancreatic [45].

In Colombia, between 1997 and 2012, the number of cancer deaths increased by 33%, now representing 15% of cancer deaths in men and 20% in women. In the same period, the total years of life lost due to cancer disease increased by 25.1% in men and 31.1% women. The largest increases (> 40%) were colon and rectum, pancreas and kidney cancer in both sexes; melanoma and bladder cancer for men and breast and ovarian cancer for women, [46-48]. Recently, Hodgkin lymphoma have been reported, with 819 new diagnosed patients. Eighty-nine (12 %) of them had Hodgkin lymphoma (HL) and 720 (88 %) had non-HL. All survival rates at 3 years were 77 % for HL and follicular lymphoma, 54 % for Diffuse large B-cell lymphoma (DLBCL), the most common form of non-HL, and 45 % for T cell lymphomas [49]. A total of 4.736 cervical cancer new cases were diagnosed with an

incidence of 21.5 per 100.000 people. In this year, mortality rate was 10.0 per 100.000 people in 2008 [50].

Skin cancer has not been a priority public health in Colombia in part because of their low mortality (approximately 1 death per 100.000 population per year). According to reports from other countries, however, skin cancer is a major public health problem in terms of mortality and healthcare costs. Based on program data US Social Security, Medicare, skin cancer costs represent more than \$ 426.000.000 by year, being one of more expensive 5 types of cancer in the United States [51]. In England, in 2008 the average cost per case of non-melanoma skin cancer was £ 889 and £ 1226, respectively. It is estimated that the cost to the NHS for skin cancer will be over £ 180 million in 2020 [52]. In Colombia, skin cancer is more prevalent than other types of cancer. In 2002, according to the National Cancer Institute, skin cancer was 663 cases among other cancers [53]. During 2003 to 2005 a study conducted in the Dermatological Center Federico Lleras Acosta, Bogota Colombia, reported an increase in the number of diagnosed cases (168.659), of which 2.184 were for malignant skin tumors. In 2005 was reported an increase for basal cell cancer of 7 cases by 1.000 compared to 2003. In the case of melanoma, increased from 2.7 per 10.000 in 2003, to 13 per 10.000 in 2005 [54].

According to the Institute of Hydrology, Meteorology and Environmental Studies of Colombia. (IDEAM), the values of atmospheric ozone in Colombia are below levels assumed as a minimum for the entire country, confirming solar ultraviolet radiation as a risk of serious consideration for the future development of skin carcinogenesis [55]. Nevertheless, the National Plan for Cancer Control in Colombia 2010-2019, claimed to have no magnitude data of cases of skin cancer in the country, excluding it from the estimated values. However, it is considered the cancer with highest incidence in Colombia.

Despite advances in early diagnosis and treatment, cancer is a major cause of death in Colombia, with a growing impact on population health. New strategies are necessary to reduce the number of death per year. Recent studies propose different target proteins important in carcinogenesis processes, such as DNA methyltransferases as important regulators of cell function epigenetic [1, 56, 57] as well as inflammation-promoting proteins such as COX-2 and iNOS [58, 59], suggesting that inhibition of these proteins may be useful cancer treatment. Natural compounds have been reported as promissory source for drug discovery. About 50% of current cancer therapeutics are derived from natural sources. Paclitaxel, a natural compound, isolated and structurally elucidated for the first time in the late 1960s from the stem bark of western yew (*T. brevifolia* Nutt.) discovered as agent that acted by promoting the irreversible assembly of tubulin into microtubules [60]. Paclitaxel is

approved for the cancer treatment. However, its market price is very high at \$ 600.000 per kg [61]. The searching for compounds capable of inhibiting cancer related target, remains a subject of great interest worldwide being natural compounds, known by its capabilities and assimilation by the human body, a good alternative. For all these aspects, the international scientific community has focused its efforts on the search for new sources of naturally occurring active ingredients as potential anti-cancer [62-64].

1.4. OBJECTIVES AND THESIS STRUCTURE

This work was performed in order to identify natural compounds that may interact with targets protein involved in cancer. The content was structured in four main steps, as follows:

- Identification of natural compounds that interact with COX-2.
- Searching of natural compounds with potential modulation on iNOS activity.
- Virtual screening for identification of natural compounds as inhibitors of DNMTs.
- Evaluation *in vitro* of natural compounds as inhibitors of DNMT1, antineoplastic activity, and its interaction with human albumin by spectroscopic methods.

Chapter 2, entitled as introduction, describe the main aspects and state-of-the-art knowledge on cancer mechanism, the role of natural compounds as chemopreventive agents, and explanation of different methods used to search promising compounds for cancer prevention and treatment. The subsequent chapters (1-5) shown the abstract, materials and methods, results and discussions, and conclusions of each single step. The main contributions of this thesis project are presented in Chapter 7, entitled conclusions and final remarks.

In Chapter 3, the interaction of bioactive natural products present in the diet was evaluated on COX-2, by *in silico* approach utilizing AutoDock Vina, GOLD and Surflex-Dock (SYBYL-X) docking programs. Theoretical affinity for reported COX-2 inhibitors significantly correlated with reported median inhibitory concentrations. Moreover, synergistic action of curcumin on celecoxib-induced inhibition of COX-2 may occur allosterically, as this natural compound docks to a place different from the inhibitor binding site.

Natural compounds commonly found in foods were identified in Chapter 4 as potential modulators of inducible nitric oxide synthase (iNOS), employing AutoDock Vina molecular docking protocols. Results presented here indicated some chemicals presented in food may be acting by direct on iNOS enzyme.

Advanced computational tools were performed for searching of new DNMTs inhibitors from natural compounds in Chapter 5. A classifier LDA-based QSAR model for classification of active/inactive 800 natural molecules from natural compounds. Subsequent docking calculations were performed on DNA methyltransferase (DNMTs) structures by AutoDock Vina and Surflex-Dock, this method is proposed as a computational strategy for identifying DNMTs inhibitors, with application in the identification of new anticancer drugs.

Finally, in Chapter 6, the anticancer activity of natural DNA methyltransferase inhibitors and interaction with human serum albumin were evaluated. Natural products, gambogic acid, phloridzin and digoxin, identified *in silico* with potential to interact with DNMTs were evaluated by *in vitro* assays for DNA methylation inhibi

tion and cytotoxic activity, and the interaction of these natural compounds with human serum albumin was studied using spectroscopic methods (UV-VIS, quenching of fluoresce and circular dichroism) and molecular docking protocols.

1.5. REFERENCES

[1] Liu, L., Li, J., Kundu, J.K., Surh, Y.-J. Piceatannol inhibits phorbol ester-induced expression of COX-2 and iNOS in HR-1 hairless mouse skin by blocking the activation of NF- κ B and AP-1. *Inflammat Res.* 2014, 63, 1013-21.

[2] Katiyar, S.K., Singh, T., Prasad, R., Sun, Q., Vaid, M. Epigenetic Alterations in Ultraviolet Radiation-Induced Skin Carcinogenesis: Interaction of Bioactive Dietary Components on Epigenetic Targets. *Photochem Photobiol.* 2012, 88, 1066-74.

[3] Kerr, J.F., Winterford, C.M., Harmon, B.V. Apoptosis. Its significance in cancer and cancer therapy. *Cancer.* 1994, 73, 2013-26.

[4] Nordling, C. A new theory on the cancer-inducing mechanism. *British J Cancer.* 1953, 7, 68.

[5] Barreto, J.A., O'Malley, W., Kubeil, M., Graham, B., Stephan, H., Spiccia, L. Nanomaterials: applications in cancer imaging and therapy. *Adv Mater.* 2011, 23.

[6] Siegel, R., Naishadham, D., Jemal, A. Cancer statistics, 2012. *CA Cancer J Clin.* 2012, 62, 10-29.

[7] Harris, C.C. Chemical and physical carcinogenesis: advances and perspectives for the 1990s. *Cancer Res.* 1991, 51, 5023s-44s.

[8] Humans, I.W.G.o.t.E.o.C.R.t. Biological agents. Volume 100 B. A review of human carcinogens. IARC monographs on the evaluation of carcinogenic risks to humans/World Health Organization, International Agency for Research on Cancer. 2012, 100, 1.

[9] Doll, R., Cook, P. Summarizing indices for comparison of cancer incidence data. *Int J Cancer.* 1967, 2, 269-79.

[10] Thun, M.J., DeLancey, J.O., Center, M.M., Jemal, A., Ward, E.M. The global burden of cancer: priorities for prevention. *Carcinogenesis.* 2010, 31, 100-10.

[11] Clifford, G.M., Polesel, J., Rickenbach, M., Dal Maso, L., Keiser, O., Kofler, A., et al. Cancer risk in the Swiss HIV Cohort Study: associations with immunodeficiency, smoking, and highly active antiretroviral therapy. *J Natl Cancer Inst.* 2005, 97, 425-32.

[12] Ferlay, J., Soerjomataram, I., Ervik, M., Dikshit, R., Eser, S., Mathers, C., et al. Cancer Incidence and Mortality Worldwide: IARC CancerBase No. 11 [Internet]. Lyon, France: International Agency for Research on Cancer. GLOBOCAN. 2013; 2012 v1. 0, htt p. globocan. iarc. fr. Accessed. 2015, 30.

[13] Knudson, A.G. Hereditary cancer, oncogenes, and antioncogenes. *Cancer Res.* 1985, 45, 1437-43.

[14] Marnett, L.J. Oxyradicals and DNA damage. *Carcinogenesis.* 2000, 21, 361-70.

[15] Organization, W.H. Cancer control: knowledge into action: WHO guide for effective programmes, World Health Organization, 2007.

[16] Miller, B. Cancer: We Can Win The War Against Cancer By Aggressively pursuing Prevention, Oak Publication Sdn Bhd, 2005.

[17] Smith, R.A., Cokkinides, V., Eyre, H.J. Cancer screening in the United States, 2007: a review of current guidelines, practices, and prospects. *CA Cancer J Clin.* 2007, 57, 90-104.

[18] Sabatino, S.A., Habarta, N., Baron, R.C., Coates, R.J., Rimer, B.K., Kerner, J., et al. Interventions to increase recommendation and delivery of screening for breast, cervical, and colorectal cancers by healthcare providers: systematic reviews of provider assessment and feedback and provider incentives. *Am J Prevent Med.* 2008, 35, S67-S74.

[19] Hanahan, D., Weinberg, R.A. Hallmarks of cancer: the next generation. *cell.* 2011, 144, 646-74.

[20] Nguyen, D.X., Bos, P.D., Massagué, J. Metastasis: from dissemination to organ-specific colonization. *Nat Rev Cancer.* 2009, 9, 274-84.

[21] Joyce, J.A., Pollard, J.W. Microenvironmental regulation of metastasis. *Nat Rev Cancer.* 2009, 9, 239-52.

[22] Ovadje, P., Roma, A., Steckle, M., Nicoletti, L., Arnason, J.T., Pandey, S. Advances in the research and development of natural health products as main stream cancer therapeutics. *Evid Based Compl Alternat Med* 2015, 2015.

[23] Harvey, A.L., Edrada-Ebel, R., Quinn, R.J. The re-emergence of natural products for drug discovery in the genomics era. *Nat Rev Drug Dis.* 2015, 14, 111-29.

[24] De Monte, C., Carradori, S., Secci, D., D'Ascenzio, M., Guglielmi, P., Mollica, A., et al. Synthesis and pharmacological screening of a large library of 1, 3, 4-thiadiazolines as innovative therapeutic tools for the treatment of prostate cancer and melanoma. *Eur J Med Chem.* 2015, 105, 245-62.

[25] Walls, B., Jordan, L., Diaz, L., Miller, R. Targeted therapy for cutaneous oncology: a review of novel treatment options for non-melanoma skin cancer: part I. *J Drugs Dermatol.* 2014, 13, 947-52.

[26] D'Orazio, J., Jarrett, S., Amaro-Ortiz, A., Scott, T. UV Radiation and the Skin. *Int J Mol Sci.* 2013, 14, 12222-48.

[27] Nandakumar, V., Vaid, M., Tollefsbol, T.O., Katiyar, S.K. Aberrant DNA hypermethylation patterns lead to transcriptional silencing of tumor suppressor genes in UVB-exposed skin and UVB-induced skin tumors of mice. *Carcinogenesis*. 2011, 32, 597-604.

[28] Liggett, W., Sidransky, D. Role of the p16 tumor suppressor gene in cancer. *J Clin Oncol*. 1998, 16, 1197-206.

[29] Zhai, Y., Dang, Y., Gao, W., Zhang, Y., Xu, P., Gu, J., et al. P38 and JNK signal pathways are involved in the regulation of phlorizin against UVB-induced skin damage. *Experimen Dermatol*. 2015.

[30] Vicentini, F.T.M.C., He, T., Shao, Y., Fonseca, M.J.V., Verri Jr, W.A., Fisher, G.J., et al. Quercetin inhibits UV irradiation-induced inflammatory cytokine production in primary human keratinocytes by suppressing NF- κ B pathway. *J Dermatol Sci*. 2011, 61, 162-8.

[31] Koehn, F.E., Carter, G.T. The evolving role of natural products in drug discovery. *Nat Rev Drug Discov*. 2005, 4, 206-20.

[32] Sahu, S., Saraf, S., Kaur, C.D. Biocompatible nanoparticles for sustained topical delivery of anticancer phytoconstituent quercetin. *Pakistan journal of biological sciences: PJBs*. 2013, 16, 601-9.

[33] Taveira, S.F., de Campos, A., Luciana, M., de Santana, D.C., Nomizo, A., de Freitas, L.A.P., et al. Development of cationic solid lipid nanoparticles with factorial design-based studies for topical administration of doxorubicin. *J Biomed Nanotechnol*. 2012, 8, 219-28.

[34] Mangalathillam, S., Rejinold, N.S., Nair, A., Lakshmanan, V.-K., Nair, S.V., Jayakumar, R. Curcumin loaded chitin nanogels for skin cancer treatment via the transdermal route. *Nanoscale*. 2012, 4, 239-50.

[35] Bar-Sela, G., Epelbaum, R., Schaffer, M. Curcumin as an anti-cancer agent: review of the gap between basic and clinical applications. *Curr Med Chem*. 2010, 17, 190-7.

[36] Yao, K., Chen, H., Lee, M.-H., Langfald, A., Kim, M.O., Yu, D.H., et al. Kaempferol suppresses solar ultraviolet radiation-induced skin cancers by targeting RSK2 and MSK1. *Cancer Res*. 2014, 7, 958-67.

[37] Ibbotson, S. Topical 5-aminolaevulinic acid photodynamic therapy for the treatment of skin conditions other than non-melanoma skin cancer. *British J Dermatol*. 2002, 146, 178-88.

[38] Afaq, F., Katiyar, S. Dietary Phytochemicals and Chemoprevention of Solar Ultraviolet Radiation-Induced Skin Cancer. In: *Nutraceuticals and Cancer*, Sarkar, F.H. Ed., Springer Netherlands, 2012, pp. 295-321.

[39] Litterman, N.K., Lipinski, C.A., Bunin, B.A., Ekins, S. Computational prediction and validation of an expert's evaluation of chemical probes. *J Chem Inf Model*. 2014, 54, 2996-3004.

[40] Barelrier, S., Eidam, O., Fish, I., Hollander, J., Figaroa, F., Nachane, R., et al. Increasing chemical space coverage by combining empirical and computational fragment screens. *ACS Chem Biol*. 2014, 9, 1528-35.

[41] Sliwoski, G., Kothiwale, S., Meiler, J., Lowe, E.W. Computational methods in drug discovery. *Pharmacol Rev*. 2014, 66, 334-95.

[42] Patil, S.P., Ballester, P.J., Kerezsi, C.R. Prospective virtual screening for novel p53–MDM2 inhibitors using ultrafast shape recognition. *J Comput Aided Mol Des.* 2014, 28, 89-97.

[43] Kumar, V., Krishna, S., Siddiqi, M.I. Virtual screening strategies: Recent advances in the identification and design of anti-cancer agents. *Methods.* 2015, 71, 64-70.

[44] Tuccinardi, T., Poli, G., Dell'Agnello, M., Granchi, C., Minutolo, F., Martinelli, A. Receptor-based virtual screening evaluation for the identification of estrogen receptor β ligands. *J Enzyme Inhib Med Chem.* 2014, 1-9.

[45] Siegel, R.L., Miller, K.D., Jemal, A. Cancer statistics, 2016. *CA Cancer J Clin.* 2016, 66, 7-30.

[46] de Vries, E., Arroyave, I., Pardo, C., Wiesner, C., Murillo, R., Forman, D., et al. Trends in inequalities in premature cancer mortality by educational level in Colombia, 1998–2007. *J Epidemiol Comm Health.* 2015, 69, 408-15.

[47] De Vries, E., Meneses, M.X., Piñeros, M. Años de vida perdidos como una medida de carga de cáncer en Colombia, 1997-2012. *Biomédica.* 2016, 36.

[48] Angel, J., Ibarra, J., Diaz, S., Lehmann, C., Garcia, M., Guzman, L., et al. Clinical behavior of breast cancer in men in a Latin American population. *Rev Colomb Cancerol.* 2015, 19, 150-5.

[49] Combariza, J.F., Lombana, M., Torres, A.M., Castellanos, A.M., Arango, M. General features and epidemiology of lymphoma in Colombia. A multicentric study. *Ann Hematol.* 2015, 94, 975-80.

[50] Muñoz, N., Bravo, L.E. Epidemiology of cervical cancer in Colombia. *Salud Publica Mex.* 2014, 56, 431-9.

[51] Sanchez, G., Nova, J., de la Hoz, F. Risk factors for basal cell carcinoma: a study from the national dermatology center of Colombia. *Act Dermo-Sifiliograf* 2012, 103, 294-300.

[52] Vallejo-Torres, L., Morris, S., Kinge, J., Poirier, V., Verne, J. Measuring current and future cost of skin cancer in England. *J Pub Health.* 2013, fdt032.

[53] Pardo, C., Murillo, R., Piñeros, M., Castro, M.Á. Casos nuevos de cáncer en el Instituto Nacional de Cancerología, Colombia, 2002. *Rev Colomb Cancerol.* 2003, 7, 4-19.

[54] Nova-Villanueva, J., Sánchez-Vanegas, G., de Quintana, L.P. Cáncer de Piel: Perfil Epidemiológico de un Centro de Referencia en Colombia. *Rev Salud Pub.* 2007, 9, 4.

[55] Colombia. Ministerio de Ambiente, Vivienda y Desarrollo Territorial. . Ozono. Bogotá: IDEAM. 2002.

[56] Kala, R., Shah, H.N., Martin, S.L., Tollefsbol, T.O. Epigenetic-based combinatorial resveratrol and pterostilbene alters DNA damage response by affecting SIRT1 and DNMT enzyme expression, including SIRT1-dependent γ -H2AX and telomerase regulation in triple-negative breast cancer. *BMC cancer.* 2015, 15, 1.

[57] Kim, H., Ramirez, C.N., Su, Z.-Y., Kong, A.-N.T. Epigenetic modifications of triterpenoid ursolic acid in activating Nrf2 and blocking cellular transformation of mouse epidermal cells. *J Nutr Biochem.* 2015.

[58] Maini, S., Fahlman, B.M., Krol, E.S. Flavonols Protect Against UV Radiation-Induced Thymine Dimer Formation in an Artificial Skin Mimic. *J Pharm Pharmaceut Sci.* 2015, 18.

[59] Paredes-Gonzalez, X., Fuentes, F., Jeffery, S., Saw, C.L.L., Shu, L., Su, Z.Y., et al. Induction of NRF2-mediated gene expression by dietary phytochemical flavones apigenin and luteolin. *Biopharmaceut Drug Disp.* 2015, 36, 440-51.

[60] Atanasov, A.G., Waltenberger, B., Pferschy-Wenzig, E.-M., Linder, T., Wawrosch, C., Uhrin, P., et al. Discovery and resupply of pharmacologically active plant-derived natural products: A review. *Biotechnology Adv.* 2015, 33, 1582-614.

[61] Howat, S., Park, B., Oh, I.S., Jin, Y.-W., Lee, E.-K., Loake, G.J. Paclitaxel: biosynthesis, production and future prospects. *N Biotechnol.* 2014, 31, 242-5.

[62] Reddy, L., Odhav, B., Bhoola, K. Natural products for cancer prevention: a global perspective. *Pharmacol Therap.* 2003, 99, 1-13.

[63] Mann, J. Natural products in cancer chemotherapy: past, present and future. *Nat Rev Cancer.* 2002, 2, 143-8.

[64] Ramos, A.A., Castro-Carvalho, B., Prata-Sena, M., Dethoup, T., Buttachon, S., Kijjoa, A., et al. Crude extracts of marine-derived and soil fungi of the genus *Neosartorya* exhibit selective anticancer activity by inducing cell death in colon, breast and skin cancer cell lines. *Pharmacogn Res.* 2016, 8, 8.

Chapter 2



CHAPTER 2. INTRODUCTION TO THE CANCER

2.1. CANCER OVERVIEW

2.1.1 Definition

Cancer is a group of diseases characterized by uncontrolled growth and propagation of abnormal cells causing death in most patients. This disease can be caused by external factors (snuff, chemicals, radiation and infectious organisms) and internal factors (hereditary, hormones, immune conditions, and mutations in metabolism) [65-67]. Also, combinations of these initiate or promote carcinogenic processes. In most cancers, development requires several stages taking place for many years. Cancer is the second leading cause of death worldwide. In 2012, more than 14 million new cases of cancer worldwide were diagnosed (Figure 2.1). Overall statistics estimate this number will reach 19 million by 2025 [68]. Currently, the number of people who die by cancer are more than twice than those die by AIDS, malaria or tuberculosis.

Most common causes of cancer death reported in 2012

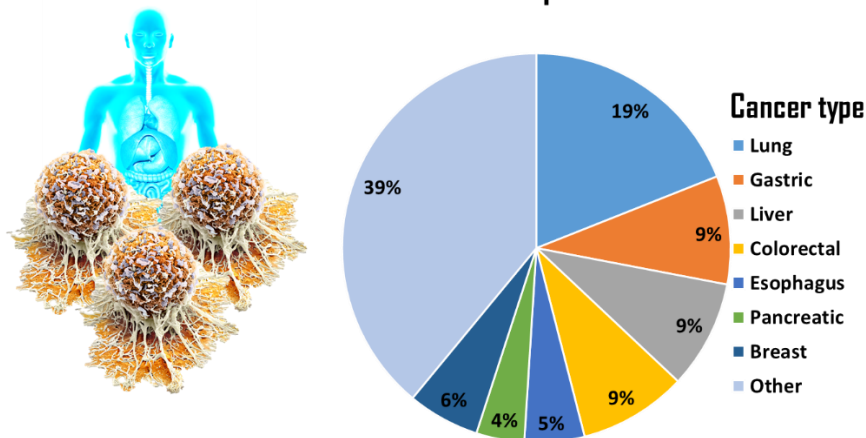


Figure 2.1. Reported deaths from Cancer worldwide, 2012.

2.1.2 Cancer cells and cancer stem cells

Cancer cells are the basis of disease; initiate cells and tumor progression, leading oncogenic mutations of tumor suppressor genes that define cancer as a genetic disease [69]. Cancer cells within tumors have been described as reasonably homogeneous population cells to tumor progression [70]. Many human tumors are histologically different, presenting regions defined by different degrees of differentiation, proliferation, vascularity, inflammation, and/or invasiveness [71]. In recent years, however, they have accumulated evidence pointing to the existence of a new dimension of intratumoral heterogeneity and a subclass of neoplastic cells within tumors, called cancer stem (CSC) cells [72].

2.1.3 Proposed cancer development mechanisms

Recent studies have identified hallmark features that promote carcinogenic processes. Together these distinctive features provide extensive mechanistic framework which explain the transformation multistage carrying a normal cell to its lethal metastatic counterpart (Figure 2.2) [73]. Cancer mainly includes six biological skills during their development, which constitute an organizing principle for the rationalization of its complexity. These features include activating invasion and metastasis, enabling replicative immortality, evading growth suppressors, evading immune destruction, genome instability and mutation, inducing angiogenesis, energy metabolism reprogramming, evading cell death, sustaining tumor proliferative signaling and inflammation-promoting [19]. In addition to cancer cells, some tumors

contain an apparently normal recruited cells that contribute to the acquisition of the distinctive features in the tumor microenvironment used to develop new ways for cancer treatment [19, 20].

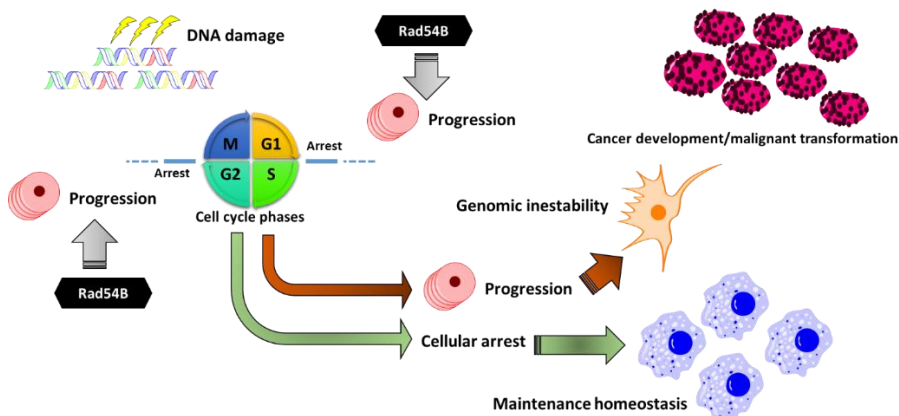


Figure 2.2. A basic mechanism of cancer development. Rad54B instead inactivates the arrest and promotes cell cycle progression.

2.2. DNA METHYLATION IN SKIN CANCER

Changes in DNA methylation have been examined in squamous cell carcinoma. Global hypomethylation increase in advanced cancer. The silencing of tumor suppressor genes, including MLH-1, BRCA1 and MGMT hypermethylation associated with CpG islands is an early event in skin carcinogenesis murine. However, DNA hypermethylation is also seen in the disease progression [74, 75]. Changes in DNA methylation also observed in human melanoma, through hypermethylation of tumor-related, including WIF1, TFPI2, RASSF1A genes, and SOCS1 have been associated with advanced melanoma [76]. These changes affect the expression of a large number of genes. However, the impact of altered expression of individual genes is not entirely clear [74]. These studies indicate that alterations in DNA methylation is an important epigenetic event in melanoma and non-melanoma skin that contributes to the progression of the disease, although there is not enough information to understand the role of individual changes in gene expression of the disease [77]. In addition, other mechanisms have been proposed, including nuclear factor-kappa (NF- κ B), activator protein-1 (AP-1) and signal transducer and activator of transcription 3 (STAT3), as well as, inflammatory enzyme cyclooxygenase-2 (COX-2) and inducible nitric oxide synthase (iNOS) [1].

2.3. MOLECULAR PROTEIN-LIGAND DOCKING

The discovery of naturally bioactive compounds with anti-cancer properties represents one of the efforts in recent decades, in order to develop therapeutic treatments for this disease of high incidence worldwide. In drug discovery methodologies, the information about the potential activity compound promissory, usually is directed to the structural basis from receptor and ligand through a protocol of molecular docking (Figure 2.3), as first step prior to experimental evaluation [78], the most commonly used programs for this purpose are GOLD [79], Surflex-Dock [80] and AutoDock Vina [81]. Being AutoDock Vina the most widely used one for this purpose.

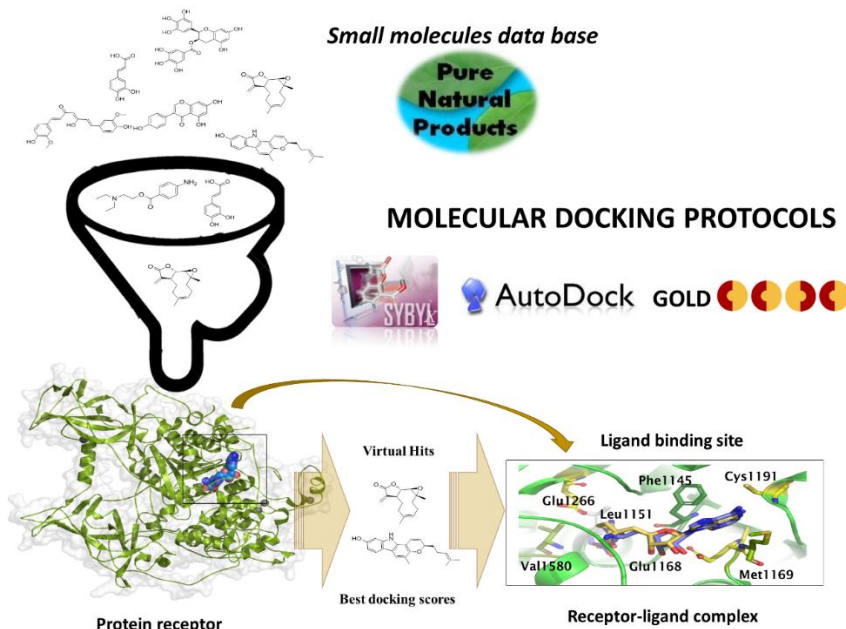


Figure 2.3. Schematic representation for molecular docking protocols. Computational tools combined with statistical methods facilitate and increase the probability of success in the selection of promissory compounds.

2.3.1 GOLD (*Genetic Optimization for Ligand Docking*).

This program uses a scoring function called convenience (fitness) to classify different modes of ligand binding to the protein. It consists of four terms: a) the score hydrogen bonds protein-ligand, b) score Van der Waals force protein-ligand, c) the contribution to the convenience due to intramolecular hydrogen bonds in the ligand and d) the contribution due to the intramolecular ligand tension. It also has a

mechanism for positioning the ligand in the binding site with attachment points, and finally uses a search algorithm to explore possible binding modes [79].

2.3.2 Surflex-Dock (Sybyl Program)

Surflex-Dock, uses a function of empirical score and patented search engine to find the ligand binding site of the protein. Surflex-Dock has an idealized active site of the ligand to the protein called protomol target to generate putative poses molecules or molecular fragments. These putative poses are scored using the scoring function "Hammerhead" which also serves as a function of local optimization of poses. The results of the coupling for all molecules are organized according to the total score "Total score" represented in $-\log(K_d)$, K_d is the dissociation constant [80].

2.3.3 AutoDock Vina

AutoDock Vina, is a program used for molecular docking and virtual screening, which combines some of the advantages of functions based on empirical knowledge and scoring functions: empirical information is extracted from both the conformational preferences of the receptor-ligand complex and experimental measurements of affinity. Ligands are classified based on a scoring function of energy, to accelerate the score calculation, thought a grid based on protein-ligand interaction [81].

2.4. NATURALLY OCCURRING COMPOUNDS AND THEIR APPLICATION IN MEDICINE

The natural compounds have been widely used in traditional medicine, considered as a viable option for the development of new drugs alternative, becoming a valuable long-term source leading to the discovery of new and effective drugs. Statistical data show that natural bioactive compounds and their derivatives, contribute about one-third of the drugs most currently sold on the market [82].

Natural bioactive compounds in fruits and vegetables (Figure 2.4), have been considered as promising options for different clinical trials aimed at finding alternatives for the prevention of diseases involving inflammatory processes in some stage, such as cancer [83, 84]. Many of these natural bioactive dietary compounds have been reported with important pharmacological effects, which can significantly alter the activity of therapeutic agents function by modulating biochemical pathways [85]. There have been numerous therapeutic areas benefited greatly by the rich diversity of scaffolds for drugs generated by the study of physicochemical properties of natural products, due to their ability to interact with many specific drug targets within the cell and indeed in recent years have been a source of inspiration for most models applied drugs on diseases with high incidence worldwide, mainly in inflammatory and carcinogenic diseases [86].

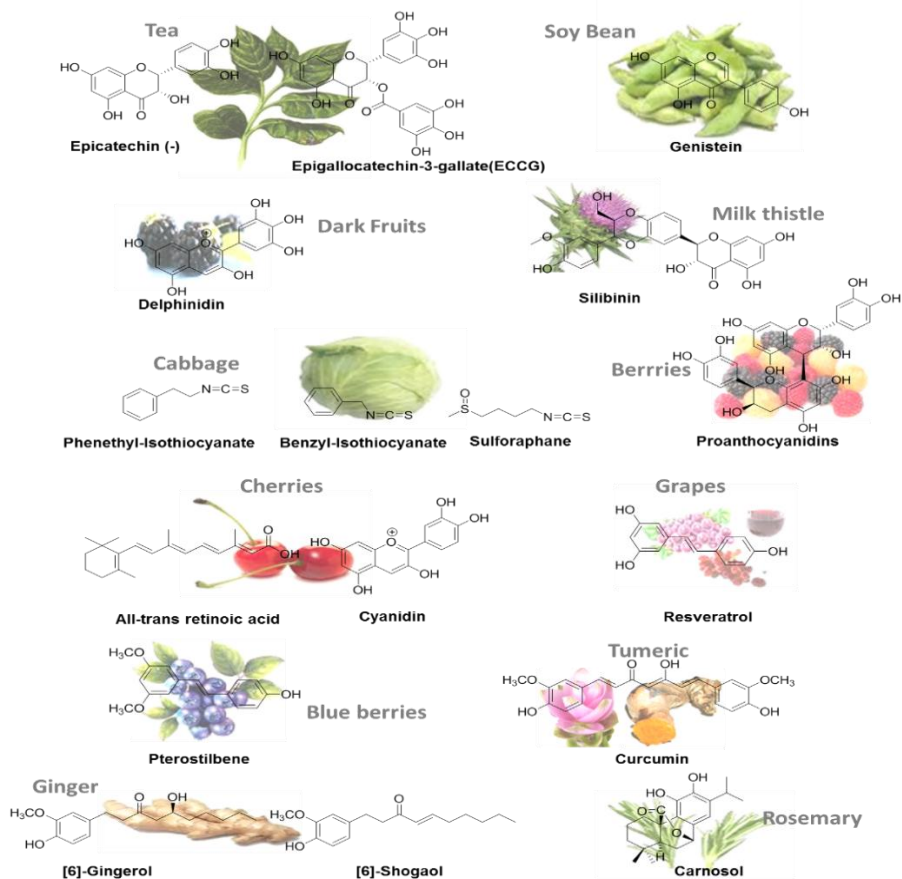


Figure 2.4. Some bioactive compounds and their natural sources.

2.5. MOLECULAR BIOLOGY ASSAYS (PCR/RFLP)

Molecular biology techniques are those used to isolate or extract high-purity DNA, analyze it to see their status, cut and paste (birth of genetic engineering), amplifying a region in an enormous number of molecules (cloning fragments bacteria or other vectors such as viruses and PCR) [87], cutting a region with restriction enzymes to see if a mutation is present or a restriction site is lost (mutation analysis by RFLP or restriction fragment length polymorphism), mean differences in the sizes of the restriction fragments due to polymorphisms in DNA, among others [88].

Innumerable applications of these techniques and perhaps the most commonly used today is PCR, followed by restriction enzymes and detection of fragments on a gel or followed by a polyacrylamide gel having more definition for separating fragments with few bases of differences [89-92]. When both PCR and restriction enzymes analysis are used, they are called PCR/RFLP (Polymerase Chain Reaction - Restriction Fragment Length Polymorphism). These techniques can be used for detecting alleles of a normal and mutated gene (inherited diseases) or to distinguish bacterial or viral strains or more favorable alleles for a characteristic of interest productive then apply to the selection [88].

2.6. CELL VIABILITY ASSAYS

Cellular cytotoxicity is defined as a change in basic cellular functions leading to a damage which may be detected. From this occurs, different authors have developed batteries in vitro tests to predict the toxic effects of drugs and chemicals, using experimental models and primary cultures isolated from organs as established cell lines [93]. Among the most known and already validated tests are testing Neutral Red Uptake, kenacid binding to blue and finally the reduction assay bromide 3-(4,5 dimethylthiazo-2-yl) -2,5 diphenyltetrazolium (MTT) [94].

2.6.1 MTT Assays

This is a method used to determine cell viability, given by the number of cells present in the culture which is able to be measured by the formation of a colored compound, due to a reaction that takes place in the mitochondria of viable cells. The MTT [3-(4, 5-dimethyl-2-thiazolyl) -2, 5-diphenyl -2H- tetrazolium bromide]-is taken up by cells and reduced by mitochondrial succinic dehydrogenase enzyme to a formazan insoluble form [94]. The reaction product, formazan is retained in the cells and can be released by solubilizing them [95]. Thus, it is quantified the amount of reduced MTT by a colorimetric procedure that occurs as a result of the discoloration reaction from yellow to blue [96].

2.7. SPECTROSCOPIC METHODS USED TO EVALUATE PROTEIN-LIGAND INTERACTIONS

Spectroscopy is the study of interaction of electromagnetic radiation with atoms and molecules. These interactions, which include absorption or emission, are highly sensitive testing of atomic and molecular structures [97]. A briefly definition of spectroscopic techniques used in this work for evaluation of human serum albumin with natural compounds is presented below.

2.7.1 UV-VIS Spectroscopy

The ultraviolet-visible spectrophotometry or UV-Vis spectrometry involves photon spectroscopy in the region of ultraviolet-visible radiation. This technique is complementary to fluorescence spectrometry, dealing with transitions from the excited state to the ground state, while the absorption spectroscopy is measured from ground state to the excited state [98]. These properties make to UV-VIS spectroscopy applicable for the study of protein-ligand interaction.

2.7.2 Fluorescence Spectroscopy

Fluorescence Spectrometry (also called fluorometry or spectrofluorometry) is a type of spectroscopy that analyzes fluorescence of a sample. A beam of light is used, usually ultraviolet light, which excites the electrons of the molecules of certain compounds and causes them to emit light of a lower energy, visible light generally (but not necessarily). A complementary technique is the UV-VIS spectrometry. Fluorescence spectroscopy can be inferred about the interaction of a ligand with a protein or macromolecule as well as the calculation of different thermodynamic parameters that generate information about the type of interaction in a particular system. [99].

2.7.3 Circular Dichroism

It is the differential absorption by an asymmetric molecule (in our case, the polypeptide chain) of two circularly polarized light beams (left and right) direction is measured through the ellipticity parameter (θ , theta), an angle it is measured in degrees. Plane-polarized light becomes elliptical by effect of an optically active chromophore. The asymmetry of the chromophores in proteins (amides, aromatic groups and S-S bridges) is induced by interaction with neighboring groups and estimate secondary structure content detect conformational changes measure ligand binding [100]. This spectroscopic technique has been usefull in prediction of canonical secondary structure contents for proteins based on empirically-defined spectroscopic signatures derived from proteins with known three-dimensional structures [101].

2.8. REFERENCES

[1] Shrivastava, N., Kamal, S., Varma, A. Cancer and Its Biology. A Textbook of Molecular Biotechnology. 2009, 401.

[2] Montesano, R., Hall, J. Environmental causes of human cancers. Eur J Cancer. 2001, 37, 67-87.

[3] Lichtenstein, P., Holm, N.V., Verkasalo, P.K., Iliadou, A., Kaprio, J., Koskenvuo, M., et al. Environmental and heritable factors in the causation of cancer—analyses of cohorts of twins from Sweden, Denmark, and Finland. *N Engl J Med*. 2000, 343, 78-85.

[4] NCI, N.C.I., 2016.

[5] Zhou, B.-B.S., Zhang, H., Damelin, M., Geles, K.G., Grindley, J.C., Dirks, P.B. Tumour-initiating cells: challenges and opportunities for anticancer drug discovery. *Nat Rev Drug Dis*. 2009, 8, 806-23.

[6] Hermann, P.C., Huber, S.L., Herrler, T., Aicher, A., Ellwart, J.W., Guba, M., et al. Distinct populations of cancer stem cells determine tumor growth and metastatic activity in human pancreatic cancer. *Cell Stem Cell*. 2007, 1, 313-23.

[7] Eliceiri, B.P., Cheresh, D.A. The role of av integrins during angiogenesis: insights into potential mechanisms of action and clinical development. *J Clin Invest*. 1999, 103, 1227-30.

[8] Clevers, H. The cancer stem cell: premises, promises and challenges. *Nat Med*. 2011, 313-9.

[9] Yasuhara, T., Suzuki, T., Katsura, M., Miyagawa, K. Rad54B serves as a scaffold in the DNA damage response that limits checkpoint strength. *Nat Commun*. 2014, 5.

[10] Hanahan, D., Weinberg, R.A. Hallmarks of cancer: the next generation. *cell*. 2011, 144, 646-74.

[11] Nguyen, D.X., Bos, P.D., Massagué, J. Metastasis: from dissemination to organ-specific colonization. *Nat Rev Cancer*. 2009, 9, 274-84.

[12] Saha, K., Hornyak, T.J., Eckert, R.L. Epigenetic cancer prevention mechanisms in skin cancer. *The AAPS journal*. 2013, 15, 1064-71.

[13] Fraga, M.F., Herranz, M., Espada, J., Ballestar, E., Paz, M.F., Ropero, S., et al. A mouse skin multistage carcinogenesis model reflects the aberrant DNA methylation patterns of human tumors. *Cancer Res*. 2004, 64, 5527-34.

[14] Tanemura, A., Terando, A.M., Sim, M.-S., van Hoesel, A.Q., de Maat, M.F., Morton, D.L., et al. CpG island methylator phenotype predicts progression of malignant melanoma. *Clin Cancer Res*. 2009, 15, 1801-7.

[15] van den Hurk, K., Niessen, H.E., Veeck, J., van den Oord, J.J., van Steensel, M.A., Zur Hausen, A., et al. Genetics and epigenetics of cutaneous malignant melanoma: a concert out of tune. *BBA Rev Cancer*. 2012, 1826, 89-102.

[16] Liu, L., Li, J., Kundu, J.K., Surh, Y.-J. Piceatannol inhibits phorbol ester-induced expression of COX-2 and iNOS in HR-1 hairless mouse skin by blocking the activation of NF- κ B and AP-1. *Inflammat Res*. 2014, 63, 1013-21.

[17] Cavasotto, C.N., Orry, W., Andrew, J. Ligand docking and structure-based virtual screening in drug discovery. *Curr Top Med Chem*. 2007, 7, 1006-14.

[18] Verdonk, M.L., Cole, J.C., Hartshorn, M.J., Murray, C.W., Taylor, R.D. Improved protein–ligand docking using GOLD. *Proteins: Struct Funct Bioinf*. 2003, 52, 609-23.

[19] Jain, A.N. Surflex-Dock 2.1: robust performance from ligand energetic modeling, ring flexibility, and knowledge-based search. *J Comp Aided Mol Des*. 2007, 21, 281-306.

[20] Trott, O., Olson, A.J. AutoDock Vina: improving the speed and accuracy of docking with a new scoring function, efficient optimization, and multithreading. *J Comput Chem*. 2010, 31, 455-61.

[21] Zhou, X., Li, Y., Chen, X. Computational identification of bioactive natural products by structure activity relationship. *J Mol Graph Modell.* 2010, 29, 38-45.

[22] Thoppil, R.J., Bishayee, A. Terpenoids as potential chemopreventive and therapeutic agents in liver cancer. *World J Hepatol.* 2011, 3, 228-49.

[23] Lucas, L., Russell, A., Keast, R. Molecular mechanisms of inflammation. Anti-inflammatory benefits of virgin olive oil and the phenolic compound oleocanthal. *Curr Pharm Des.* 2011, 17, 754-68.

[24] Lila, M.A., Raskin, I. Health-related Interactions of Phytochemicals. *J Food Sci.* 2005, 70, R20-R7.

[25] Mishra, B.B., Tiwari, V.K. Natural products: an evolving role in future drug discovery. *Eur J Med Chem.* 2011, 46, 4769-807.

[26] Mirhendi, H., Makimura, K., Khoramizadeh, M., Yamaguchi, H. A one-enzyme PCR-RFLP assay for identification of six medically important *Candida* species. *Nihon Ishinkin Gakkai Zasshi.* 2006, 47, 225-9.

[27] Girish, P., Anjaneyulu, A., Viswas, K., Shivakumar, B., Anand, M., Patel, M., et al. Meat species identification by polymerase chain reaction-restriction fragment length polymorphism (PCR-RFLP) of mitochondrial 12S rRNA gene. *Meat Sci.* 2005, 70, 107-12.

[28] AlSuhaibani, E., Voudouris, C., Al-Atiyat, R., Kotzamumin, A., Vontas, J., Margaritopoulos, J. Identification of a point mutation in the *ace1* gene of *Therioaphis trifolli maculata* and detection of insecticide resistance by a diagnostic PCR-RFLP assay. *Bull Entomol Res.* 2015, 105, 712-6.

[29] Dowgier, G., Mari, V., Losurdo, M., Larocca, V., Colaianni, M.L., Cirone, F., et al. A duplex real-time PCR assay based on TaqMan technology for simultaneous detection and differentiation of canine adenovirus types 1 and 2. *J Virol Methods.* 2016, 234, 1-6.

[30] Sousa, D.R.T.d., Santos, C.S.d.S., Wanke, B., Júnior, S., Santos, M.C.d., Cruz, K.S., et al. PCR-RFLP as a useful tool for diagnosis of invasive mycoses in a healthcare facility in the North of Brazil. *Electron J Biotech.* 2015, 18, 231-5.

[31] Xu, W., Morris, U., Aydin-Schmidt, B., Msellem, M.I., Shakely, D., Petzold, M., et al. SYBR green real-time PCR-RFLP assay targeting the *Plasmodium* cytochrome b gene—a highly sensitive molecular tool for malaria parasite detection and species determination. *PLoS one.* 2015, 10, e0120210.

[32] Rampersad, S.N. Multiple applications of Alamar Blue as an indicator of metabolic function and cellular health in cell viability bioassays. *Sensors.* 2012, 12, 12347-60.

[33] Stockert, J.C., Blázquez-Castro, A., Cañete, M., Horobin, R.W., Villanueva, Á. MTT assay for cell viability: Intracellular localization of the formazan product is in lipid droplets. *Acta Histochem.* 2012, 114, 785-96.

[34] Lim, S.-W., Loh, H.-S., Ting, K.-N., Bradshaw, T.D., Allaudin, Z.N. Reduction of MTT to Purple Formazan by Vitamin E Isomers in the Absence of Cells. *Trop Life Sci Res.* 2015, 26, 111.

[35] Liu, C., Hou, L., Liu, L., Qu, Z., Wang, X., Sun, X., et al. In Vitro Cytotoxicity Evaluation of Highly Absorbent Foam Dressings Based on Silver Zirconium Phosphate via IC50 Value. *J Biomat Nanobiotech.* 2016, 7, 37.

[36] Holdgate, G., Geschwindner, S., Breeze, A., Davies, G., Colclough, N., Temesi, D., et al. Biophysical methods in drug discovery from small molecule to pharmaceutical. *Methods Mol Biol.* 2013,1008, 327-55.

[37] Enyedy, É.A., Dömötör, O., Bali, K., Hetényi, A., Tuccinardi, T., Keppler, B.K. Interaction of the anticancer gallium (III) complexes of 8-hydroxyquinoline and maltol with human serum proteins. *J Biol Inorg Chem.* 2015, 20, 77-88.

[38] Domínguez-García, M., Ortega-Zúñiga, C., Meléndez, E. New tungstenocenes containing 3-hydroxy-4-pyrone ligands: antiproliferative activity on HT-29 and MCF-7 cell lines and binding to human serum albumin studied by fluorescence spectroscopy and molecular modeling methods. *J Biol Inorg Chem.* 2013, 18, 195-209.

[39] Narváez-Pita, X., Ortega-Zuniga, C., Acevedo-Morantes, C.Y., Pastrana, B., Olivero-Verbel, J., Maldonado-Rojas, W., et al. Water soluble molybdenocene complexes: Synthesis, cytotoxic activity and binding studies to ubiquitin by fluorescence spectroscopy, circular dichroism and molecular modeling. *J Inorg Biochem.* 2014, 132, 77-91.

[40] Lopes, J.L., Miles, A.J., Whitmore, L., Wallace, B.A. Distinct circular dichroism spectroscopic signatures of polyproline II and unordered secondary structures: Applications in secondary structure analyses. *Protein Sci.* 2014, 23, 1765-72.

Chapter 3



CHAPTER 3. POTENTIAL INTERACTION OF NATURAL DIETARY BIOACTIVE COMPOUNDS WITH COX-2

3.1. ABSTRACT

Bioactive natural products present in the diet play an important role in several biological processes, and many have been involved in the alleviation and control of inflammation-related diseases. These actions have been linked to both gene expression modulation of pro-inflammatory enzymes, such as cyclooxygenase 2 (COX-2), and to an action involving a direct inhibitory binding on this protein. In this study, several food-related compounds with known gene regulatory action on inflammation have been examined *in silico* as COX-2 ligands, utilizing AutoDock Vina, GOLD and Surflex-Dock (SYBYL) as docking protocols. Curcumin and all-*trans* retinoic acid presented the maximum absolute AutoDock Vina-derived binding affinities (9.3 kcal/mol), but genistein, apigenin, cyanidin, kaempferol, and docosahexaenoic acid, were close to this value. AutoDock Vina affinities and GOLD scores for several known COX-2 inhibitors significantly correlated with reported median inhibitory concentrations ($R^2=0.462$, $P<0.001$ and $R^2=0.238$, $P=0.029$, respectively), supporting the computational reliability of the predictions made by our docking simulations. Moreover, docking analysis insinuate the synergistic action of curcumin on celecoxib-induced inhibition of COX-2 may occur allosterically, as this natural compound docks to a place different from the inhibitor binding site. These results suggest that the anti-inflammatory properties of some food-derived molecules could be the result of their direct binding capabilities to COX-2, and this process can be modeled using protein-ligand docking methodologies.

3.2. INTRODUCTION

Foods have small amounts of bioactive compounds that act as extra nutritional constituents [1]. The diversity of these chemicals is large and some of the most representative include flavonoids, isothiocyanates, proanthocyanidins, terpenoids, carotenoids, anthocyanins, and omega-3 polyunsaturated fatty acids, among many others [2]. The presence of these natural bioactive molecules in fruits and foods has been considered relevant, not only due to their unique organoleptic properties, but also because of their beneficial effects on human health, as demonstrated in numerous studies [3,4]. A recent review paper by Pan et al [2], detailed how natural bioactive compounds exert their anti-inflammatory activities by modulating gene expression of diverse inflammation-related genes. However, it is also well known that some anti-inflammatory molecules carry out their action by directly inhibiting inflammatory proteins such cyclooxygenase 2 (COX-2) [5]. This enzyme catalyzes the first step in the synthesis of prostaglandins, thromboxanes and other eicosanoids in several inflammatory processes [6].

Although several natural products have been shown to modulate COX-2 expression [7,8,9], it is not clear if those are able to directly interact with the gene product or its modulating transcription factors. Computational chemistry offers the possibility to explore these interactions through protein-ligand docking procedures. Docking methods are valuable tools for drug development, and most current approaches assume a rigid receptor structure to allow virtual screening of large numbers of possible ligands and putative binding sites on a receptor molecule [10]. Among those tools used for this purpose are AutoDock Vina, GOLD and Surflex-Dock (SYBYL) [11,12,13]. Docking strategies generate binding or affinity scores for different sites and poses on targets, and the protein 'hits' identified by using this method can serve as potential candidates for experimental validation [14,15].

In this study, docking methodologies were used to test the ability of 29 natural bioactive compounds, isolated from different food sources, to bind COX-2. In addition, ligands known to bind COX-2 were submitted to docking protocols to establish relationships between their biological activity and the predicted binding affinities.

3.3. MATERIALS AND METHODS

3.3.1. Protein and ligand structure preparation

Experimental coordinates of three COX-2 structures (PDB_codes: 1CX2, 1PPX and 1CVU) were obtained from Protein Data Bank (PDB) [16] and prepared with SYBYL 8.1.1 package [17]. Anti-inflammatory natural products chosen to perform this

study were those reported to modulate expression of genes related to inflammation [2]. All these chemicals are present in foods and vegetables (Table 3.1), and they have been proven to have good anti-inflammatory properties. Structures were drawn with SYBYL 8.1.1 package, exactly as presented by Pan 2009, and optimized using DFT at the B3LYP/6-31G level, and calculations were carried out with Gaussian 03 package program [18]. The resultant geometry was translated to Mol2 format with Open Babel [19]. To determine structural similarities between 1CX2, 1PPX and 1CVU, a molecular superposition was conducted using SYBYL 8.1.1 program.

Table 3.1. Evaluated natural products and their sources.

Compound	Dietary source	Reference
Apigenin	Celery	[20]
Tangeretin	Citrus peel	[21]
Silybinin	Milk thistle	[22]
Cyanidin	Cherries	[23]
Delphinidin	Dark fruits	[24]
Genistein	Soybean	[25]
Epicatechin	and Green tea	[26]
epigallocatechin-3-gallate		
Naringenin	Citrus peel	[27]
Quercetin and Kaempferol	Broccoli	[28]
5-hydroxy-3,6,7,8,3',4'-hexamethoxyflavone	Citrus peel	[29]
Curcumin	Turmeric powder and curcuma	[30,31]
Resveratrol	Grape skins and red wine	[32]
[6]-gingerol and [6]-shogaol	Ginger	[33]
Carnosol	Rosemary	[34]
Pterostilbene	Blueberries	[35]
Benzyl isothiocyanate	and Cabbage	[36]
Phenethyl isothiocyanate		
Sulforaphane	Cabbage	[37]
Proanthocyanidins	Berries	[38]
All- <i>trans</i> retinoic acid	Carrot, peppers and broccoli	[39,40]
Menthone	Mentha	[41]
Lycopene and β -carotene	Tomato and carrot	[42,43]
Lutein	Spinach and eggs	[44]
Eicosapentaenoic acid	and Fish and fish oil	[45,46]
Docosahexaenoic acid		

3.3.2. Protein-ligand docking calculations

The feasibility of natural compounds to be ligands for COX-2 structures was evaluated using molecular docking. This was performed utilizing three different programs that rely on several distinct scoring functions to evaluate the performance of the protein-ligand docking: AutoDock Vina, Surflex-Dock (SYBYL) and GOLD program.

AutoDock Vina combines some advantages of knowledge-based potentials and empirical scoring functions: it extracts empirical information from both the conformational preferences of the receptor-ligand complex and from experimental affinity measurements. Ligands are ranked based on an energy scoring function and, to speed up the score calculation, a grid-based protein-ligand interaction is used [11]. The docking site for the ligands on 1CX2, 1PXX and 1CVU was defined by establishing a cube at the geometrical center of the native ligand present in each one of the evaluated PDB structures, with the dimensions $24 \times 24 \times 24 \text{ \AA}$, covering the ligand binding site with a grid point spacing of 0.375 \AA . The coordinates X, Y and Z for 1CX2 from center grid boxes were 25.374, 21.657 and 17.292; for 1PXX 27.058, 24.431 and 15.437, and finally for 1CVU 25.277, 22.358 and 49.308, respectively. Ten runs were performed per each ligand, and for each run the best pose was saved. Finally, the average binding affinity for best poses was accepted as the binding affinity value for a particular complex.

GOLD utilizes a score function called fitness to rank different binding modes. It comprises four terms: the protein–ligand hydrogen-bond score, the protein-ligand van der Waals score, the contribution to the fitness due to intramolecular hydrogen bonds in the ligand and the contribution due to intramolecular strain in the ligand. It also has a mechanism for placing the ligand in the binding site using fitting points; and finally, it uses a search algorithm to explore possible binding modes [12]. The docking site was defined for each structure (1CX2, 1PXX and 1CVU) using the same coordinates X, Y and Z employed to localize the binding site with AutoDock Vina. A radius sphere of 10 \AA was defined around the geometrical center of the native ligand for each evaluated protein. For each independent algorithm run, a maximum number of 125.000 operations were performed. Operator weights for crossover, mutation, and migration were set in mode auto, the maximum distance between hydrogen donors and fitting points was set to 3.0 \AA , and non-bonded Van der Waals energies were cut-off at 6.0 \AA .

The Surflex-Dock module of SYBYL is a molecular docking unit that performs flexible alignments. Its results are presented as both docking accuracy and screening

utility [13]. The docking procedure was started with the protomol generation. The protomol was created using a ligand-based approach (native ligand for each COX-2 structure). Proto_threshold was set to 0.5 and proto_bloat was left at 0 as a default parameter. For each protein-ligand pair, twenty top ranked docked solutions were saved and the Surflex-Dock score presented as the mean for these values.

These docking platforms were also used to calculate docking scores for COX-2 inhibitors, SC558 and diclofenac, as well as for the natural substrate arachidonic acid. These molecules were also obtained from PDB. All protein-ligand docking calculations conducted on COX-2 proteins were performed using the inhibitor binding site on the crystal structure (PDB: 1CX2 and 1PPX) or the substrate binding site (PDB: 1CVU). These binding sites are the same in these COX-2 structures. In all cases, affinities were reported as the mean value obtained for 10 docking runs per ligand.

3.3.3. Identification of residues interacting with the natural bioactive compounds on COX-2 binding site

The identification of protein residues that interact with the natural bioactive compounds having the greatest affinities was carried out using LigandScout 3.0 [47]. This program creates simplified pharmacophores to detect the number and type of primary existing ligand-residue interactions on the protein active site.

3.3.4. Docking validation with biological data for COX-2 inhibitors

The 2D structures and the biological data of 21 COX-2 inhibitors were obtained from the PubChem chemical library [48] and literature [49,50]. Docking procedures were performed with three docking tools: AutoDock Vina, GOLD and Surflex-Dock [11,12,13], following the same protocols previously described for studied natural products. The biological data consisted of median inhibitory concentrations (IC_{50}), and the details of the testing protocols and materials are available on PubChem BioAssay [48]. The relationship between AutoDock Vina-calculated affinities of inhibitors on the three tested COX-2 (average values) and experimental activity data ($\text{Log}IC_{50}$) was performed by linear correlation [51], using Graph InStat Software (Version 3.06, 2003).

3.3.5. Theoretical approach to study the synergistic effect between curcumin and celecoxib on COX-2

It has been reported that curcumin acts synergistically with celecoxib in the inhibition of prostaglandin E2 synthesis by COX-2 [52, 53]. In order to gain insight in this process, we performed docking simulations on the whole COX-2 (3LN1) structure with both compounds. Aiming to evaluate if the curcumin shares the same binding site as celecoxib, a series of 500 AutoDock Vina docking runs were performed using the following docking parameters. The docking procedure on the 3LN1 structure was performed by establishing a cube with the dimensions $60 \times 84 \times 72 \text{ \AA}$ covering the whole protein (Chain A), with a grid point spacing of 1.0 \AA , using as center of the grid box the protein itself.

3.4. RESULTS AND DISCUSSION

3.4.1. Structural similarities of COX-2 structures

The superpositioning of the 3D COX-2 structures (PDB: 1CX2, 1CVU and 1PXX) as well as the RMSD values for each pair of them are presented in Figure 3.1. As can be seen, these three-dimensional structures of COX-2 have only minor differences (sequence identity > 99.5 and RMSD $< 0.507 \text{ \AA}$).

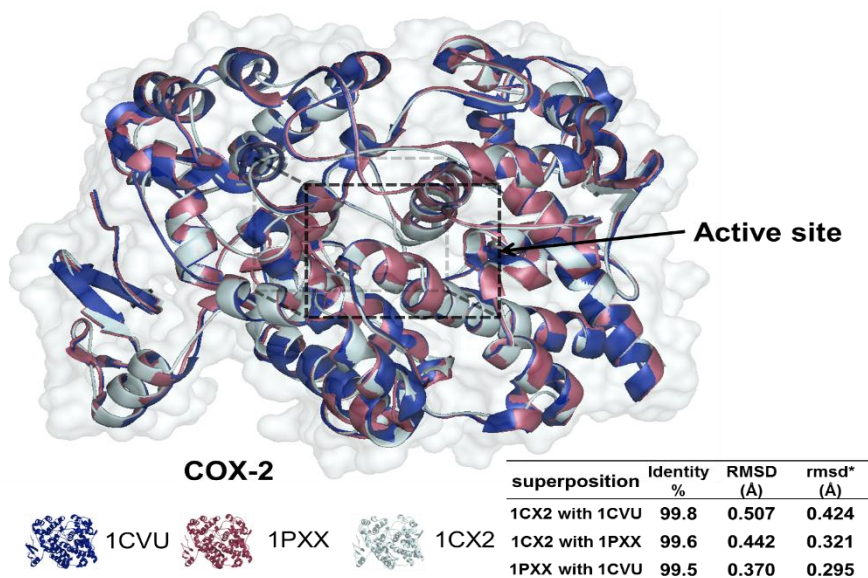


Figure 3.1. 3D-Superposition of COX-2 structures (1CVU, 1PXX and 1CX2), showing sequence identity and RMSD values. *RMSD for the binding site.

3.4.2. Docking calculations using AutoDock Vina, GOLD and SYBYL programs

The docking affinities of natural products for different COX-2, as calculated by three distinct docking programs are presented in Table 3.2. Results indicate that compared to the examined natural products, AutoDock Vina-calculated binding affinities for SC558, diclofenac (inhibitors) and arachidonic acid (substrate) were more consistent in terms of the magnitude of the expected predicted value, than the values generated for the scores calculated by GOLD and SYBYL. In the case of GOLD, the presence of the nitrogen seems to generate conflicting scores (negative values) for diclofenac, and high variability for binding scores obtained for the different COX-2 structures. SYBYL, on the other hand, also showed considerable variability for the scores obtained for the COX-2 structures. Therefore, successive calculations and discussions are referred solely to results provided by AutoDock Vina.

Table 3.2. Docking results for natural bioactive compound on three COX-2 structures.

Protein Name: Cyclooxygenase-2 (COX-2)	PDB codes								
	1CX2			1PXX			1CVU		
Compound	AV ^a Affinity (kcal/mol)	G Fitness	S Total Score	AV Affinity (kcal/mol)	G Fitness	S Total Score	AV Affinity (kcal/mol)	G Fitness	S Total Score
Curcumin	-8.4	51.41	7.60	-8.7	52.18	5.44	-9.3	52.62	7.03
Silibinin	-7.8	25.33	4.67	-3.6	44.59	0.79	-7.8	37.70	3.97
Apigenin	-8.4	47.99	5.24	-8.6	49.48	4.96	-8.9	48.68	6.08
Genistein	-8.4	43.42	4.49	-9.1	49.05	5.13	-8.8	48.03	5.15
Naringenin	-8.3	50.78	6.04	-8.4	49.66	5.89	-8.6	47.11	5.43
[6]-Shogahol	-8.0	54.43	9.10	-7.6	49.73	8.34	-7.8	53.17	7.02
[6]-Gingerol	-8.0	55.73	7.54	-7.6	46.76	8.24	-7.7	55.00	7.69
Docosahexaenoic acid	-7.7	63.84	9.10	-7.5	60.62	9.57	-8.8	64.05	10.73
Cyanidin	-7.6	46.71	5.25	-8.1	49.41	3.24	-8.9	51.37	5.70
Quercetin	-7.6	46.78	5.84	-8.1	49.55	4.57	-8.8	47.97	6.23
Resveratrol	-7.6	45.19	5.11	-8.0	47.15	6.49	-8.0	46.02	5.31
Eicosapentaenoic acid	-7.4	59.86	9.37	-7.5	58.10	8.98	-8.5	61.63	8.78
Tangeretin	-7.5	48.91	3.90	-7.7	65.16	6.82	-8.1	60.72	5.21
Epicatechin	-7.4	43.09	6.32	-8.5	47.23	5.19	-8.7	46.58	5.68
Kaempferol	-7.6	46.93	4.13	-7.9	48.48	3.85	-8.8	47.29	4.45
Delphinidin	-7.1	48.64	5.79	-8.1	49.77	3.84	-8.4	50.75	6.04
Pterostilbene	-6.9	49.10	6.94	-7.9	49.03	7.15	-8.2	48.09	6.79
All-trans retinoic acid	-7.2	36.84	5.08	-7.3	39.23	5.36	-9.3	46.28	6.90
Carnosol	-6.8	17.40	2.81	-5.6	44.06	4.33	-8.1	48.73	5.56
Menthone	-6.3	29.56	3.30	-6.6	30.11	4.15	-6.6	29.63	4.03

Table 3.2. continued

Benzylisothiocyanate	-5.9	39.73	2.83	-6.0	40.34	3.19	-6.1	39.02	2.95
Phenethylisothiocyanate	-6.1	44.28	4.42	-6.1	41.84	3.48	-6.5	38.86	3.29
Epigallocatechin-3-gallate	-7.2	52.43	4.88	-6.7	54.01	3.26	-8.2	59.86	6.43
B-Carotene	-5.7	20.8	6.58	3.3	-103.52	5.60	-6.1	-21.11	6.66
Lycopene	-5.3	20.59	5.33	-5.6	21.64	3.20	-7.6	2.11	4.04
5-Hydroxy-3,6,7,8,3',4'-Hexamethoxyflavone	-6.1	48.27	8.33	-6.7	55.94	9.59	-7.9	49.00	8.06
Sulforaphane	-4.4	45.61	3.38	-4.7	42.94	4.04	-4.8	43.43	3.72
Lutein	-3.9	31.69	4.99	3.6	-89.77	4.56	-5.6	-65.32	2.77
Proanthocyanidin B2	-1.8	-44.04	2.70	3.8	-48.54	-1.26	-4.5	-39.79	1.15
SC558 (Inhibitor)	-10.7	51.75	6.03	-10.0	45.21	5.59	-10.1	43.44	4.55
Diclofenac (Inhibitor)	-8.0	-122.97	4.42	-8.6	-119.46	5.46	-8.8	-117.28	2.24
Arachidonic acid (Substrate)	-8.0	59.70	8.64	-7.5	58.18	9.58	-7.8	66.83	10.81

^a. Docking scoring function values calculated for each protein: AV, AutoDock Vina; G, GOLD; S, Surflex-Dock (SYBYL).

According to the AutoDock Vina-obtained affinity values (kcal/mol), several natural compounds are potential ligands for COX-2, with best scores obtained for PDB: 1CVU, including curcumin, all-*trans* retinoic acid (greatest docking scores, with identical mean absolute affinity value of 9.3 kcal/mol), as well as genistein, apigenin, cyanidin, kaempferol and docosahexaenoic acid.

3.4.3. Interaction between residues in COX-2 and natural products

The complex COX-2 (PDB: 1CVU) with curcumin and all-*trans* retinoic acid, as well as the interactions between residues in the protein binding site and these ligands are shown in Figure 3.2. Both ligands fit into the same binding site (Figure 2A).

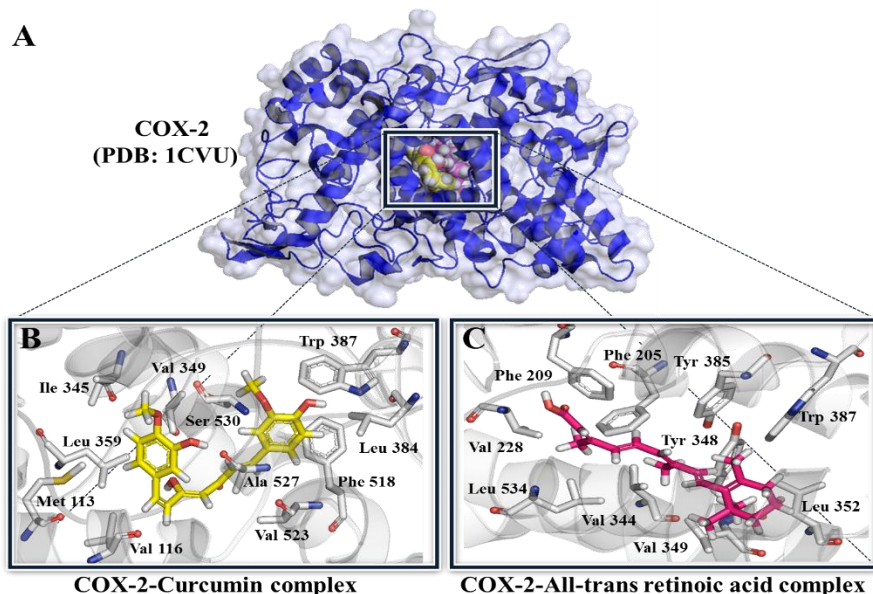


Figure 3.2. 3D structure of COX-2(1CVU)-ligand complexes. (A) COX-2 bound to curcumin or all-*trans* retinoic acid (box). (B) Residues in the interaction COX-2-curcumin. (C) Residues in the interaction COX-2-all-*trans* retinoic acid.

The most important residues on the 1CVU-curcumin complex (Figure 2B) are Met113, Val116, Ile345, Val349, Leu359, Leu384, Trp387, Phe518, Ala527, Val523, and Ser530. Most interactions are hydrophobic and aromatic in nature, except for Ser 530, which interacts with curcumin through a hydrogen bond. For the 1CVU-all-*trans* retinoic acid complex (Figure 2C), relevant aminoacids are Phe205, Phe209, Val228, Val344, Tyr348, Val349, Leu352, Tyr385, Trp387, and Leu534, showing only

hydrophobic interactions with the ligand. Most of these residues have also been reported for chemicals having strong interactions with COX-2 [54,55]. The most favorable conformation resulted from the docking of curcumin into the active site of COX-2 is similar to that experimentally found for the COX-2 substrate arachidonic acid (Figure 3.3). Accordingly, it is plausible to suggest that curcumin may be exerting its action by acting as a competitive inhibitor of arachidonic acid during prostaglandin E₂ synthesis by COX-2.

Among many natural products with known anti-inflammatory properties, curcumin is one of the most commonly referenced [56-59]. It is a phenolic yellow pigment present in curry powder, which has been associated with beneficial effects on human health as a result of its consumption in food [2]. It has been shown that curcumin exhibits antioxidant, anti-inflammatory and pro-apoptotic activities. Other food-related phenolic compounds with anti-inflammatory properties have also been reported in grapes, peanuts, blueberries, cranberries and red wine [60].

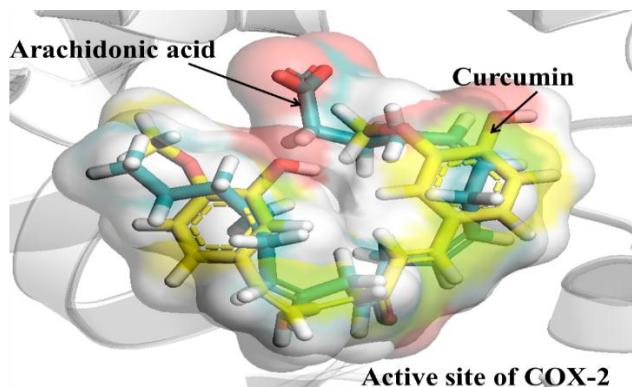


Figure 3.3. Docking conformation of curcumin and arachidonic acid (experimental) on the active site of COX-2 (1CVU).

All-*trans* retinoic acid is a terpenoid derived from the mevalonate and isopentenyl pyrophosphate pathway [61]. This compound has been used for the treatment or alleviation of inflammatory diseases [62]. Other molecules that docked into COX-2 were genistein, apigenin, cyanidin and kaempferol. These are flavonoids commonly present in foods that have been used for the treatment of many diseases, mainly due to their anti-allergic, antiviral, anti-inflammatory and vasodilatory properties [63,64,65,66,67]. Similarly, docosahexaenoic acid has been reported to possess systemic anti-inflammatory effects and cardiovascular protection [68].

Although values obtained by docking analysis should be considered just as a theoretical approximation, this information could be useful to explore possible mechanisms by which these chemicals behave as anti-inflammatory compounds, in particular if those could directly bind proteins such as COX-2.

3.4.4. Relationship between biological activity of COX-2 inhibitors and protein-ligand docking data

In order to determine if affinity values calculated by AutoDock Vina, as well as the scores calculated by GOLD and Surflex-Dock, could be utilized as an indication of the likeliness of a compound to behave as a COX-2 inhibitor, a group of 21 active compounds with confirmed inhibition activity, reported in PubChem BioAssay database [48], were docked to COX-2 (PDB: 1CX2, 1PXX and 1CVU). The PubChem chemical structure identifier (CID), biological activity (IC_{50}), AutoDock Vina affinity values, GOLD and Surflex-Dock scores for these compounds, and the biological activity ($\text{Log}IC_{50}$) are shown in Table 3.3. The relationships between biological activity and docking data are presented in Figure 3.4. Results suggest that for all examined docking tools, COX-2 activity follows a linear relationship only with binding affinity (AutoDock Vina) and the docking scores from GOLD, being highly significant with the first one. Although the magnitude of the correlation was moderate ($R^2 = 0.462$, $P < 0.001$), this value is similar to that obtained for other docking studies [69].

Moreover, data showed that ligands with absolute affinities greater than 10 kcal/mol have a better chance of interaction with COX-2. For instance, celecoxib, SC558, and 2,3-diarylphenyl sulfonamide have absolute affinity values greater than 10 kcal/mol and low IC_{50} . However, molecules with absolute affinities values around 9 kcal/mol have also a good probability of acting as COX-2 inhibitors. This is reassured when biological data is revised for our food-derived COX-2 inhibitors that presented best affinity values. Median inhibitory concentrations (IC_{50}) tested in different cell lines for curcumin (range 2 μM to 15 μM) [70,71,72,73,74,75], all-*trans* retinoic acid (20.5 μM) [76], genistein (range: <15 μM to 200 μM) [77,78,79], apigenin (range: 8.04 μM to 50 μM) [77,80], cyanidin (range: 40 μM to 90 μM) [81,82], kaempferol (range: <15 μM to 50 μM) [77,80], docosahexaenoic acid (range: 9.8 μM to 30 μM) [83,84], naringenin (7.9 \pm 1.9 μM) [85], [6]-Shogahol, (2,1 μM) [86], resveratrol (range: 3.06 μM) [87], eicosapentaenoic acid (7,1 μM) [83] are supporting evidence that these compounds can modulate COX-2 activity not only at mRNA but also at the protein level.

Table 3.3. Calculated affinities (AutoDock Vina), binding scores values (GOLD and SYBYL) and median inhibitory concentrations [IC₅₀] for selected COX-2 inhibitors.

COX-2 structure	PDB_code:1CX2			PDB_code:1PXX		
	AV Affinity (kcal/mol)	G Fitness	S Total Score	AV Affinity (kcal/mol)	G Fitness	S Total Score
Valdecoxib (AID: 162347)	-9.5±0.0	65.86±0.02	4.80±0.00	-8.5±0.0	61.78±0.02	4.62±0.00
Celecoxib (AID: 270014)	-10.8±0.0	68.42±0.02	6.63±0.00	-9.7±0.0	65.53±0.06	8.14±0.00
Meloxicam (AID: 162326)	-7.4±0.1	35.65±0.62	5.96±0.00	-7.0±0.0	38.51±0.15	3.90±0.00
Piroxicam (AID: 162326)	-8.3±0.0	39.06±0.04	3.54±0.00	-8.0±0.0	35.07±0.24	3.80±0.00
Diclofenac (AID: 313125)	-8.0±0.0	-122.97±0.07	4.42±0.00	-8.6±0.0	-119.24±0.24	5.46±0.00
Flosulide (AID: 162338)	-8.5±0.0	67.40±0.08	7.35±0.00	-8.8±0.0	63.56±0.14	6.47±0.00
Tenidap (AID: 160880)	-8.4±0.1	56.04±0.15	6.47±0.00	-8.3±0.0	61.57±0.08	4.20±0.00
Nimesulide (AID: 162655)	-7.6±0.0	57.79±0.10	6.77±0.00	-7.6±0.0	56.15±0.13	5.28±0.00
Etodolac (AID: 52141)	-7.2±0.1	49.14±0.23	7.09±0.00	-7.9±0.0	45.72±0.13	6.05±0.00
Rofecoxib (AID: 241308)	-9.8±0.0	63.49±0.04	6.60±0.00	-8.8±0.0	60.60±0.03	7.47±0.00
Dup 697 (AID: 162346)	-9.9±0.2	73.47±0.04	6.18±0.00	-9.5±0.0	69.63±0.09	5.88±0.00
L-745337 (AID: 162346)	-9.3±0.0	62.69±0.18	6.92±0.00	-10.9±0.0	63.73±0.03	6.19±0.00
SC558 Filizola, [49]	-10.7±0.2	51.75±0.25	6.03±0.00	-10.0±0.1	45.21±0.36	5.59±0.00
NS 398 (AID: 46852)	-7.6±0.0	60.55±0.07	6.23±0.00	-7.7±0.0	57.99±0.05	5.18±0.00
SC-58125 (AID: 162346)	-10.2±0.2	69.83±0.10	6.72±0.00	-9.6±0.2	67.76±0.08	6.40±0.00
CID: 10459826 (AID: 254745)	-7.0±0.1	60.72±0.64	6.28±0.00	-7.3±0.0	27.84±1.31	7.27±0.00
CID: 10895294 (AID: 162484)	-9.4±0.0	73.59±0.03	7.25±0.00	-7.6±0.0	69.78±0.08	7.55±0.00

Table 3.3. continued

CID: 9885354 (AID: 162507)	-10.6±0.0	68.32±0.03	7.49±0.00	-9.4±0.0	65.24±0.06	8.29±0.00
2,3-diarylcyclobutenone methylsulfone Dewitt, [50]	-9.4±0.0	66.20±0.03	6.64±0.00	-8.7±0.0	64.91±0.09	5.34±0.00
2,3-diarylphenyl sulfonamide Dewitt, [50]	-11.0±0.0	66.32±0.05	6.80±0.00	-10.7±0.0	65.70±0.03	7.27±0.00
2,3-diarylthiazolotriazole methylsulfone Dewitt, [50]	-8.9±0.0	66.62±0.03	7.23±0.00	-9.3±0.0	72.88±0.05	6.42±0.00

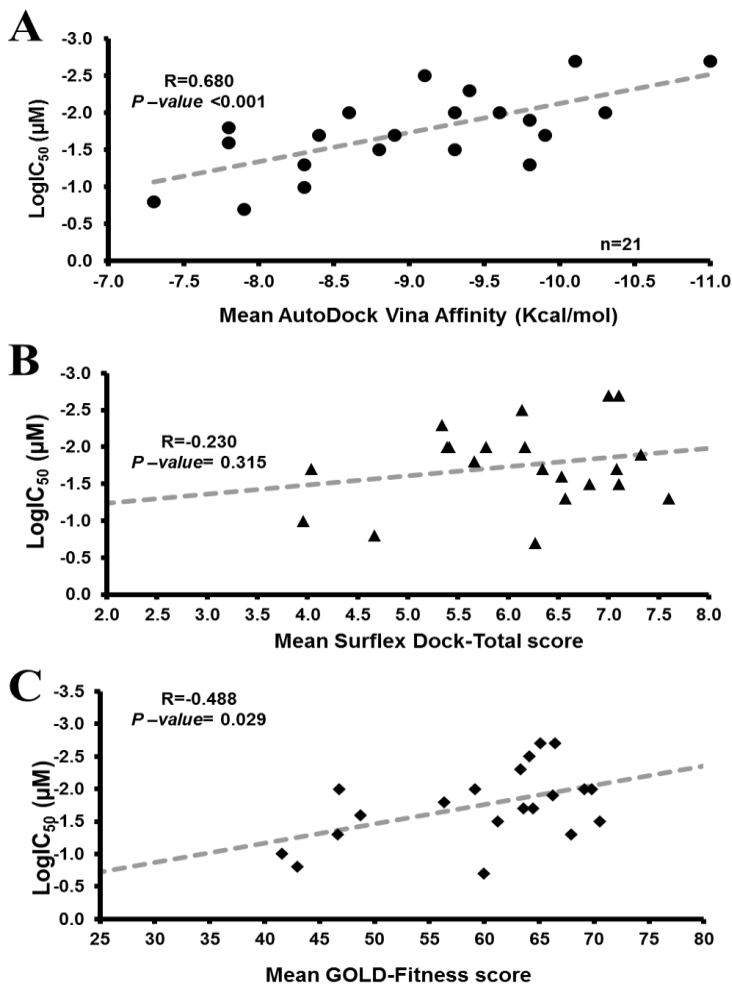


Figure 3.4. Correlation between docking theoretical data for inhibitors on COX-2 structures (1CX2, 1PXX and 1CVU) and their half maximal inhibitory concentration (Log IC₅₀). (A) AutoDock Vina, (B) GOLD and (C) Surflex-Dock. The regression line is shown for illustrative purposes. The GOLD score value for diclofenac (-119.90 ± 0.11) was not included in the analysis.

3.4.5. Docking curcumin and celecoxib on COX-2

It is known that some of the chemicals studied here can modulate COX-2 activity not only by competitive inhibition, but also by allosteric binding [52,53]. It has been shown that curcumin produces a synergistic effect with celecoxib, a highly selective COX-2 inhibitor, almost abolishing all enzyme activity [52,53]. In order to determine if this additive process occurs due to curcumin (both the keto and the enol forms) binding on a site different from that used by celecoxib, a series of 500 AutoDock Vina docking runs were performed on the protein isolated from the complex COX-2-celecoxib (PDB: 3LN1), and the results are presented in Figure 5. Celecoxib docks onto COX-2 (PDB: 3LN1) on two different sites (Figure 3.5A). As expected, the most favorable was the active site of COX-2 (binding frequency, bf, 96.8%) (Figure 3.5B), as found in the crystal structure of the celecoxib:COX-2 complex (PDB: 3LN1). An additional site (bf, 3.2%) was detected by the docking simulations, but it is less energetically favorable (-8.8 kcal/mol vs. -11.2 kcal/mol). On the other hand, in addition to the active site (celecoxib site), curcumin in the keto form prefers two additional (allosteric) sites on COX-2 (Figure 3.5C) with binding frequencies of 38.6% and 38.2% (Figure 3.5D).

A different trend is observed for the enol form of curcumin. This form does not dock on the active site at all when the whole protein (3LN1) is used as docking surface (Figure 3.5E), and it docks mainly to site 2 (bf, 94.12%), and in a minor grade to site 3 (bf, 5.88%) (Figure 3.5F); however these interactions are less favorable than those detected for the keto form.

It is important to keep in mind that results from docking the keto and enol forms of curcumin on the whole protein surface (3LN1) are different from those acquired when the enol form is docked directly into the active site of 1CX2, 1PXX and 1CVU. In these last cases, the absolute binding affinities were greater by approximately 1-2 kcal/mol. The docking of the keto form of curcumin onto the active site of COX-2 generates not only different affinity values depending on the site, but also distinct spatial orientations. These last changes could require additional docking energy and this could be a reason explaining why this curcumin form prefers the other binding sites, where the docking implies less inner molecular consumption.

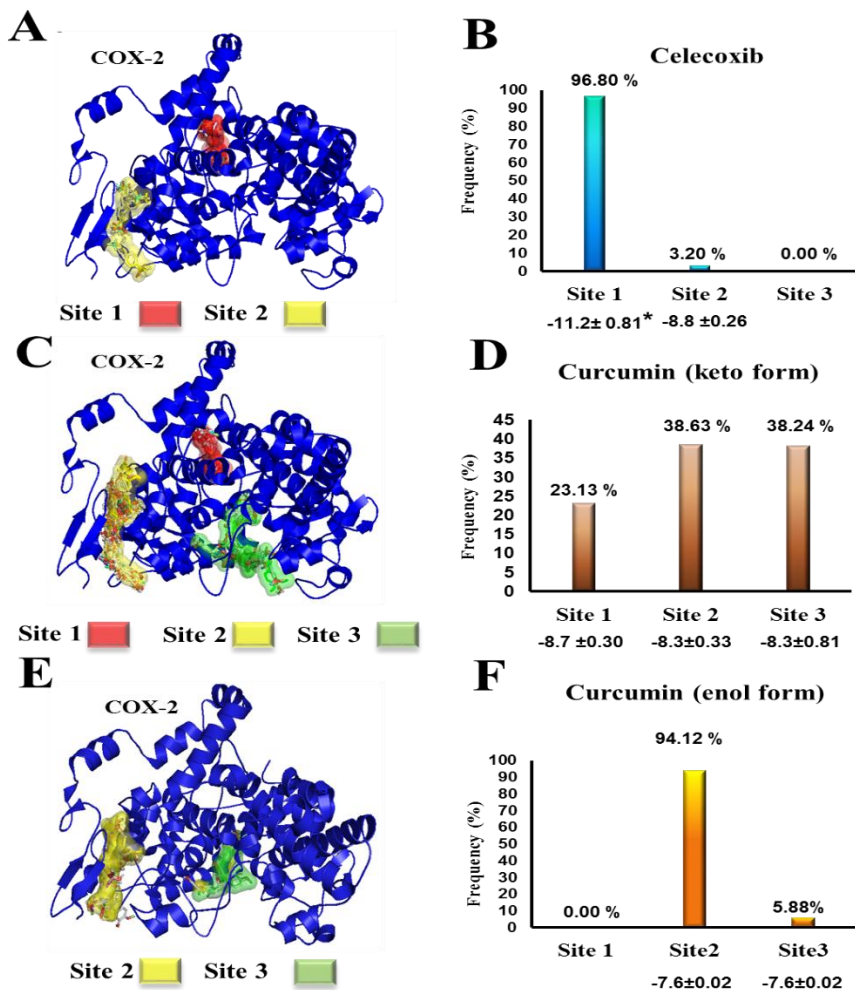


Figure 3.5. Celecoxib (A) and curcumin (keto, C; enol E) binding sites on COX-2, and ligand binding site preferences for each one of them (B, D, and F, respectively). *The affinity values (mean \pm standard deviation, $n = 500$) in kcal/mol obtained for each protein–ligand complex are shown in below site.

Docking runs ($n=100$) for celecoxib and the two curcumin forms, performed using the three docking tools examined in this work, on the three binding sites predicted for curcumin (keto form, PubChem) using AutoDock Vina are shown in Table 3.4. Results showed that AutoDock Vina, GOLD and Surflex-Dock predicted that celecoxib prefers only the known inhibitor binding site (Site 1). In the case of

curcumin, all three docking tools suggested that both forms of this natural product can at some point interact with any of the three binding sites. However, there are minor changes in the preferences based on the curcumin form and the docking tool used. Taken together, these results suggest that independent from the tautomeric state of curcumin, it has the ability to interact with COX-2 on a binding site different from celecoxib.

Table 3.4. Binding affinity (AutoDock Vina) and binding score values (GOLD and Surflex-Dock) for curcumin (keto and enol forms) and celecoxib (inhibitor) on different predicted binding sites (1, 2, and 3) on COX-2.

Compound	Site 1			Site 2		
	AV (kcal/mol)	G Fitness	S Total Score	AV (kcal/mol)	G Fitness	S Total Score
Celecoxib	-11.9	68.54	9.50	-9.0	61.04	6.05
Curcumin (keto)	-8.4	56.51	6.71	-8.8	52.58	7.24
Curcumin (enol)	-8.6	48.39	7.40	-8.7	51.97	9.58

Compound	Site 3		
	AV (kcal/mol)	G Fitness	S Total Score
Celecoxib	-7.2	60.87	4.53
Curcumin (keto)	-8.0	52.64	8.75
Curcumin (enol)	-8.3	51.52	7.40

AV. AutoDock Vina; G. GOLD; S. Surflex-Dock (SYBYL).

This *in silico* evaluation of curcumin binding on COX-2 offers a plausible explanation for the synergism observed for celecoxib and curcumin to inhibit the action of the enzyme. It also showed that the size of the used docking grid can have profound differences in the results. However, it was clear that for both keto and enol forms, a binding site different from the active site is preferred by curcumin, although this process is less energetically favorable.

Although the mechanisms involved in the anti-inflammatory action of chemicals present in edible plants may comprise distinct pathways, some of the compounds examined here are known for their actions on the regulation of transcription factors such as nuclear factor-kappa B (NF κ B) [88,89], signal transducers and activation of transcription-1 (STAT-1) [90], peroxisome proliferator-activated receptor gamma (PPAR γ) [91], NF-E2-related factor-2 (Nrf2) [92], and also in the inhibition of mitogen-activated protein kinase (MAPK) (ERK, JNK, and p38) phosphorylation [93],

among many other targets. These mechanisms may indeed alter the expression of COX-2. However, as shown here, it may be equally important to consider their direct action at the protein level, in order to have a better knowledge of their pharmacological benefits. In addition, it is clear that computational chemistry is a powerful tool that speeds up and lowers the cost of those approaches leading to find therapeutic agents to promote human health.

3.5. CONCLUSIONS

In silico docking calculations performed with AutoDock Vina showed that binding affinities obtained for some natural compounds on COX-2, such as curcumin and all-*trans* retinoic acid, are of similar magnitude than those generated for known inhibitors of this protein. Affinities from AutoDockVina and scores given by the docking software GOLD showed significant correlations with experimental data for COX-2 inhibition. Docking studies performed with curcumin and celecoxib, this last a synthetic inhibitor of COX-2, suggest that curcumin may be able to bind this protein both competitively and allosterically. Therefore, natural products present in the diet are important not only as transcriptional regulators of COX-2, but also they may modulate its enzyme activity to control inflammatory processes.

3.6. REFERENCES

- [1] Kitts, D.D. Bioactive substances in food: identification and potential uses. *Can J Physiol Pharmacol.* 1994, 72, 423-424.
- [2] Pan, M.H., Lai, C.S., Dushenkov, S., Ho, C.T. Modulation of inflammatory genes by natural dietary bioactive compounds. *J Agric Food Chem.* 2009, 57, 4467-447.
- [3] Bohlin, L., Göransson, U., Alsmark, C., Wedén, C., Backlund, A. Natural products in modern life science. *Phytochem Rev.* 2010, 9, 279-301.
- [4] Shen, C.L., Yeh, J.K., Cao, J., Wang, J.S. Green tea and bone metabolism. *Nutr Res.* 2009, 29, 437-456.
- [5] Chakraborti, A.K., Garg, S.K., Kumar, R., Motiwala, H.F., Jadhavar, P.S. Progress in COX-2 inhibitors: a journey so far. *Curr Med Chem.* 2010, 17, 1563-1593.
- [6] Kiefer, J.R., Pawlitz, J.L., Moreland, K.T., Stegeman, R.A., Hood, W.F., Gierse, J.K., Stevens, A.M., Goodwin, D.C., Rowlinson, S.W., Marnett, L.J., Stallings, W.C., Kurumbail, R.G. Structural insights into the stereochemistry of the cyclooxygenase reaction. *Nature* 2000, 405, 97-101.
- [7] Wilken, R., Veena, M.S., Wang, M.B., Srivatsan, E.S. Curcumin: a review of anti-cancer properties and therapeutic activity in head & neck squamous cell carcinoma. *Mol Cancer* 2011, 10, 12.
- [8] Frasca, G., Panico, A.M., Bonina, F., Messina, R., Rizza, L., Musumeci, G., Rapisarda, P., Cardile, V. Involvement of inducible nitric oxide synthase and cyclooxygenase-2 in the anti-inflammatory effects of a red orange extract in human chondrocytes. *Nat Prod Res.* 2010, 24, 1469-1480.

- [9] Jin, M., Suh, S.J., Yang, J.H., Lu, Y., Kim, S.J., Kwon, S., Jo, T.H., Kim, J.W., Park, Y.I., Ahn, G.W., Lee, C.K., Kim, C.H., Son, J.K., Son, K.H., Chang, H.W. Anti-inflammatory activity of bark of *Dioscorea batatas* DECNE through the inhibition of iNOS and COX-2 expressions in RAW264.7 cells via NF- κ B and ERK1/2 inactivation. *Food Chem Toxicol.* 2010, 48, 3073-3079.
- [10] May, A., Zacharias, M. Accounting for global protein deformability during protein-protein and protein-ligand docking. *BBA- Proteins Proteom* 2005, 1754, 225-231.
- [11] Trott, O., Olson, A.J. AutoDock Vina: improving the speed and accuracy of docking with a new scoring function, efficient optimization and multithreading. *J Comput Chem.* 2009, 31, 455-461.
- [12] Verdonk, M.L., Cole, J.C., Hartshorn, M.J., Murray, C.W., Taylor, R.D. Improved protein-ligand docking using GOLD. *Proteins: Struct Funct Gen.* 2003, 52, 609-623.
- [13] Jain, A.N., Surflex-Dock 2.1: Robust performance from ligand energetic modeling, ring flexibility, and knowledge-based search. *J Comput Aided Mol Des.* 2007, 21, 281-306.
- [14] Tang, Y., Zhu, W., Chen, K., Jiang, H. New technologies in computer-aided drug design: Toward target identification and new chemical entity discovery. *Drug Discov Today Tech.* 2006, 3, 307-313.
- [15] Utsintong, M., Talley, T.T., Taylor, P.W., Olson, A.J., Vajragupta, O. Virtual screening against alpha-cobratoxin. *J Biomol Screen.* 2009, 14, 1109-1118.
- [16] RCSB PDB Protein Data Bank | Home www.pdb.org/pdb/home/home.do.
- [17] SYBYL molecular modeling software, Version 8.1. 2007,. Tripos, St. Louis, MO, U.S.A.
- [18] Frisch, M., Trucks, G., Schlegel, H., Scuseria, G., Robb, M., Cheeseman, J., et al. Gaussian 03, revision B. 05; Gaussian. Inc., Pittsburgh, PA. 2003, 12478.
- [19] Guha, R., Howard, M.T., Hutchison, G.R., Murray-Rust, P., Rzepa, H., Steinbeck, C., Wegner, J.K., Willighagen, E. The blue obelisk -- interoperability in chemical informatics. *J Chem Inf Model.* 2006, 46, 991-998.
- [20] Yao, Y., Sang, W., Zhou, M., Ren, G. Phenolic composition and antioxidant activities of 11 celery cultivars. *J Food Sci.* 2010, 75, 9-13.
- [21] Stuetz, W., Prapamontol, T., Hongsibsong, S., Biesalski, H.K. Polymethoxylated flavones, flavanone glycosides, carotenoids, and antioxidants in different cultivation types of tangerines (*Citrus reticulata* Blanco cv. Sainampueng) from Northern Thailand. *J Agric Food Chem.* 2010, 58, 6069-6074.
- [22] Abenavoli, L., Capasso, R., Milic, N., Capasso, F. Milk thistle in liver diseases: past, present, future. *Phytother Res.* 2010, 24, 1423-1432.
- [23] Sarić, A., Sobocanec, S., Balog, T., Kusić, B., Sverko, V., Dragović-Uzelac, V., Levaj, B., Cosić, Z., Safranko, Z.M., Marotti, T. Improved antioxidant and anti-inflammatory potential in mice consuming sour cherry juice (*Prunus cerasus* cv. Maraska). *Plant Foods Hum Nutr.* 2009, 64, 231-237.
- [24] Castellarin, S.D., Di Gaspero, G. Transcriptional control of anthocyanin biosynthetic genes in extreme phenotypes for berry pigmentation of naturally occurring grapevines. *BMC Plant Biol.* 2007, 30, 7-46.

[25] Basini, G., Bussolati, S., Santini, S.E., Grasselli, F. The impact of the phyto-oestrogen genistein on swine granulosa cell function. *J Anim Physiol Anim Nutr (Berl)*. 2010, 94, 374-382.

[26] Wang, P., Aronson, W.J., Huang, M., Zhang, Y., Lee, R.P., Heber, D., Henning, S.M. Green tea polyphenols and metabolites in prostatectomy tissue: Implications for Cancer prevention. *Cancer Prev Res*. 2010, 3, 985-993.

[27] Lien, L.T., Yeh, H.S., Su, W.T. Effect of adding extracted hesperetin, naringenin and pectin on egg cholesterol, serum traits and antioxidant activity in laying hens. *Arch Anim Nutr*. 2008, 62, 33-43.

[28] Vasanthi, H.R., Mukherjee, S., Das, D.K. Potential health benefits of broccoli- a chemico-biological overview. *Mini Rev Med Chem*. 2009, 9, 749-759.

[29] Lai, C.S., Li, S., Chai, C.Y., Lo, C.Y., Ho, C.T., Wang, Y.J., Pan, M.H. Inhibitory effect of citrus 5-hydroxy-3,6,7,8,3',4'-hexamethoxyflavone on 12-O-tetradecanoylphorbol 13-acetate-induced skin inflammation and tumor promotion in mice. *Carcinogenesis* 2007, 28, 2581-2588.

[30] Kaura, S., Modib, N.H., Pandac, D., Roya, N. Probing the binding site of curcumin in *Escherichia coli* and *Bacillus subtilis* FtsZ - A structural insight to unveil antibacterial activity of curcumin. *Eur J Med Chem*. 2010, 45, 4209-4214.

[31] Rasyid, A., Rahman, A.R., Jaalam, K., Lelo, A. Effect of different curcumin dosages on human gall bladder. *Asia Pac J Clin Nutr*. 2002, 11, 314-318.

[32] Kalantari, H., Das, D.K. Physiological effects of resveratrol. *Biofactors*. 2010, 36, 401-406.

[33] Weng, C.J., Wu, C.F., Huang, H.W., Ho, C.T., Yen, G.C. Anti-invasion effects of 6-shogaol and 6-gingerol, two active components in ginger, on human hepatocarcinoma cells. *Mol Nutr Food Res*. 2010, 54, 1618-1627.

[34] Bernardes, W.A., Lucarini, R., Tozatti, M.G., Souza, M.G., Andrade Silva, M.L., da Silva Filho, A.A., Martins, C.H., Miller Crotti, A.E., Pauletti, P.M., Groppo, M., Cunha, W.R. Antimicrobial activity of *Rosmarinus officinalis* against oral pathogens: relevance of carnosic acid and carnosol. *Chem Biodivers*. 2010, 7, 1835-1840.

[35] Alosi, J.A., McDonald, D.E., Schneider, J.S., Privette, A.R., McFadden, D.W. Pterostilbene inhibits breast cancer in vitro through mitochondrial depolarization and induction of caspase-dependent apoptosis. *J Surg Res*. 2010, 161, 195-201.

[36] Visanji, J.M., Duthie, S.J., Pirie, L., Thompson, D.G., Padfield, P.J. Dietary isothiocyanates inhibit Caco-2 cell proliferation and induce G2/M phase cell cycle arrest, DNA damage, and G2/M checkpoint activation. *J Nutr*. 2004, 134, 3121-3126.

[37] Skupinska, K., Misiewicz-Krzeminska, I., Lubelska, K., Kasprzycka-Guttman, T. The effect of isothiocyanates on CYP1A1 and CYP1A2 activities induced by polycyclic aromatic hydrocarbons in MCF7 cells. *Toxicol In Vitro*. 2009, 23, 763-771.

[38] Déziel, B.A., Patel, K., Neto, C., Gottschall-Pass, K., Hurta, R.A. Proanthocyanidins from the american cranberry (*Vaccinium macrocarpon*), inhibit matrix metalloproteinase-2 and matrix metalloproteinase-9 activity in human prostate cancer cells via alterations in multiple cellular signaling pathways. *J Cell Biochem*. 2010, 111, 742-754.

- [39] Theodosiou, M., Laudet, V., Schubert, M. From carrot to clinic: an overview of the retinoic acid signaling pathway, *Cell. Mol. Life Sci.* 67, 2010, 1423-1445.
- [40] G.L. Ambrosini, N.H. de Klerk, L. Fritschi, D. Mackerras, B. Musk, Fruit, vegetable, vitamin A intakes, and prostate cancer risk, *Prostate Cancer Prostatic Dis.* 2008, 11, 61-66.
- [41] Muhammad, S.A., Muhammad, S., Waqar, A., Masood, P., Raghav, Y. Chlorinated monoterpene ketone, acylated β -sitosterol glycosides and a flavanone glycoside from *Mentha longifolia* (Lamiaceae). *Phytochemistry* 2002, 59, 889-895.
- [42] Vogel, J.T., Tieman, D.M., Sims, C.A., Odabasi, A.Z., Clark, D.G., Klee, H.J. Carotenoid content impacts flavor acceptability in tomato (*Solanum lycopersicum*). *J Sci Food Agric.* 2010, 90, 2233-2340.
- [43] Thürmann, P.A., Steffen, J., Zwernemann, C., Aebischer, C.P., Cohn, W., Wendt, G., Schalch, W. Plasma concentration response to drinks containing beta-carotene as carrot juice or formulated as a water dispersible powder. *Eur J Nutr.* 2002, 41, 228-235.
- [44] Burns-Whitmore, B.L., Haddad, E.H., Sabaté, J., Jaceldo-Siegl, K., Tanzman, J., Rajaram, S. Effect of n-3 fatty acid enriched eggs and organic eggs on serum lutein in free-living lacto-ovo vegetarians. *Eur J Clin Nutr.* 2010, 64, 1332-1337.
- [45] Mills, J.D., Bailes, J.E., Sedney, C.L., Hutchins, H., Sears, B. Omega-3 fatty acid supplementation and reduction of traumatic axonal injury in a rodent head injury model. *J Neurosurg.* 2010, 114, 77-84.
- [46] Mann, N.J., O'Connell, S.L., Baldwin, K.M., Singh, I., Meyer, B.J. Effects of seal oil and tuna-fish oil on platelet parameters and plasma lipid levels in healthy subjects. *Lipids* 2010, 45, 669-681.
- [47] Wolber, G., Langer, T. LigandScout: 3-D pharmacophores derived from protein-bound ligands and their use as virtual screening filters. *J Chem Inf Model.* 2005, 45, 160-169.
- [48] PubChem. <http://pubchem.ncbi.nlm.nih.gov>.
- [49] Filizola, M., Perez, J.J., Palomer, A., Mauleón, D. Comparative molecular modeling study of the three-dimensional structures of prostaglandin endoperoxide H2 synthase 1 and 2 (COX-1 and COX-2). *J Mol Graph Model.* 1997, 15, 290-300.
- [50] Dewitt, D.L. Cox-2-selective inhibitors: The new super aspirins. *Mol Pharm* 1999, 55, 625-631.
- [51] Zhou, Z., Wang, Y., Bryant, S.H. Computational analysis of the cathepsin B inhibitors activities through LR-MMPBSA binding affinity calculation based on docked complex. *J Comput Chem.* 2009, 30, 2165-2175.
- [52] Lev-Ari, S., Strier, L., Kazanov, D., Madar-Shapiro, L., Dvory-Sobol, H., Pinchuk, I., Marian, B., Lichtenberg, D., Arber, N. Celecoxib and curcumin synergistically inhibit the growth of colorectal cancer cells. *Clin Cancer Res.* 2005, 11, 6738-6744.
- [53] Lev-Ari, S., Strier, L., Kazanov, D., Elkayam, O., Lichtenberg, D., Caspi, D., Arber, N. Curcumin synergistically potentiates the growth-inhibitory and pro-apoptotic effects of celecoxib in osteoarthritis synovial adherent cells. *Rheumatology* 2006, 45, 171-177.
- [54] Selvam, C., Jachak, S.M., Thilagavathi, R., Chakraborti, A.K. Design, synthesis, biological evaluation and molecular docking of curcumin analogues as antioxidant, cyclooxygenase inhibitory and anti-inflammatory agents. *Bioorg Med Chem Lett.* 2005, 15, 1793-1797.

[55] Furse, K.E., Pratt, D.A., Porter, N.A., Lybrand, T.P. Molecular dynamics simulations of arachidonic acid complexes with COX-1 and COX-2: insights into equilibrium behavior. *Biochemistry* 2006, 45, 3189-3205.

[56] Wu, S.J., Tam, K.W., Tsai, Y.H., Chang, C.C., Chao, J.C. Curcumin and saikosaponin A inhibit chemical-induced liver inflammation and fibrosis in rats. *Am J Chin Med.* 2010, 38, 99-111.

[57] Sikora, E., Scapagnini, G., Barbagallo, M. Curcumin, inflammation, ageing and age-related diseases. *Immun Ageing.* 2010, 7, 1.

[58] Moghaddam, S.J., Barta, P., Mirabolfathinejad, S.G., Ammar-Aouchiche, Z., Garza, N.T., Vo, T.T., Newman, R.A., Aggarwal, B.B., Evans, C.M., Tuvim, M.J., Lotan, R., Dickey, B.F. Curcumin inhibits COPD-like airway inflammation and lung cancer progression in mice. *Carcinogenesis* 2009, 30, 1949-1956.

[59] Jurenka, J.S. Anti-inflammatory properties of curcumin, a major constituent of *Curcuma longa*: a review of preclinical and clinical research. *Altern Med Rev.* 2009, 14, 141-153.

[60] Galati, G., Sabzevari, O., Wilson, J.X., O'Brien, P.J. Prooxidant activity and cellular effects of the phenoxy radicals of dietary flavonoids and other polyphenolics. *Toxicology* 2002, 177, 91-104.

[61] Akihisa, T., Yasukawa, K., Yamaura, M., Ukiya, M., Kimura, Y., Shimizu, N., Koichi, A. Triterpene alcohol and sterol ferulates from rice bran and their anti-inflammatory effects. *J Agric Food Chem.* 2000, 48, 2313-2319.

[62] Leelawat, K., Ohuchida, K., Mizumoto, K., Mahidol, C., Tanaka, M. All-trans retinoic acid inhibits the cell proliferation but enhances the cell invasion through up-regulation of c-met in pancreatic cancer cells. *Cancer Lett.* 2005, 224, 303-310.

[63] Li, R.R., Pang, L.L., Du, Q., Shi, Y., Dai, W.J., Yin, K.S. Apigenin inhibits allergen-induced airway inflammation and switches immune response in a murine model of asthma. *Immunopharmacol Immunotoxicol.* 2010, 32, 364-370.

[64] Vela, E.M., Knostman, K.A., Mott, J.M., Warren, R.L., Garver, J.N., Vela, L.J., Stammen, R.L. Genistein, a general kinase inhibitor, as a potential antiviral for arenaviral hemorrhagic fever as described in the Pirital virus-Syrian golden hamster model. *Antiviral Res.* 2010, 87, 318-328.

[65] Watkins, B.A., Hannon, K., Ferruzzi, M., Li, Y. Dietary PUFA and flavonoids as deterrents for environmental pollutants. *J Nutr Biochem.* 2007, 18, 196-205.

[66] Calderone, V., Chericoni, S., Martinelli, C., Testai, L., Nardi, A., Morelli, I., Breschi, M.C., Martinotti, E. Vasorelaxing effects of flavonoids: investigation on the possible involvement of potassium channels, Naunyn Schmiedebergs. *Arch Pharmacol.* 2004, 370, 290-298.

[67] Lee, K.M., Lee, K.W., Jung, S.K., Lee, E.J., Heo, Y.S., Bode, A.M., Lubet, R.A., Lee, H.J., Dong, Z. Kaempferol inhibits UVB-induced COX-2 expression by suppressing Src kinase activity. *Biochem Pharmacol.* 2010, 80, 2042-2049.

[68] Massaro, M., Habib, A., Lubrano, L., Del Turco, S., Lazzerini, G., Bourcier, T., Weksler, B.B., De Caterina, R. The omega-3 fatty acid docosahexaenoate attenuates

endothelial cyclooxygenase-2 induction through both NADP[H] oxidase and PKC ϵ inhibition. *Proc Natl Acad Sci.* 2006,103, 15184-15189.

[69] Hare, A.A., Leng, L., Gandavadi, S., Du, X., Cournia, Z., Bucala, R., Jorgensen, W.L. Optimization of N-benzyl-benzoxazol-2-ones as receptor antagonists of macrophage migration inhibitory factor (MIF). *Bioorg Med Chem Lett.* 2010, 20, 5811-5814.

[70] Gonzales, A.M., Orlando, R.A. Curcumin and resveratrol inhibit nuclear factor- κ B-mediated cytokine expression in adipocytes. *Nutr Metab.* 2008, 5, 17.

[71] Lev-Ari, S., Maimon, Y., Strier, L., Kazanov, D., Arber, N. Down-regulation of prostaglandin E2 by curcumin is correlated with inhibition of cell growth and induction of apoptosis in human colon carcinoma cell lines. *J Soc Integr Oncol.* 2006, 4, 21-26.

[72] B. Du, L. Jiang, Q. Xia, L. Zhong, Synergistic Inhibitory effects of curcumin and 5-fluorouracil on the growth of the human colon cancer cell Line HT-29. *Chemotherapy* 2006, 52, 23-28.

[73] Lev-Ari, S., Starr, A., Vexler, A., Karaush, V., Loew, V., Greif, J., Fenig, E., Aderka, D., Ben-Yosef, R. Inhibition of pancreatic and lung adenocarcinoma cell survival by curcumin is associated with increased apoptosis, down-regulation of COX-2 and EGFR and inhibition of Erk1/2 activity. *Anticancer Res.* 2006, 26, 4423-4430.

[74] Gafner, S., Lee, S.K., Cuendet, M., Barthél my, S., Vergnes, L., Labidalle, S., Mehta, R.G., Boone, C.W., Pezzuto, J.M. Biologic evaluation of curcumin and structural derivatives in cancer chemoprevention model systems. *Phytochemistry.* 2004, 65 2849-2859.

[75] J. Hong, M. Bose, J. Ju, J.H. Ryu, X. Chen, S. Sang, M.J. Lee, C.S. Yang, Modulation of arachidonic acid metabolism by curcumin and related β -diketone derivatives: effects on cytosolic phospholipase A2, cyclooxygenases and 5-lipoxygenase. *Carcinogenesis* 2004, 25, 1671-1679.

[76] Kim, B.H., Kang, K.S., Lee, Y.S. Effect of retinoids on LPS-induced COX-2 expression and COX-2 associated PGE2 release from mouse peritoneal macrophages and TNF- α release from rat peripheral blood mononuclear cells. *Toxicol Lett.* 2004, 150, 191-201.

[77] Liang, Y.C., Huang, Y.T., Tsai, S.H., Lin-Shiau, S.Y., Chen, C.F., Lin, J.K. Suppression of inducible cyclooxygenase and inducible nitric oxide synthase by apigenin and related flavonoids in mouse macrophages. *Carcinogenesis* 1999, 20 1945-1952.

[78] Dia, V.P., Berhow, M.A., Gonzalez de mejia, E. Bowman-birk inhibitor and genistein among soy compounds that synergistically inhibit nitric oxide and prostaglandin E2 pathways in lipopolysaccharide-induced macrophages. *J Agric Food Chem.* 2008, 56, 11707-11717.

[79] F. Ye, J. Wu, T. Dunn, J. Yi, X. Tong, D. Zhang. Inhibition of cyclooxygenase-2 activity in head and neck cancer cells by genistein. *Cancer Lett.* 2004, 211, 39-46.

[80] Liang, Y.C., Tsai, S.H., Tsai, D.C., Lin-Shiau, S.Y., Lin, J.K. Suppression of inducible cyclooxygenase and nitric oxide synthase through activation of peroxisome proliferator-activated receptor-Q by flavonoids in mouse macrophages. *FEBS Lett.* 2001, 496, 12-18.

[81] Wang, H., Nair, M.G., Strasburg, G.M., Chang, Y.C., Booren, A.M., Gray, J.I., DeWitt, D.L. Antioxidant and antiinflammatory activities of anthocyanins and their aglycon, cyanidin, from tart cherries. *J. Nat Prod.* 1999, 62, 294-296.

[82] Seeram, N.P., Zhang, Y., Nair, M.G. Inhibition of proliferation of human cancer cells and cyclooxygenase enzymes by anthocyanidins and catechins. *Nutr. Cancer*. 2003, 46 101-106.

[83] Ringbom, T., Huss, U. Å. Stenholm, S. Flock, L. Skattebøl, P. Perera, L. Bohlin. COX-2 inhibitory effects of naturally occurring and modified fatty acids. *J Nat Prod* 2001, 64, 745-749.

[84] Calviello, G., Di Nicuolo, F., Gragnoli, S., Piccioni, E., Serini, S., Maggiano, N., Tringali, G., Navarra, P., Ranelletti, F.O., Palozza, P. n-3 PUFAs reduce VEGF expression in human colon cancer cells modulating the COX-2/PGE2 induced ERK-1 and -2 and HIF-1 α induction pathway. *Carcinogenesis*. 2004, 25, 2303-2310.

[85] Takano-Ishikawaa, Y., Gotoa, M., Yamakia, K. Structure–activity relations of inhibitory effects of various flavonoids on lipopolysaccharide-induced prostaglandin E2 production in rat peritoneal macrophages: comparison between subclasses of flavonoids. *Phytomedicine* 2006, 13, 310-317.

[86] Tjendraputra, E., Tran, V.H., Biu-Brennan, D., Roufogalis B.D., Duke, C.C. Effect of ginger constituents and synthetic analogues on cyclooxygenase-2 enzyme in intact cells. *Bioorg Chem*. 2001, 29, 156-163.

[87] Cao, H., Yu, R., Tao, Y., Nikolic, D., van Breemen, R.B. Measurement of cyclooxygenase inhibition using liquid chromatography–tandem mass spectrometry, *J Pharm Biomed Anal*. 2011, 54, 230-235.

[88] Y.J. Surh, K.S. Chun, H.H. Cha, S.S. Han, Y.S. Keum, K.K. Park, S.S. Lee, Molecular mechanisms underlying chemopreventive activities of anti-inflammatory phytochemicals: down-regulation of COX-2 and iNOS through suppression of NF- κ B activation. *Mutat Res*. 2001, 480, 243-268.

[89] Kole, L., Giri, B., Manna, S.K., Pal, B., Ghosh, S. Biochanin-A, an isoflavon, showed anti-proliferative and anti-inflammatory activities through the inhibition of iNOS expression, p38-MAPK and ATF-2 phosphorylation and blocking NF- κ B nuclear translocation. *Eur J Pharmacol*. 2011, 653, 8-15.

[90] Chung, E.Y., Kim, B.H., Hong, J.T., Lee, C.K., Ahn, B., Nam, S.Y., Han, S.B., Kim, Y. Resveratrol down-regulates interferon- γ -inducible inflammatory genes in macrophages: molecular mechanism via decreased STAT-1 activation, *J Nutr Biochem*. 2011, 22, 902-909.

[91] Wang, H.M., Zhao, Y.X., Zhang, S., Liu, G.D., Kang, W.Y., Tang, H.D., Ding, J.Q., Chen, S.D. PPAR γ agonist curcumin reduces the amyloid-beta-stimulated inflammatory responses in primary astrocytes, *J Alzheimers Dis*. 2010, 20 1189-1199.

[92] Garg, R., Gupta, S., Maru, G.B. Dietary curcumin modulates transcriptional regulators of phase I and phase II enzymes in benzo[a]pyrene-treated mice: mechanism of its anti-initiating action, *Carcinogenesis* 2008, 29, 1022-1032.

[93] Ahn, J., Lee, H., Kim, S., Ha, T. Curcumin-induced suppression of adipogenic differentiation is accompanied by activation of Wnt/beta-catenin signaling, *Am. J. Physiol. Cell Physiol*. 2010, 298, 1510-1516.

Chapter 4



CHAPTER 4. FOOD-RELATED COMPOUNDS THAT MODULATE EXPRESSION OF INDUCIBLE NITRIC OXIDE SYNTHASE MAY ACT AS ITS INHIBITORS

4.1. ABSTRACT

Natural compounds commonly found in foods may contribute to protect cells against the deleterious effects of inflammation. These anti-inflammatory properties have been linked to the modulation of transcription factors that control expression of inflammation-related genes, including the inducible nitric oxide synthase (iNOS), rather than a direct inhibitory action on these proteins. In this study, forty two natural dietary compounds, known for their ability to exert an inhibitory effect on the expression of iNOS, have been studied *in silico* as docking ligands on two available 3D structures for this protein (PDB ID: 3E7G and PDB ID: 1NSI). Natural compounds such as silibinin and cyanidin-3-rutinoside and other flavonoids showed the highest theoretical affinities for iNOS. Docking affinity values calculated for several known iNOS inhibitors significantly correlated with their reported half maximal inhibitory concentrations ($R = 0.842$, $P < 0.0001$), suggesting the computational reliability of the predictions made by our docking simulations. Moreover, docking affinity values for potent iNOS inhibitors are of similar magnitude to those obtained for some studied natural products. Results presented here indicate that, in addition to gene expression modulation of proteins involved in inflammation, some chemicals present in food may be acting by direct binding and possible inhibiting actions on iNOS.

4.2. INTRODUCTION

The intake of natural dietary bioactive compounds is associated with low incidence of many diseases. The beneficial biological effects of these chemicals present in fruits and plant-derived-foods may be due to two of their known properties: their affinity for certain proteins and their antioxidant activity. Numerous publications have shown that, in addition to their antioxidant capacity, compounds of plant origin may regulate different signaling pathways in some diseases [1-4]. Some of this large list of molecules include isothiocyanates, proanthocyanidins, terpenoids, carotenoids, omega-3, and polyunsaturated fatty acids, among others [2, 5-8].

Among most common food-related compounds of particular importance as anti-inflammatory drugs, flavonoids play a pivotal role. These chemicals are a large and diverse group of plant phenolic that chemically are derivatives of the benzo- γ -pyrone ring, containing phenolic and pyran groups, and presenting conjugation between rings A and B, that differ according to their hydroxyl, methoxy and glycosidic side groups [9]. During metabolism, the free hydroxyl groups may be methylated, sulfated or glucuronidated. In foods, flavonoids can be found as 3-O-glycosides (anthocyanin) and polymers [10]. These natural compounds have received significant interest due to their known biological properties, in particular the prevention of inflammation [11], cancer [12], and cardiovascular diseases [13]. Several of the anti-inflammatory effects of these molecules have been associated with the inhibition of protein expression of key mediators involved in inflammation processes, such as the inducible nitric oxide synthase (iNOS) [14].

NOSs are a family of eukaryotic enzymes that produce nitric oxide (NO) from L-arginine. In mammals there are three isoforms [15]: the endothelial (eNOS) and neuronal (nNOS) isozymes are constitutively expressed [16], and through the production of low levels of NO, they are involved in the regulation of blood pressure and nerve function, respectively. In contrast, iNOS is produced in response to cytokines or pathogens [17]. NOS contains the heme group in its catalytic site, which is important for its enzymatic activity [18].

Several natural products have been presented to modulate iNOS expression [19]. However, for many of them it remains unclear if the process is the result of an interaction with inflammation-related transcription factors or the enzyme itself. Computational chemistry offers powerful tools to explore these mechanisms by using molecular docking. This method is widely utilized in drug development, and this approach generally assumes a rigid receptor structure to allow the binding of a ligand on putative binding sites on the receptor surface [20, 21]. AutoDock Vina has become one of the most frequently used docking software for this purpose. It

combines some advantages of knowledge-based potentials and empirical scoring functions, extracting empirical information from the conformational preferences of the receptor-ligand complex and from experimental affinity measurements. Ligands are ranked based on an energy scoring function and, to speed up the score calculation, a grid-based protein-ligand interaction is employed [22]. In this study, docking methods were used to theoretically evaluate the ability of 42 natural bioactive compounds, known to regulate human iNOS mRNA expression, to bind this protein.

4.3. MATERIALS AND METHODS

4.3.1. Protein Structures and Modeling of Ligands

3D structures of two human iNOS (PDB ID: 3E7G and PDB ID: 1NSI) were downloaded from Protein Data Bank (PDB)[23], prepared and aligned with Sybyl 8.1.1 program [24]. Both models have the same 3D coordinates (sequence identity = 100% and RMSD < 0.459 Å) (Figure 4.1), and minimal differences can be attributed to the resolution quality for each one (PDB ID: 3E7G = 2.20 Å and PDB ID: 1NSI = 2.55 Å).

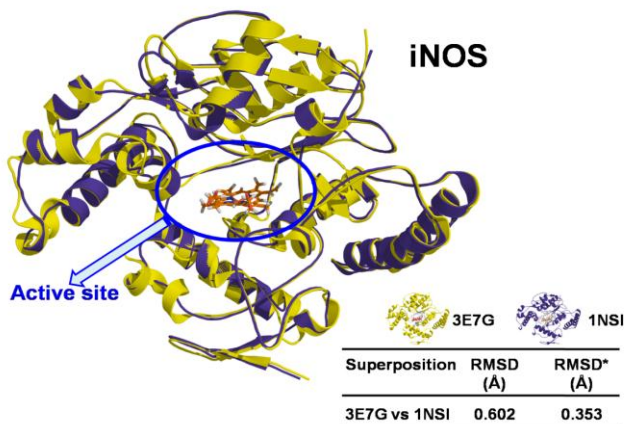


Figure 4.1. Superposition of iNOS structures (3E7G and 1NSI), showing sequence identity and RMSD values. *RMSD for the binding site.

Forty-two anti-inflammatory natural compounds, present in fruits and plant-derived-foods and belonging to different chemical groups (Figure 4.2), were chosen as protein ligands to perform this study, as they have been reported to modulate expression of genes related to inflammation [19, 25]. These compounds comprise distinct chemical families, such as anthocyanins, flavolignans, flavones, and organosulfur compounds, among others. They are considered of special relevance to

food and pharmaceutical industry because of their potential health-promoting effects, and favourable organoleptic properties. The geometries of these bioactive compounds were optimized using DFT at the B3LYP/6-31G level [26], and calculations were carried out with Gaussian 03 package program [27]. Open Babel was used to transform geometries to Mol2 format for their subsequent processing [28].

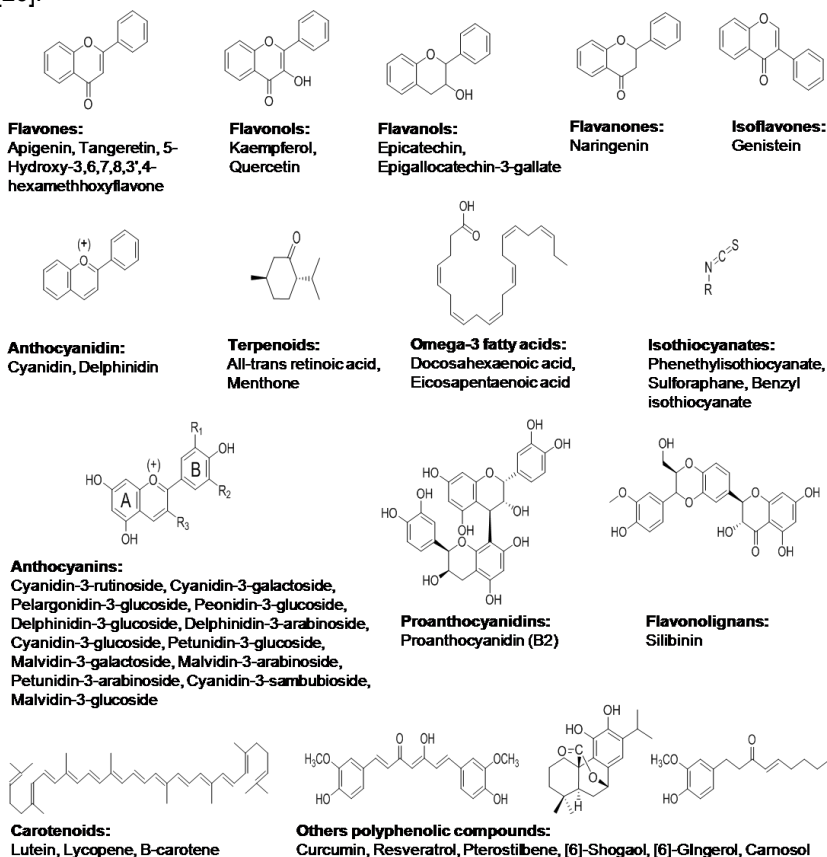


Figure 4.2. Chemical groups for food-related natural compounds used to perform docking studies on iNOS.

4.3.2. Protein-Ligand Docking Simulations

Molecular docking was utilized to evaluate the feasibility of some food-related natural compounds to form complexes with iNOS. MGL tools 1.5.0 [29] was employed to prepare protein structures for molecular docking, and protein-ligand

docking calculations were performed with AutoDock Vina 1.0 program [22], using, as the docking box, the cavity filled by the ligand in the PDB structure (PDB ID: 3E7G and PDB ID: 1NSI). The docking site for the ligands on iNOS structure (PDB ID: 3E7G) was defined by establishing a cube with the dimensions $24 \times 24 \times 24 \text{ \AA}$, covering the ligand binding site with a grid point spacing of 1.0 \AA , and centering grid boxes of 56.030, 20.374 and 79.669 in X, Y and Z dimensions, respectively. The binding site for the other iNOS structure (PDB ID: 1NSI) was defined similarly to PDB ID: 3E7G, except for the location of the centre of grid boxes, that in this case were 11.664, 63.188, and 15.995 in X, Y and Z dimensions, respectively. All calculations with AutoDock Vina included 20 number modes, an energy range of 1.5, and exhaustiveness equal to 20. Ten docking runs were executed per each ligand, saving the best obtained pose. The average affinity for best poses was computed as the affinity value for a given complex. For comparison purposes, these calculations were performed for the iNOS inhibitor AR-C95791, as well as for the natural substrate L-arginine. These molecules were extracted from their 3D complex structures, as those were the ligands bound to PDB ID: 3E7G and PDB ID: 1NSI, respectively.

4.3.3. Residues Interacting with the Natural Bioactive Compounds on iNOS Binding Site and Searching of Alternative Allosteric Binding Sites

The identification of protein residues (PDB ID: 3E7G and PDB ID: 1NSI) that interact on the binding site with those natural bioactive compounds that produced the best AutoDock Vina affinity values, was accomplished using LigandScout 3.0 [30], a package that utilizes pharmacophores to establish ligand-amino acid interactions on the target binding site. Residue-ligand interactions were visualized with PyMol program [31].

In addition, ligands for which docking complexes produced affinity values less than -9.2 kcal/mol were subjected to docking simulations ($n = 100$) over the whole protein surface, in order to identify possible allosteric binding sites. This was done by performing a docking simulation as follows: the binding site for the ligand on iNOS (PDB ID: 3E7G, chain A) was defined by forming a cube with the dimensions $66 \times 66 \times 80 \text{ \AA}$, engulfing the whole protein structure, using a grid point spacing of 1.0 \AA and center grid boxes of 60.398, 20.038 and 83.489, in X, Y and Z dimensions, respectively. The same approach was used for iNOS structure (PDB ID: 1NSI, chain A), but the dimensions of the cube were $66 \times 80 \times 66 \text{ \AA}$, and the center grid boxes were 12.344, 58.446 and 15.573 in X, Y and Z dimensions, respectively. All other docking parameters were the same as previously described.

4.3.4. Docking Validation with Biological Data for iNOS Inhibitors.

To validate the docking procedure, the 3D structures and the biological data of thirty iNOS inhibitors were obtained from PubChem chemical library (<http://pubchem.ncbi.nlm.nih.gov>) [32] and literature [33]. Docking procedures were performed with AutoDock Vina [22], following the same protocols described for natural products. The biological data consisted of the half maximal inhibitory concentration (IC_{50}) for iNOS activity, as reported for different compounds in PubChem BioAssay. Detailed information about the synthesis and purification of these iNOS inhibitors has been reported in the literature [34, 35]. These assays were conducted on A172 cells, and the activity of iNOS was induced by gamma interferon, tumor necrosis factor alpha, and interleukin 1-beta. Concomitant with cytokine addition, appropriate concentrations of compounds were added. The IC_{50} values were calculated from log-logit analysis of the data [34].

Correlation analysis [36] was used to establish relationships between AutoDock Vina-derived affinities of inhibitors on the two tested iNOS (average values) and experimental biological data ($\text{Log}IC_{50}$). Statistical analysis was performed using Graph InStat Software (Version 3.06, 2003).

4.4. RESULTS AND DISCUSSION

4.4.1. Docking Affinities of Natural Dietary Bioactive Compounds with iNOS

AutoDock Vina-calculated affinity scores obtained for natural bioactive products on examined iNOS structures (PDB ID: 3E7G, PDB ID: 1NSI) are presented in Table 4.1. Several molecules showed affinity values at least two units greater than the average obtained for all tested compounds, suggesting those may be efficient ligands for iNOS. The best docking results were observed for cyanidin-3-rutinoside (cyanidin-3-rutinoside) (-9.3 kcal/mol for PDB ID: 3E7G, and -9.5 kcal/mol for PDB ID: 1NSI) and silibinin (-9.5 kcal/mol for PDB ID: 3E7G, and -9.2 kcal/mol for PDB ID: 1NSI). However, other molecules such as the anthocyanin cyanidin-3-sambubioside, malvidin-3-arabinoside, malvidin-3-galactoside, petunidin-3-arabinoside, resveratrol and cyanidin, also presented affinity values less than -8.9 kcal/mol.

Table 4.1. AutoDock Vina-calculated affinities obtained for docking of natural bioactive compounds on iNOS.

Compound	Natural source [References]	3E7G Affinity (kcal/mol) ^a	1NSI Affinity (kcal/mol) ^a
Cyanidin-3-rutinoside	Raspberry, cherries [37, 38]	-9.3 ± 0.0	-9.5 ± 0.0
Silibinin	Milk thistle [39, 40]	-9.5 ± 0.0	-9.2 ± 0.0
Cyanidin-3-sambubioside	Peanut [41]	-9.2 ± 0.0	-8.5 ± 0.0
Malvidin-3-arabinoside	Blueberries [42]	-8.3 ± 0.0	-9.2 ± 0.0
Malvidin-3-galactoside	Berries [43]	-7.9 ± 0.0	-9.1 ± 0.0
Petunidin-3-arabinoside	Bilberry [44]	-8.5 ± 0.0	-9.0 ± 0.0
Resveratrol	Grape skins [45]	-8.9 ± 0.0	-7.5 ± 0.0
Cyanidin	Strawberries [46]	-8.9 ± 0.1	-7.1 ± 0.0
Delphinidin-3-arabinoside	Blueberries [42]	-8.2 ± 0.0	-8.8 ± 0.0
Petunidin-3-glucoside	Blueberries [42]	-8.1 ± 0.0	-8.8 ± 0.0
Peonidin-3-glucoside	Black rice [47]	-8.4 ± 0.0	-8.6 ± 0.0
Malvidin-3-glucoside	Berries [43]	-8.1 ± 0.0	-8.6 ± 0.0
Apigenin	Celery [48]	-8.4 ± 0.0	-7.7 ± 0.0
Carnosol	Rosemary [49]	-8.6 ± 0.0	-7.4 ± 0.0
Delphinidin	Dark berries [50]	-8.6 ± 0.0	-7.0 ± 0.0
Proanthocyanidin	Berries [51]	-8.5 ± 0.0	-8.5 ± 0.0
Epigallocatechin-3-gallate	Green tea [52]	-8.3 ± 0.0	-8.3 ± 0.0
Cyanidin-3-galactoside	Lingonberry [53]	-8.3 ± 0.0	-8.1 ± 0.0
Delphinidin-3-glucoside	Berries [43]	-8.1 ± 0.0	-8.3 ± 0.0
Quercetin	Broccoli [54]	-8.3 ± 0.0	-7.8 ± 0.0
Cyanidin-3-glucoside	Black rice [47]	-8.2 ± 0.0	-8.1 ± 0.0
Pelargonidin-3-glucoside	Strawberries [55]	-8.0 ± 0.0	-8.1 ± 0.0
Curcumin	Curcuma [56]	-8.1 ± 0.1	-7.8 ± 0.1
Kaempferol	Broccoli [54]	-8.1 ± 0.0	-7.7 ± 0.0
5-Hydroxy-3,6,7,8,3',4'-hexamethoxyflavone	Citrus peel [57]	-8.1 ± 0.0	-6.5 ± 0.0
All- <i>trans</i> -retinoic acid	Carrot [58]	-8.0 ± 0.1	-7.8 ± 0.0
Naringenin	Citrus peel [59]	-8.0 ± 0.0	-7.4 ± 0.0
Pterostilbene	Blueberries [60]	-7.9 ± 0.0	-7.3 ± 0.0
Tangeretin	Citrus peel [61]	-7.5 ± 0.0	-7.0 ± 0.0
Genistein	Soybean [62]	-7.5 ± 0.1	-6.9 ± 0.0

Docosahexaenoic acid	Fish and fish oil [63]	-6.4 ± 0.1	-7.5 ± 0.1
Epicatechin	Green tea [52]	-7.3 ± 0.0	-7.3 ± 0.0
[6]-Shogaol	Ginger [64]	-7.2 ± 0.1	-7.2 ± 0.0
[6]-Gingerol	Ginger [64]	-7.1 ± 0.1	-6.9 ± 0.0

Table 4.1. continued

Eicosapentaenoic acid	Fish and fish oil [63]	-6.3 ± 0.1	-7.1 ± 0.1
Phenethylisothiocyanate	Cabbage [65]	-6.1 ± 0.0	-6.1 ± 0.0
Lycopene	Tomato [66]	-6.1 ± 0.2	-4.0 ± 0.2
Benzylisothiocyanate	Cabbage [65]	-6.0 ± 0.0	-5.8 ± 0.0
Menthone	Mentha [67]	-5.8 ± 0.0	-4.7 ± 0.0
Sulforaphane	Cabbage [68]	-4.8 ± 0.0	-4.7 ± 0.0
β-Carotene	Carrot [69]	-4.8 ± 0.1	-0.5 ± 0.4
Lutein	Spinach and eggs [70]	-3.5 ± 0.0	-1.8 ± 0.9
Mean affinity (kcal/mol)		-7.6 ± 0.2	-7.3 ± 0.3
AR-C95791 (Inhibitor-iNOS)		-8.4 ± 0.0	-6.9 ± 0.0
L-Arginine (Substrate- iNOS)		-5.9 ± 0.0	-6.4 ± 0.0

^a. Mean AutoDock Vina affinity value obtained after 10 docking runs per ligand.

Surprisingly, the AutoDock Vina affinity values obtained from docking onto iNOS the ligands AR-C95791 (-8.4 kcal/mol and -6.9 kcal/mol for PDB ID: 3E7G and PDB ID: 1NSI, respectively) and L-arginine (-5.9 kcal/mol and -6.4 kcal/mol for PDB ID: 3E7G and PDB ID: 1NSI, respectively), were similar in magnitude to the average obtained for all 42 tested compounds (PDB ID: 3E7G= -7.6 ± 0.2 kcal/mol and PDB ID: 1NSI= -7.3 ± 0.3 kcal/mol).

4.4.2. iNOS Interacting Residues with Natural Compounds and Search for Allosteric Binding Sites.

The interactions observed in the iNOS (3E7G)/silibinin and iNOS (1NSI)/cyanidin-3-rutinoside complexes, as predicted by LigandScout 3.0, are shown in Figure 4.3. Clearly, the spatial poses acquired by silibinin and cyanidin-3-rutinoside (Figure 3A vs. Figure 4.3C) differ for each protein structure. The most favorable interacting residues with silibinin on 3E7G binding site were Asn354, Thr121, Tyr347 (hydrogen bond donor), Thr121 (hydrogen bond acceptor), Val352 and Arg381 (hydrophobic). Additionally, with respect to heme group, important constituent of the catalytic site of the iNOS, silibinin showed one interacting hydrogen bond (Figure 4.3B). In the case of cyanidin-3-rutinoside, interacting residues on 1NSI binding site were Ala262, Tyr373, Asp385 (hydrogen bond donor), Tyr 373 (hydrogen bond acceptor), Pro350 and Val362 (hydrophobic). The 3E7G/silibinin complex also showed interactions with the heme group, in this case three in total (two hydrogen bond acceptor and one hydrophobic interaction) (Figure 4.3D).

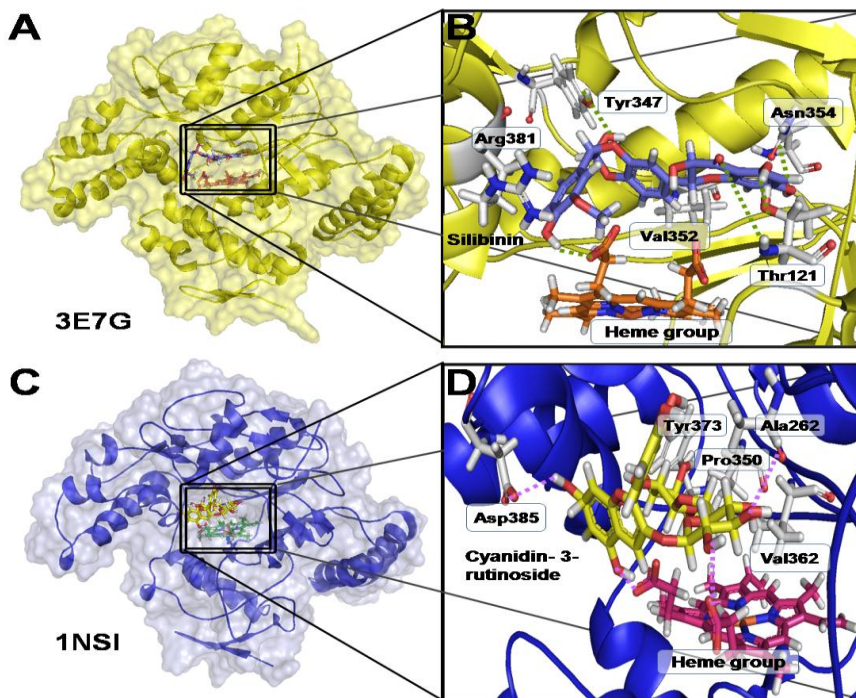


Figure 4.3. 3D view and interacting residues present in the 3E7G/silibinin (A, B) and 1NSI/cyanidin-3-rutinoside (C, D) complexes.

Cyanidin-3-rutinoside and silibinin, molecules with the best absolute affinity values for evaluated iNOS structures, were subsequently submitted to additional docking simulations, using a greater docking box covering the whole protein surface, and a total of 100 runs. This procedure showed that the ligands interacted with the proteins only at the inhibitor/substrate binding site, and no allosteric site was detected.

The complexes formed between silibinin and cyanidin-3-rutinoside with iNOS structures (PDB ID: 3E7G and PDB ID: 1NSI) involved several types of interactions. This observation implies these natural compounds behave as versatile and efficient ligands for iNOS, as they rely on a diversity of functional groups to completely accommodate into the binding site, besides presenting interesting interactions with the heme group in the active site for each one of the examined complexes (3E7G-silibinin and 1NSI/cyanidin-3-rutinoside). It is also important to mention that these compounds, which have high affinity scores (less than -9.2 kcal/mol), interact with

the iNOS only at the substrate-inhibitor binding site, suggesting that their action on this enzyme may be related to competitive inhibition with the substrate.

Results presented here have shown that some food-derived molecules with known capacity of regulating iNOS expression, are good ligands for this pro-inflammatory protein. This finding may in part explain some anti-inflammatory effects attributed to the intake of bioactive natural compounds [71-75]. Cyanidin-3-rutinoside, an anthocyanin present in raspberries and cherries [37, 38], and silibinin, also known as silybin, a widely used flavonolignan from milk thistle [39, 40], were the compounds with greater *in silico* binding affinities for iNOS. The high binding affinity registered for silibinin (-9.5 kcal/mol for PDB ID: 3E7G), and cyanidin-3-rutinoside, may suggest a possible direct iNOS inhibition, in addition to the down regulation of the genes experimentally demonstrated [76]. Silibinin has been associated with down-regulates inducible of nitric oxide synthase in human lung carcinoma [77]. Moreover, cyanidin-3-rutinoside has been reported to regulate the expression of iNOS and cyclooxygenase-2 (COX-2) in cell-based assays [78, 79]. Extracts with high content of pelargonidin-3-glucoside, cyanidins and other anthocyanins, have also been reported as inhibitors of iNOS expression in lung carcinoma cells in mice [80]. Blueberry extracts with significant levels of anthocyanins, such as malvidin, petunidin, and peonidin, compounds that are similar to some evaluated here, have been reported to possess the ability to attenuate the expression and activity of iNOS and COX-2 proteins [81]. In the case of iNOS, the inhibitory effects of these extracts on enzyme activity have been evaluated reaching an IC₅₀ value of 36 µg/mL [82].

It is important to mention that in addition to the natural compounds present in foods that were evaluated in this study [120], there are many other naturally occurring chemicals, such as mangiferin, rogersinol, and withaferin, among others, that have the ability to reduce NO production by attenuating the expression of iNOS [83-85].

4.4.3. Docking Validation with Biological Data

It should be pointed out that results from docking analysis only provide theoretical insight about plausible mechanisms involved in the anti-inflammatory properties of these compounds. In order to explore if affinity values calculated by AutoDock Vina may be used as a measure of the likeliness of a particular compound to behave as an iNOS inhibitor, a group of thirty active compounds with confirmed inhibitory activity on iNOS, reported in PubChem BioAssay database [32], were docked to iNOS isoforms (PDB ID: 3E7G and PDB ID: 1NSI), and their affinities calculated by AutoDock Vina [22]. The biological activity of validation compounds comprises a wide

range of IC_{50} values, from nanomolar to micromolar concentrations, including values reported for compounds classified as potent inhibitors of iNOS activity [86, 87]. Moreover, this activity has been reported to be isoform-specific, as significant differences on enzyme inhibition have been shown when iNOS activity was compared to those elicited by the endothelial nitric oxide synthase (eNOS) and neuronal nitric oxide synthase (nNOS) [34].

The name or PubChem chemical structure identifier (CID), AutoDock Vina affinity value, and biological activity (IC_{50}) for reported iNOS inhibitors are presented in Table 4.2. The relationship between the biological activity (IC_{50}) and the mean binding affinity obtained for both iNOS structures are shown in Figure 4.4. The data indicated the inhibition of iNOS activity follows a linear relationship with the theoretical binding affinity for these compounds.

The relationship observed between biological activity ($\log IC_{50}$) and *in silico* binding affinity values for known iNOS inhibitors is mostly linear in nature (Figure 4.4), and our results ($R = 0.842$, $P < 0.0001$) are much better than those reported for similar studies [88]. The data revealed ligands can be divided in two groups based on their affinity scores. Molecules with affinity scores less than -8.0 kcal/mol are likely to have IC_{50} values equal or lower than $0.1 \mu\text{M}$. In contrast, those with values higher than -8.0 kcal/mol will have less chance to inhibit iNOS. Moreover, those natural compounds with absolute affinity scores less than -9.0 kcal/mol, such as CID 16116045, CID 16115115, and CID 16114995 are good candidates to have IC_{50} values in the sub nanomolar range.

Table 4.2. AutoDock Vina-calculated affinities of selected inhibitors for iNOS and their half maximal inhibitory concentrations (IC₅₀).

iNOS inhibitor	AID/Reference	PDB ID: 3E7G	PDB ID: 1NSI	Affinity mean ^a	IC ₅₀ (μM)	LogIC ₅₀ (μM)
		Affinity (kcal/mol)	Affinity (kcal/mol)			
Pimagedine	AID: 92004	-4.0 ± 0.0	-4.4 ± 0.0	-4.2 ± 0.0	3.9	0.59
AMT	[33]	-4.7 ± 0.1	-4.4 ± 0.1	-4.6 ± 0.1	3.6	0.56
N(G)-iminoethylornithine	AID: 92181	-5.5 ± 0.0	-6.2 ± 0.0	-5.9 ± 0.1	2.2	0.34
L-NIL	AID: 92009	-5.8 ± 0.1	-6.3 ± 0.1	-6.0 ± 0.1	1.3	0.11
Targinine	AID: 92143	-5.8 ± 0.1	-6.7 ± 0.0	-6.2 ± 0.1	0.86	-0.07
Nitroarginine	AID: 92143	-6.1 ± 0.1	-6.9 ± 0.0	-6.5 ± 0.1	0.67	-0.17
AR-C95791	AID: 92009	-8.4 ± 0.0	-6.9 ± 0.0	-7.7 ± 0.2	0.35	-0.46
CID10398018	AID: 92144	-6.4 ± 0.0	6.6 ± 0.1	-6.5 ± 0.0	0.25	-0.60
Etiron	AID: 92011	-4.1 ± 0.1	-4.1 ± 0.0	-4.1 ± 0.0	0.16	-0.80
CID 10011896	AID: 92011	-4.2 ± 0.1	-4.3 ± 0.0	-4.2 ± 0.0	0.14	-0.85
CID 3863	AID: 92004	-5.9 ± 0.0	-6.2 ± 0.1	-6.0 ± 0.0	0.1	-1.00
CID 16116298	AID: 280474	-7.6 ± 0.0	-6.7 ± 0.0	-7.2 ± 0.1	0.1	-1.00
CID 16116293	AID: 280474	-8.4 ± 0.0	-9.2 ± 0.0	-8.8 ± 0.1	0.1	-1.00
CID 16115471	AID: 280474	-8.1 ± 0.1	-8.6 ± 0.0	-8.3 ± 0.1	0.066	-1.18
CID 16115345	AID: 280474	-8.1 ± 0.0	-9.0 ± 0.0	-8.6 ± 0.1	0.066	-1.18
CID 44420709	AID: 280474	-8.7 ± 0.0	-8.7 ± 0.0	-8.7 ± 0.0	0.033	-1.48
CID 16116564	AID: 280474	-8.1 ± 0.0	-8.5 ± 0.0	-8.3 ± 0.0	0.012	-1.92
CID 16115897	AID: 280474	-8.3 ± 0.0	-8.9 ± 0.0	-8.6 ± 0.1	0.01	-2.00
CID 16115611	AID: 280474	-9.8 ± 0.0	-9.1 ± 0.0	-9.5 ± 0.1	0.0054	-2.27
CID 16115606	AID: 280474	-8.6 ± 0.0	-9.6 ± 0.0	-9.5 ± 0.1	0.0041	-2.39
CID 16115472	AID: 280474	-8.1 ± 0.0	-8.8 ± 0.0	-8.4 ± 0.1	0.0035	-2.46
CID 16115342	AID: 280474	-9.5 ± 0.0	-9.1 ± 0.0	-9.3 ± 0.0	0.003	-2.52
CID 16114996	AID: 280474	-9.9 ± 0.0	-10.5 ± 0.0	-10.2 ± 0.0	0.0027	-2.57

Table 4.2. continued

CID 16115233	AID: 280474	-7.7 ± 0.0	-8.4 ± 0.0	-8.1 ± 0.1	0.0015	-2.82
CID 16115115	AID: 280474	-10.4 ± 0.1	-10.4 ± 0.0	-10.4 ± 0.0	0.0011	-2.96
CID 16114992	AID: 280474	-9.2 ± 0.0	-9.9 ± 0.0	-9.5 ± 0.1	0.001	-3.00
CID 16114995	AID: 280474	-10.2 ± 0.0	-11.1 ± 0.0	-10.7 ± 0.1	0.00096	-3.02
CID 16116046	AID: 280474	-9.9 ± 0.1	-10.1 ± 0.0	-10.0 ± 0.0	0.0008	-3.10
CID 16116045	AID: 280474	-9.8 ± 0.0	-10.3 ± 0.0	-10.0 ± 0.1	0.00067	-3.17
CID 16115896	AID: 280474	-8.7 ± 0.0	-9.1 ± 0.0	-8.9 ± 0.1	0.0005	-3.30

^a Average affinity between the scores obtained for two iNOS structures (PDB ID: 3E7G and PDB ID: 1NSI), AID: Assay ID (PubChem Bioassay), CID: Compound ID (PubChem Compound), IC₅₀: Half maximal inhibitory concentration.

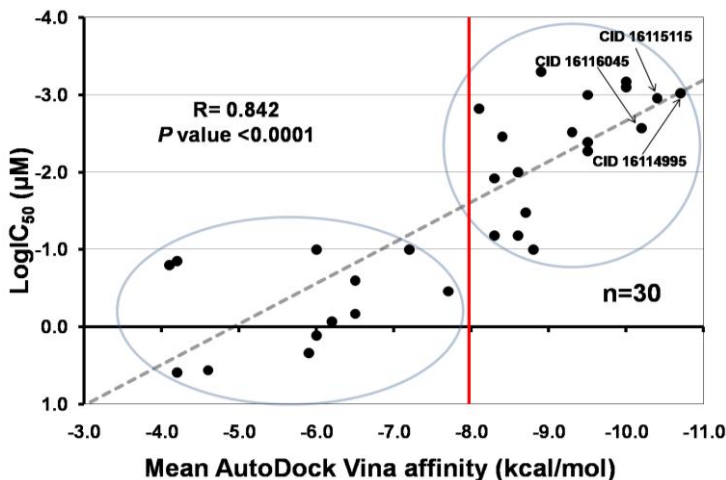


Figure 4.4. Correlation between the mean affinities calculated by AutoDock Vina in 3E7G and 1NSI for iNOS inhibitors and their half maximal inhibitory concentration [LogC₅₀]. The regression line ($Y = 0.375X + 1.820$) was added for illustrative purposes. Circles show molecules with high (upper) and low (lower) biological activity.

Interestingly, two natural compounds evaluated here (silibinin and cyanidin-3-rutinoside) presented absolute affinity scores less than -9.2 kcal/mol for both iNOS. These values are even better than those obtained for well-known inhibitors such as pimagedine, AMT, L-NIL, nitroarginine, targinine, and etiron [32, 33]. These results could help explaining some of their benefic effects on human health, not only by their known modulation of transcription factors [19], but also by their behavior as iNOS inhibitors. In general, flavonoids and anthocyanins present good theoretically capacity to bind and inhibit iNOS. Although the anti-inflammatory properties of natural compounds may occur through multiple mechanisms, the exploration of a direct action at the protein level by docking simulations provides insights regarding their pharmacological benefits.

4.5. CONCLUSIONS

In conclusion, docking analysis data suggested that it is plausible that in addition to their role mediating transcription regulation of inflammation-related genes, some food-related, such as silibinin (flavolignan) and cyanidin-3-rutinoside (anthocyanin), may exert direct inhibitory action on iNOS. Future research will focus on experimental evaluation of these results, using the iNOS model to design new derivatives of these natural bioactive compounds.

4.6. REFERENCES

- [1] Day, B.J. Antioxidants as potential therapeutics for lung fibrosis. *Antiox Red Sign.* 2008, 10, 355-70.
- [2] Song, F.-L., Gan, R.-Y., Zhang, Y., Xiao, Q., Kuang, L., Li, H.-B. Total phenolic contents and antioxidant capacities of selected Chinese medicinal plants. *Int J Mol Sci.* 2010, 11, 2362-72.
- [3] Lü, J.M., Lin, P.H., Yao, Q., Chen, C. Chemical and molecular mechanisms of antioxidants: experimental approaches and model systems. *J Cell Mol Med.* 2010, 14, 840-60.
- [4] Kamat, C.D., Gadal, S., Mhatre, M., Williamson, K.S., Pye, Q.N., Hensley, K. Antioxidants in central nervous system diseases: preclinical promise and translational challenges. *J Alzheimers Dis.* 2008, 15, 473-93.
- [5] Kris-Etherton, P.M., Hecker, K.D., Bonanome, A., Coval, S.M., Binkoski, A.E., Hilpert, K.F., et al. Bioactive compounds in foods: their role in the prevention of cardiovascular disease and cancer. *Am J Med.* 2002, 113, 71-88.
- [6] Delcourt, C., Korobelnik, J.-F., Barberger-Gateau, P., Delyfer, M.-N., Rougier, M.-B., Le Goff, M., et al. Nutrition and age-related eye diseases: the Alienor (Antioxydants, Lipides Essentiels, Nutrition et maladies OculaiRes) Study. *J Nutr Health Aging.* 2010, 14, 854-61.
- [7] Wang, S.Y., Chen, C.-T., Sciarappa, W., Wang, C.Y., Camp, M.J. Fruit quality, antioxidant capacity, and flavonoid content of organically and conventionally grown blueberries. *J Agric Food Chem.* 2008, 56, 5788-94.
- [8] Xia, E.-Q., Deng, G.-F., Guo, Y.-J., Li, H.-B. Biological activities of polyphenols from grapes. *Int J Mol Sci.* 2010, 11, 622-46.
- [9] Heim, K.E., Tagliaferro, A.R., Bobilya, D.J. Flavonoid antioxidants: chemistry, metabolism and structure-activity relationships. *J Nutr Biochem.* 2002, 13, 572-84.
- [10] Hammerstone, J.F., Lazarus, S.A., Schmitz, H.H. Procyanidin content and variation in some commonly consumed foods. *J Nutr.* 2000, 130, 2086S-92S.
- [11] Nichols, J.A., Katiyar, S.K. Skin photoprotection by natural polyphenols: anti-inflammatory, antioxidant and DNA repair mechanisms. *Arch Dermatol Res.* 2010, 302, 71-83.
- [12] Rahman, M.A., Amin, A.R., Shin, D.M. Chemopreventive potential of natural compounds in head and neck cancer. *Nutr Cancer.* 2010, 62, 973-87.
- [13] Hooper, L., Kroon, P.A., Rimm, E.B., Cohn, J.S., Harvey, I., Le Cornu, K.A., et al. Flavonoids, flavonoid-rich foods, and cardiovascular risk: a meta-analysis of randomized controlled trials. *Am J Clin Nutr.* 2008, 88, 38-50.
- [14] Zaslaver, M., Offer, S., Kerem, Z., Stark, A.H., Weller, J.I., Eliraz, A., et al. Natural compounds derived from foods modulate nitric oxide production and oxidative status in epithelial lung cells. *J Agric Food Chem.* 2005, 53, 9934-9.
- [15] Bian, K., Murad, F. Nitric oxide (NO)--biogenesis, regulation, and relevance to human diseases. *Front Biosci.* 2003, 8, d264-78.
- [16] Garcin, E.D., Arvai, A.S., Rosenfeld, R.J., Kroeger, M.D., Crane, B.R., Andersson, G., et al. Anchored plasticity opens doors for selective inhibitor design in nitric oxide synthase. *Nat Chem Biol.* 2008, 4, 700-7.

- [17] Rosenfeld, R.J., Garcin, E.D., Panda, K., Andersson, G., Åberg, A., Wallace, A.V., et al. Conformational changes in nitric oxide synthases induced by chlorzoxazone and nitroindazoles: crystallographic and computational analyses of inhibitor potency. *Biochemistry*. 2002, 41, 13915-25.
- [18] Li, D., Stuehr, D.J., Yeh, S.-R., Rousseau, D.L. Heme distortion modulated by ligand-protein interactions in inducible nitric-oxide synthase. *J Biol Chem*. 2004, 279, 26489-99.
- [19] Pan, M.-H., Lai, C.-S., Dushenkov, S., Ho, C.-T. Modulation of inflammatory genes by natural dietary bioactive compounds. *J Agric Food Chem*. 2009, 57, 4467-77.
- [20] May, A., Zacharias, M. Accounting for global protein deformability during protein-protein and protein-ligand docking. *BBA- Protein Proteom*. 2005, 1754, 225-31.
- [21] Maldonado-Rojas, W., Olivero-Verbel, J. Potential interaction of natural dietary bioactive compounds with COX-2. *J Mol Graph Model*. 2011, 30, 157-66.
- [22] Trott, O., Olson, A.J. AutoDock Vina: improving the speed and accuracy of docking with a new scoring function, efficient optimization, and multithreading. *J Comput Chem*. 2010, 31, 455-61.
- [23] www.pdb.org/pdb/home/home.do. Protein Data Bank (RCSB PDB). 2011.
- [24] Tripos:St. Louis, M. SYBYL 8.1. molecular modeling software. Tripos: St. Louis, MO, USA, 2007., USA, 2007., Vol. 8.1.
- [25] Hwang, Y.P., Choi, J.H., Yun, H.J., Han, E.H., Kim, H.G., Kim, J.Y., et al. Anthocyanins from purple sweet potato attenuate dimethylnitrosamine-induced liver injury in rats by inducing Nrf2-mediated antioxidant enzymes and reducing COX-2 and iNOS expression. *Food Chem Toxicol*. 2011, 49, 93-9.
- [26] Li, J., Shi, R., Yang, C., Zhu, X. Exploration of the binding of benzimidazole-biphenyl derivatives to hemoglobin using docking and molecular dynamics simulation. *Int J Biol Macromol*. 2011, 48, 20-6.
- [27] Frisch, M., Trucks, G., Schlegel, H., Scuseria, G., Robb, M., Cheeseman, J., et al. Gaussian 03, revision B. 05; Gaussian. Inc., Pittsburgh, PA. 2003, 12478.
- [28] Guha, R., Howard, M.T., Hutchison, G.R., Murray-Rust, P., Rzepa, H., Steinbeck, C., et al. The Blue Obelisk-interopability in chemical informatics. *J Chem Inf Mod*. 2006, 46, 991-8.
- [29] Sanner, M.F. Python: a programming language for software integration and development. *J Mol Graph Model*. 1999, 17, 57-61.
- [30] Wolber, G., Langer, T. LigandScout: 3-D pharmacophores derived from protein-bound ligands and their use as virtual screening filters. *J Chem Inf Model*. 2005, 45, 160-9.
- [31] DeLano, W.L. The PyMOL Molecular Graphics System; . DeLano Scientific LLC: San Carlos, C., USA, Ed., 1998–2003.
- [32] <http://pubchem.ncbi.nlm.nih.gov>. PubChem 2011.
- [33] Nakane, M., Klinghofer, V., Kuk, J.E., Donnelly, J.L., Budzik, G.P., Pollock, J.S., et al. Novel potent and selective inhibitors of inducible nitric oxide synthase. *Mol Pharmacol*. 1995, 47, 831-4.
- [34] Davey, D.D., Adler, M., Arnaiz, D., Eagen, K., Erickson, S., Guilford, W., et al. Design, synthesis, and activity of 2-imidazol-1-ylpyrimidine derived inducible nitric oxide synthase dimerization inhibitors. *J Med Chem*. 2007, 50, 1146-57.

[35] Connolly, S., Aberg, A., Arvai, A., Beaton, H.G., Cheshire, D.R., Cook, A.R., et al. 2-Aminopyridines as highly selective inducible nitric oxide synthase inhibitors. Differential binding modes dependent on nitrogen substitution. *J Med Chem.* 2004, 47, 3320-3.

[36] Zhou, Z., Wang, Y., Bryant, S.H. Computational analysis of the cathepsin B inhibitors activities through LR-MMPBSA binding affinity calculation based on docked complex. *J Comput Chem.* 2009, 30, 2165-75.

[37] Feng, R., Ni, H.-M., Wang, S.Y., Tourkova, I.L., Shurin, M.R., Harada, H., et al. Cyanidin-3-rutinoside, a natural polyphenol antioxidant, selectively kills leukemic cells by induction of oxidative stress. *J Biol Chem.* 2007, 282, 13468-76.

[38] Šarić, A., Sobočanec, S., Balog, T., Kušić, B., Šverko, V., Dragović-Uzelac, V., et al. Improved antioxidant and anti-inflammatory potential in mice consuming sour cherry juice (*Prunus Cerasus* cv. Maraska). *Plant Foods Hum Nutr.* 2009, 64, 231-7.

[39] Yin, F., Liu, J., Ji, X., Wang, Y., Zidichouski, J., Zhang, J. Silibinin: A novel inhibitor of A β aggregation. *Neurochem Int.* 2011, 58, 399-403.

[40] Abenavoli, L., Capasso, R., Milic, N., Capasso, F. Milk thistle in liver diseases: past, present, future. *Phytother Res.* 2010, 24, 1423-32.

[41] Cheng, J.-C., Kan, L.-S., Chen, J.-T., Chen, L.-G., Lu, H.-C., Lin, S.-M., et al. Detection of cyanidin in different-colored peanut testae and identification of peanut cyanidin 3-sambubioside. *J Agric Food Chem.* 2009, 57, 8805-11.

[42] Wang, L.-S., Stoner, G.D. Anthocyanins and their role in cancer prevention. *Cancer Lett.* 2008, 269, 281-90.

[43] Hosseinian, F.S., Beta, T. Saskatoon and wild blueberries have higher anthocyanin contents than other Manitoba berries. *J Agric Food Chem.* 2007, 55, 10832-8.

[44] Ichiyonagi, T., Shida, Y., Rahman, M.M., Hatano, Y., Konishi, T. Bioavailability and tissue distribution of anthocyanins in bilberry (*Vaccinium myrtillus* L.) extract in rats. *J Agric Food Chem.* 2006, 54, 6578-87.

[45] Kalantari, H., Das, D.K. Physiological effects of resveratrol. *Biofactors.* 2010, 36, 401-6.

[46] Reber, J.D., Eggett, D.L., Parker, T.L. Antioxidant capacity interactions and a chemical/structural model of phenolic compounds found in strawberries. *Int J Food Sci Nutr.* 2011, 62, 445-52.

[47] Chen, P.-N., Kuo, W.-H., Chiang, C.-L., Chiou, H.-L., Hsieh, Y.-S., Chu, S.-C. Black rice anthocyanins inhibit cancer cells invasion via repressions of MMPs and u-PA expression. *Chem Biol Interact.* 2006, 163, 218-29.

[48] Yao, Y., Sang, W., Zhou, M., Ren, G. Phenolic composition and antioxidant activities of 11 celery cultivars. *J Food Sci.* 2010, 75, C9-C13.

[49] Bernardes, W.A., Lucarini, R., Tozatti, M.G., Souza, M.G., Andrade Silva, M.L., da Silva Filho, A.A., et al. Antimicrobial activity of *Rosmarinus officinalis* against oral pathogens: relevance of carnosic acid and carnosol. *Chem Biodivers.* 2010, 7, 1835-40.

[50] Castellarin, S.D., Di Gaspero, G. Transcriptional control of anthocyanin biosynthetic genes in extreme phenotypes for berry pigmentation of naturally occurring grapevines. *BMC Plant Biol.* 2007, 7, 1.

[51] Deziel, B.A., Patel, K., Neto, C., Gottschall-Pass, K., Hurta, R.A. Proanthocyanidins from the American Cranberry (*Vaccinium macrocarpon*) inhibit matrix metalloproteinase-2 and matrix metalloproteinase-9 activity in human prostate cancer cells via alterations in multiple cellular signalling pathways. *J Cell Biochem.* 2010, 111, 742-54.

[52] Wang, P., Aronson, W.J., Huang, M., Zhang, Y., Lee, R.-P., Heber, D., et al. Green tea polyphenols and metabolites in prostatectomy tissue: implications for cancer prevention. *Cancer Prev Res.* 2010, 3, 985-93.

[53] Lehtonen, H.-M., Rantala, M., Suomela, J.-P., Viitanen, M., Kallio, H. Urinary excretion of the main anthocyanin in lingonberry (*Vaccinium vitis-idaea*), cyanidin 3-O-galactoside, and its metabolites. *J Agric Food Chem.* 2009, 57, 4447-51.

[54] Vasanthi, H.R., Mukherjee, S., Das, D.K. Potential health benefits of broccoli-a chemico-biological overview. *Mini Rev Med Chem.* 2009, 9, 749-59.

[55] Mullen, W., Edwards, C.A., Serafini, M., Crozier, A. Bioavailability of pelargonidin-3-O-glucoside and its metabolites in humans following the ingestion of strawberries with and without cream. *J Agric Food Chem.* 2008, 56, 713-9.

[56] Rasyid, A., Rahman, A.R.A., Jaalam, K., Lelo, A. Effect of different curcumin dosages on human gall bladder. *Asia Pac J Clin Nutr.* 2002, 11, 314-8.

[57] Lai, C.-S., Li, S., Chai, C.-Y., Lo, C.-Y., Ho, C.-T., Wang, Y.-J., et al. Inhibitory effect of citrus 5-hydroxy-3, 6, 7, 8, 3', 4'-hexamethoxyflavone on 12-O-tetradecanoylphorbol 13-acetate-induced skin inflammation and tumor promotion in mice. *Carcinogenesis.* 2007, 28, 2581-8.

[58] Theodosiou, M., Laudet, V., Schubert, M. From carrot to clinic: an overview of the retinoic acid signaling pathway. *Cell Mol Life Sci.* 2010, 67, 1423-45.

[59] Lien, T.F., Yeh, H.S., Su, W.T. Effect of adding extracted hesperetin, naringenin and pectin on egg cholesterol, serum traits and antioxidant activity in laying hens. *Arch Anim Nutr.* 2008, 62, 33-43.

[60] Alosi, J.A., McDonald, D.E., Schneider, J.S., Privette, A.R., McFadden, D.W. Pterostilbene inhibits breast cancer in vitro through mitochondrial depolarization and induction of caspase-dependent apoptosis. *J Surgical Res.* 2010, 161, 195-201.

[61] Stuetz, W., Prapamontol, T., Hongsibsong, S., Biesalski, H.-K. Polymethoxylated flavones, flavanone glycosides, carotenoids, and antioxidants in different cultivation types of tangerines (*Citrus reticulata* Blanco cv. Sainampueng) from Northern Thailand. *J Agric Food Chem.* 2010, 58, 6069-74.

[62] Basini, G., Bussolati, S., Santini, S., Grasselli, F. The impact of the phyto-oestrogen genistein on swine granulosa cell function. *J Anim Physiol Anim Nutr.* 2010, 94, e374-e82.

[63] Mann, N.J., O'Connell, S.L., Baldwin, K.M., Singh, I., Meyer, B.J. Effects of seal oil and tuna-fish oil on platelet parameters and plasma lipid levels in healthy subjects. *Lipids.* 2010, 45, 669-81.

[64] Weng, C.J., Wu, C.F., Huang, H.W., Ho, C.T., Yen, G.C. Anti-invasion effects of 6-shogaol and 6-gingerol, two active components in ginger, on human hepatocarcinoma cells. *Mol Nutr Food Res.* 2010, 54, 1618-27.

[65] Visanji, J.M., Duthie, S.J., Pirie, L., Thompson, D.G., Padfield, P.J. Dietary isothiocyanates inhibit Caco-2 cell proliferation and induce G2/M phase cell cycle arrest, DNA damage, and G2/M checkpoint activation. *Journal Nutr.* 2004, 134, 3121-6.

[66] Vogel, J.T., Tieman, D.M., Sims, C.A., Odabasi, A.Z., Clark, D.G., Klee, H.J. Carotenoid content impacts flavor acceptability in tomato (*Solanum lycopersicum*). *J Sci Food Agric.* 2010, 90, 2233-40.

[67] Ali, M.S., Saleem, M., Ahmad, W., Parvez, M., Yamdagni, R. A chlorinated monoterpene ketone, acylated β -sitosterol glycosides and a flavanone glycoside from *Mentha longifolia* (Lamiaceae). *Phytochemistry.* 2002, 59, 889-95.

[68] Skupinska, K., Misiewicz-Krzeminska, I., Lubelska, K., Kasprzycka-Guttman, T. The effect of isothiocyanates on CYP1A1 and CYP1A2 activities induced by polycyclic aromatic hydrocarbons in Mcf7 cells. *Toxicol In Vitro.* 2009, 23, 763-71.

[69] Thürmann, P.A., Steffen, J., Zwernemann, C., Aebischer, C.-P., Cohn, W., Wendt, G., et al. Plasma concentration response to drinks containing β -carotene as carrot juice or formulated as a water dispersible powder. *Eur J Nutr.* 2002, 41, 228-35.

[70] Burns-Whitmore, B., Haddad, E., Sabaté, J., Jaceldo-Siegl, K., Tanzman, J., Rajaram, S. Effect of n-3 fatty acid enriched eggs and organic eggs on serum lutein in free-living lacto-ovo vegetarians. *Eur J Clin Nutr.* 2010, 64, 1332-7.

[71] Salado, C., Olaso, E., Gallot, N., Valcarcel, M., Egilegor, E., Mendoza, L., et al. Resveratrol prevents inflammation-dependent hepatic melanoma metastasis by inhibiting the secretion and effects of interleukin-18. *J Transl Med.* 2011, 9, 59.

[72] Au, A., Hasenwinkel, J., Frondoza, C. Silybin inhibits interleukin-1 β -induced production of pro-inflammatory mediators in canine hepatocyte cultures. *J Vet Pharmacol Ther.* 2011, 34, 120-9.

[73] Mauray, A., Felgines, C., Morand, C., Mazur, A., Scalbert, A., Milenkovic, D. Bilberry anthocyanin-rich extract alters expression of genes related to atherosclerosis development in aorta of apo E-deficient mice. *Nutr Metab Card Dis.* 2012, 22, 72-80.

[74] Seymour, E., Lewis, S.K., Urcuyo-Llanes, D.E., Tanone, I.I., Kirakosyan, A., Kaufman, P.B., et al. Regular tart cherry intake alters abdominal adiposity, adipose gene transcription, and inflammation in obesity-prone rats fed a high fat diet. *J Med Food.* 2009, 12, 935-42.

[75] Karlsen, A., Retterstøl, L., Laake, P., Paur, I., Kjølrsrud-Bøhn, S., Sandvik, L., et al. Anthocyanins inhibit nuclear factor- κ B activation in monocytes and reduce plasma concentrations of pro-inflammatory mediators in healthy adults. *J Nutr.* 2007, 137, 1951-4.

[76] Ramasamy, K., Dwyer-Nield, L.D., Serkova, N.J., Hasebroock, K.M., Tyagi, A., Raina, K., et al. Silibinin prevents lung tumorigenesis in wild-type but not in iNOS $^{-/-}$ mice: potential of real-time micro-CT in lung cancer chemoprevention studies. *Clin Cancer Res.* 2011, 17, 753-61.

[77] Chittezhath, M., Deep, G., Singh, R.P., Agarwal, C., Agarwal, R. Silibinin inhibits cytokine-induced signaling cascades and down-regulates inducible nitric oxide synthase in human lung carcinoma A549 cells. *Mol Cancer Ther.* 2008, 7, 1817-26.

[78] Zikri, N.N., Riedl, K.M., Wang, L.-S., Lechner, J., Schwartz, S.J., Stoner, G.D. Black raspberry components inhibit proliferation, induce apoptosis, and modulate gene expression in rat esophageal epithelial cells. *Nutr Cancer*. 2009, 61, 816-26.

[79] Jin, X.-H., Ohgami, K., Shiratori, K., Suzuki, Y., Koyama, Y., Yoshida, K., et al. Effects of blue honeysuckle (*Lonicera caerulea* L.) extract on lipopolysaccharide-induced inflammation in vitro and in vivo. *Exp Eye Res*. 2006, 82, 860-7.

[80] Khan, N., Afaq, F., Kweon, M.-H., Kim, K., Mukhtar, H. Oral consumption of pomegranate fruit extract inhibits growth and progression of primary lung tumors in mice. *Cancer Res*. 2007, 67, 3475-82.

[81] Llaua, F., Joseph, J., McDonald, J., Kalt, W. Attenuation of iNOS and COX-2 by blueberry polyphenols. *J Funct Foods*. 2009, 1, 274-83.

[82] Pergola, C., Rossi, A., Dugo, P., Cuzzocrea, S., Sautebin, L. Inhibition of nitric oxide biosynthesis by anthocyanin fraction of blackberry extract. *Nitric oxide*. 2006, 15, 30-9.

[83] Leiro, J.M., Alvarez, E., Arranz, J.A., Siso, I.G., Orallo, F. In vitro effects of mangiferin on superoxide concentrations and expression of the inducible nitric oxide synthase, tumour necrosis factor- α and transforming growth factor- β genes. *Biochem Pharmacol*. 2003, 65, 1361-71.

[84] Chin, Y.-W., Park, E.Y., Seo, S.-Y., Yoon, K.-D., Ahn, M.-J., Suh, Y.-G., et al. A novel iNOS and COX-2 inhibitor from the aerial parts of *Rodgersia podophylla*. *Bioorg Med Chem Lett*. 2006, 16, 4600-2.

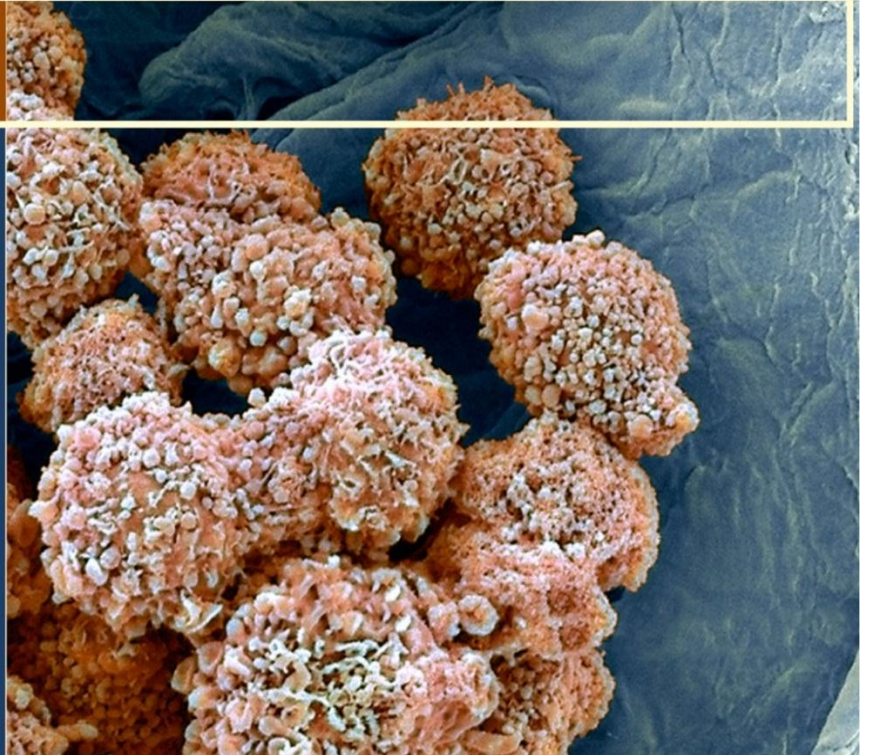
[85] Oh, J.H., Lee, T.-J., Park, J.-W., Kwon, T.K. Withaferin A inhibits iNOS expression and nitric oxide production by Akt inactivation and down-regulating LPS-induced activity of NF- κ B in RAW 264.7 cells. *Eur J Pharmacol*. 2008, 599, 11-7.

[86] Cheshire, D.R., Åberg, A., Andersson, G.M., Andrews, G., Beaton, H.G., Birkinshaw, T.N., et al. The discovery of novel, potent and highly selective inhibitors of inducible nitric oxide synthase (iNOS). *Bioorg Med Chem Lett*. 2011, 21, 2468-71.

[87] Le Bourdonnec, B., Leister, L.K., Ajello, C.A., Cassel, J.A., Seida, P.R., O'Hare, H., et al. Discovery of a series of aminopiperidines as novel iNOS inhibitors. *Bioorg Med Chem Lett*. 2008, 18, 336-43.

[88] Hare, A.A., Leng, L., Gandavadi, S., Du, X., Cournia, Z., Bucala, R., et al. Optimization of N-benzyl-benzoxazol-2-ones as receptor antagonists of macrophage migration inhibitory factor (MIF). *Bioorg Med Chem Lett*. 2010, 20, 5811-4.

Chapter 5



CHAPTER 5. COMPUTATIONAL FISHING OF NEW DNA METHYLTRANSFERASE INHIBITORS FROM NATURAL PRODUCTS

5.1. ABSTRACT

DNA methyltransferase inhibitors (DNMTis) have become an alternative for cancer therapies. However, only two DNMTis have been approved as anticancer drugs, although with some restrictions. Natural products (NPs) are a promising source of drugs. In order to find NPs with novel chemotypes as DNMTis, 47 compounds with known activity against these enzymes were used to build a LDA-based QSAR model for active/inactive molecules (93% accuracy) based on molecular descriptors. This classifier was employed to identify potential DNMTis on 800 NPs from NatProd Collection. 447 selected compounds were docked on two human DNA methyltransferase (DNMTs) structures (PDB codes: 3SWR and 2QRV) using AutoDock Vina and Surflex-Dock, prioritizing according to their score values, contact patterns at 4 Å and molecular diversity. Six consensus NPs were identified as virtual hits against DNMTs, including 9,10-dihydro-12-hydroxygambogic, phloridzin, 2',4'-dihydroxychalcone 4'-glucoside, daunorubicin, pyrromycin and centaurein. This method is an innovative computational strategy for identifying DNMTis, useful in the identification of potent and selective anticancer drugs.

5.2. INTRODUCTION

DNA methylation is a covalent biochemical modification defined as an epigenetic change important in the regulation of gene expression [1, 2]. The progression of DNA methylation involves a cycle of demethylation, *de novo* methylation, and methylation maintenance, catalyzed by family enzymes known as DNA methyltransferases (DNMTs, EC#: 2.1.1.37) [3-5]. These are responsible of transferring a methyl group from S-adenosyl-L-methionine (SAM) to the carbon-5 position of cytosine in DNA. This mechanism has been proposed for several authors (Figure 5.1) [6-9].

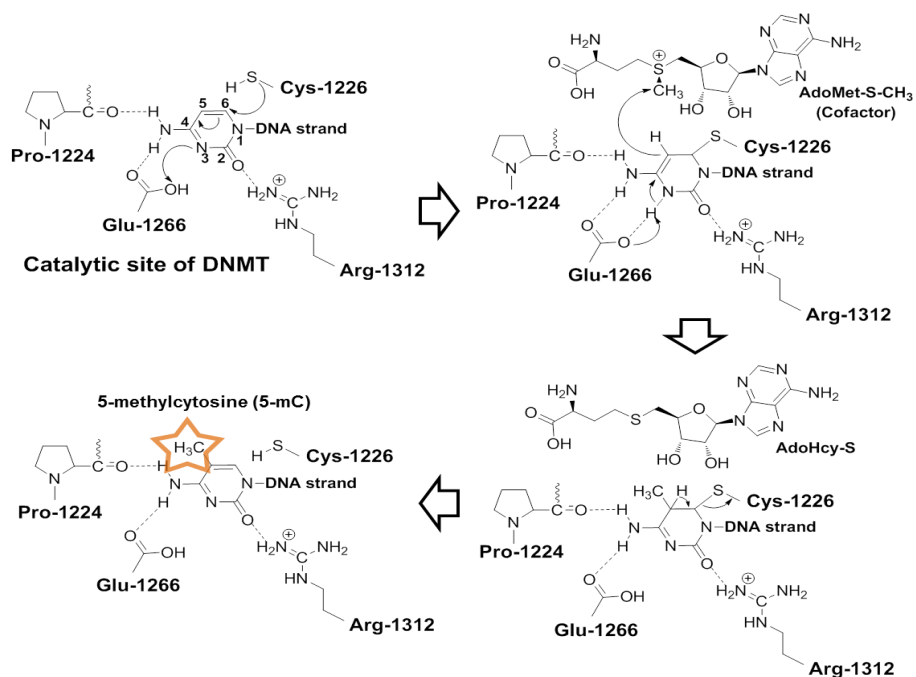


Figure 5.1. Mechanism of cytosine DNA methylation catalyzed by DNMTs. DNMTs contain a conserved cysteine residue that attacks the C(6) atom of cytosine forming a covalent bond. A nucleophilic attack occurs on the methyl group of S-adenosyl-L-methionine (AdoMet), which is converted to S-adenosyl-L-homocysteine (AdoHcy-S). The last step comprises β-elimination across the C(5)-C(6) bond, releasing the enzyme.

Currently, three types of cytosine-5 DNMTs have been identified, including two *de novo* DNA methyltransferases; DNMT3A and DNMT3B, which establish the methylation patterns during embryonic development in mammals and in differentiated cells [10, 11]; and DNMT1, the most abundant and active of these enzymes

responsible for copying the methylation pattern of DNA during cell division [12, 13]. It has been shown that DNMT1 plays an important role in carcinogenesis [12, 14], therefore, these targets are of particular interest to search for specific inhibitors [15-17].

The inhibition of DNMTs activity has been presented as a possible pathway to reactivate genes silenced by methylation of their promoters in different diseases, including cancer [1, 12, 18]. The relationship between the hypermethylation of promoter of tumor suppressor genes and cancer development has been clearly demonstrated [3, 4, 19], suggesting DNMTs as promising drug targets for the discovery of new and more potent/selective anticancer drugs [20]. To date, several DNMT inhibitors (DNMTis) of different structural classes have been published; basically categorized as nucleoside DNMTis and non-nucleoside analogue DNMTis, Figure 5.2 [16, 21]. DNMTis nucleosides, cytosine analogs, have been studied in several cancer types [22, 23]. Most of these compounds that inhibit the activity of DNMT have been related with significant "off target" effects [24], a fact that has prevented their use with pharmacological purposes. However, two of them, azacitidine and decitabine, have been approved by FDA (Food and Drug Administration) for the treatment of myelodysplastic syndromes [25, 26]. Moreover, non-nucleoside DNMTis, such as RG-108 [27], which was identified via virtual screening methods; and SGI-1027, a quinoline derivative, have been proposed as DNMTis [28, 29]. However, the weak inhibitory activity of these compounds [30] indicates a need for the search of more effective inhibitors in the future.

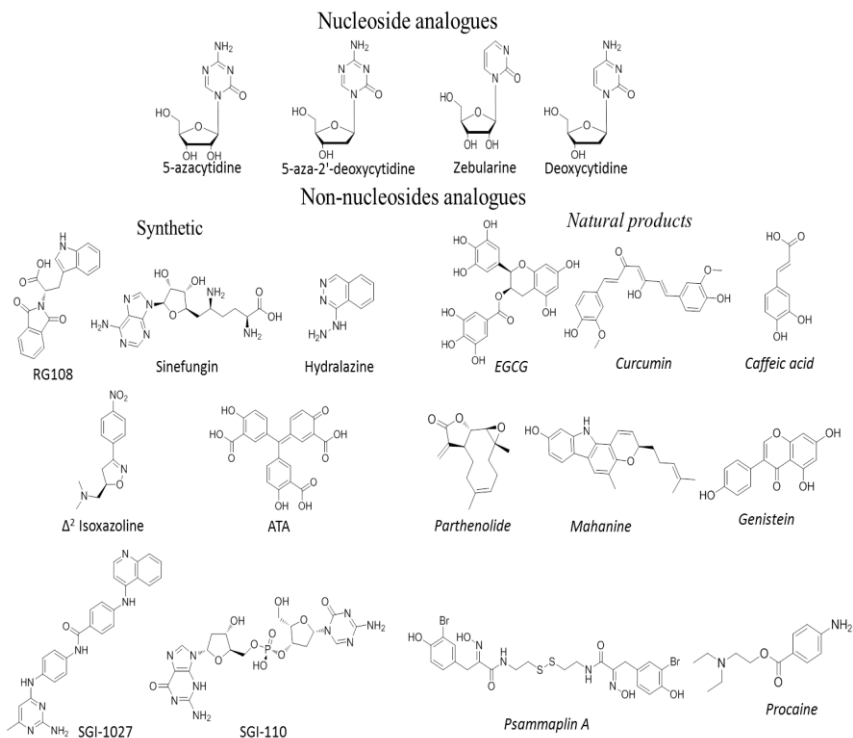


Figure 5.2. Chemical structure of representative known nucleoside analogues and non-nucleoside DNMTis, classified as synthetic and natural products.

Natural products (NPs) are a promissory source of drugs due to their molecular diversity and low toxicity. It is estimated that 60% of approved drugs are derived from natural sources [31-33]. To date, several NPs have been proposed as DNMT inhibitors [34, 35]. Some studies have shown epigallocatechin-3-gallate (EGCG) [36], curcumin [34], genistein [37], psammaplin A [38], mahanine [39], caffeic acid [40], laccic acid [41], among others. However, they exhibit no significant inhibitory pharmacological activity.

Computational tools help to elucidate the basic structural requirements of the inhibitors for activity against DNMT. The increase in the number of available crystallographic DNMTs structures has prompted the use of computational molecular docking and structure-based approaches for search DNMTis [27-29]. Computational and experimental screening methodologies have served to identify promissory DNMTis, for instance NSC 14778. Recently, two new DNMTis (SW155246 and SID49645275) have been discovered using experimental high-throughput screening

(HTS) and they have been proposed as molecular scaffold for discovering new DNMTis [42- 44]. However, they showed a lack of pharmacological information, specific of DNMTs. For this reason, the systematic searching of new promissory compounds with DNA hypomethylating activity by using NPs data sets is a great path and an urgent need to discover new and more effective DNMTis. Recently, Medina-Franco et al, shown that NPs are a rich source for demethylating agents that need to be rigorously characterized in theoretical and/or experimental studies [45].

The main aim of this report was to develop a virtual screening to find potential DNMTis on 800 NPs from NatProd Collection, MicroSource Discovery Systems (www.msdiscovery.com/natprod.html). The protocol included a Linear Discriminant Analysis (LDA)-based QSAR model from a set of 47 active/inactive molecules against DNMTs, with further optimization of the promising compounds by molecular docking procedures, and finally, a selection based on molecular diversity by *k*-means cluster analysis. Following this multistep approach, six consensus NPs hits with new chemotypes as inhibitors of DNMTs were identified.

5.3. MATERIALS AND METHODS

5.3.1 LDA-based Discriminant Model

A set of 47 diverse compounds reported in the literature as active and not active against DNMTs were used to develop a discriminant model, employing 32 compounds as training set and the other 15 as test set as shown in Table 5.1. Molecules in each group were randomly selected. Compounds were downloaded from PubChem database (<http://pubchem.ncbi.nlm.nih.gov/>), and their 3D structures were optimized using molecular mechanic methods, with Tripos force field with Gasteiger charges, a gradient convergence of 0.05 kcal/mol and a maximum number of optimization iterations of 1000. All calculations were performed using SYBYL-X 2.0 package [46].

Table 5.1. Compounds tested against DNMTs used for Building (training set) and Validating (test set) the LDA-based Discriminant Model.

No.	Active (Inhibitor) ^a	No.	Inactive
Training set			
1	RG108	20	NCS622444
2	5-azacytidine	21	NCS137546
3	5-Fluoro-2'-deoxycytidine	22	NCS319745
4	Zebularine	23	NCS106084
5	Deoxycytidine	24	NCS54162
6	EGCG	25	NCS158324
7	Genistein	26	NCS348926
8	Curcumin	27	CHEMBL1780248
9	Caffeic acid	28	NCS4092
10	Procaine	29	NCS21970
11	Hydralazine	30	NCS19555
12	Nanaomycin A	31	NCS27292
13	SGI-110	32	NCS303530
14	AdoHcy (SAH)		
15	Parthenolide		
16	Mahanine		
17	NCS97317		
18	Chlorogenic acid		
19	Δ^2 Isoxazoline		
Test set			
1	Aurintricarboxylic acid (ATA)	10	NCS408488
2	RG108-1	11	NCS56071
3	5-aza-2'-deoxycytidine	12	NCS154957
4	5,6-Dihydro-5-azacytidine	13	NCS138419
5	Aza-Adomet	14	NCS345763
6	Laccaic acid A	15	NCS27278
7	Psammaphin A		
8	SGI-1027		
9	Sinefungin		

^a Compounds in this study have been previously evaluated against DNMTs activity, Natural DNMTs in *italics*.

A LDA-based QSAR model was developed for classification of compounds as active or inactive against DNMTs. A whole set of 0-3D MDs were calculated employing DRAGON 5.5 program [47]. LDA-based QSAR model was developed using forward stepwise procedure as feature selection method (wrapper strategy) in STATISTICA 8.0 software [48], and the principle of parsimony (Occam's Razor) was established selecting the best model. Statistical parameters such as, Wilks' λ (U-statistic), square Mahalanobis distance (D^2), Fisher ratio (F) with the corresponding p -level ($p(F)$), as well as the percentage of good classification (accuracy) in both training and test sets were used to assess the quality and performance of the model [49]. In order to increase the hit chance, the classification probabilities produced by LDA-based QSAR model were used for subsequent selection of compounds. A NP is classified as active if $\Delta P\% > 50\%$ or as inactive if $\Delta P\%$ the otherwise, being $\Delta P\% = [P(\text{Active}) - P(\text{Inactive})] \times 100$, $P(\text{Active})$ and $P(\text{Inactive})$ are the probabilities to be active or inactive according to the classifier model.

In addition to the greedy-based wrapper method, we initially employed several unsupervised and supervised methods based on the computation of Shannon's entropy type measures for make a drastic dimension reduction of all DRAGON MDs [50, 51]. This algorithm has been implemented in an *in house* computer program denominated IMMAN (acronym for Information Theory based Chemometric Analysis) [52]. This approach has been employed to compare proposed MDs and various families of indices reported in the literature, as well as MD computing software [53]. Six different types of MDs from different families were finally selected in the model, including: information index (SIC2), 3D-moRSE descriptor (Mor13m), 2D autocorrelation (GATS5m), Randić molecular profile (SHP2), topological descriptor (ZM2V), and atomic centered-fragment (H-047).

5.4. Molecular Docking with AutoDock Vina and Surflex-Dock

The feasibility of NPs to work as inhibitors of DNMTs was evaluated with two docking programs frequently used for virtual screening, AutoDock Vina [54, 55, 56] and Surflex-Dock [57]; which are based on different score functions to evaluate the binding mode of a ligand onto a receptor.

5.4.1. Preparation and selection of crystallographic structures of DNMTs for molecular docking with NPs

Ten available mammalian DNMT structures (DNMT1, PDB codes: 3AV4, 3AV5, 3AV6, 3EPZ, 3PT6, 3PT9, 3PTA, 3SWR, 4DA4 and DNMT3A, PDB code: 2QRV) were downloaded from Protein Data Bank (<http://www.rcsb.org/pdb/home/>) and prepared with SYBYL-X 2.0 package for molecular docking. This process consisted of removing water molecules and other ligands, with subsequent repairing and

fixation of amide in side chains. Optimization protocols were performed using Powell conjugate gradient method; with dielectric constant value of 1.0, gradient convergence fixed to 0.005 kcal mol⁻¹, maximum number of iterations at 1000, and Kollman United/All-atoms force fields with AMBER charges.

A comparative structural analysis for DNMTs was performed with SYBYL-X 2.0 by multiple sequence alignments (% of identity, %ID) and spatial similarity (RMSD in Å) [58]. Based on these results, two representative DNMTs crystallographic structures were selected for protein-ligand docking protocols: DNMT1 (3SWR) and DNMT3A (2QRV).

5.4.2. Docking calculations of NPs on DNMTs

Docking calculations with AutoDock Vina program for NPs on selected DNMT structures (3SWR and 2QRV) were defined by establishing a cube at the geometric center of the co-crystallized ligand present on each selected DNMTs (3SWR-sinefungin and 2QRV-SAH), with dimensions 30 × 30 × 30 Å, covering the catalytic site and cofactor binding site (SAM) in the enzyme, employing a grid point spacing of 1.0 Å. The x, y, and z coordinates for the center grid boxes on 3SWR were -4.93, -2.66 and 33.36, whereas for 2QRV were 106.61, 45.73 and -1.71, respectively. Three docking runs were performed for each ligand, and the pose with the highest absolute value of affinity (kcal/mol) was saved. Finally, the mean affinity value for best poses was taken as the value of the binding affinity for a particular complex [54, 59].

The NPs that presented the best affinities with AutoDock Vina were additionally evaluated with Surflex-Dock, following a protomol generation approach based on the proximal residues to the co-crystallized ligand present in the crystallographic of selected DNMT structures using a threshold of 0.5 Å and bloat of 0, with the others parameters set as default. All docking calculations for ligands were performed keeping the same parameters (20 poses each), using only the highest ranked pose by Surflex-Dock [57, 60].

In order to validate the results obtained with AutoDock Vina and Surflex-Dock, the experimental ligands, sinefungin and SAH, were docked to the crystal structure of human DNMT1 (3SWR) and human DNMT3A (2QRV) [45], respectively. In total, 100 docking runs were performed with AutoDock Vina and Surflex-Dock for each ligand, using the same parameters described above for docking of NPs on DNMTs.

5.4.3. Identification of main interaction of selected NPs on DNMTs binding site

Identification of interacting residues at distances less than to 4 Å was carried out using Pymol program [61] in order to identify those most likely involved in the

inhibition mechanism of DNMTs [62]. The interaction nature of the residues that interact with selected NPs on DNMTs binding site was performed using LigandScout 3.1 program [63, 64], which utilizes simplified pharmacophores to detect the number and type of existing ligand-residue interactions on the protein active site for a particular protein-ligand complex. The most important DNMTs-NPs complexes were visualized with PyMol program [61] depicting the binding mode for selected NPs.

5.4.4. Molecular docking validation using biological information for DNMT1 Inhibitors

Compared to DNMT3A and DNMT3B, DNMT1 is most targeted to search for inhibitors as its high enzyme activity is the greatest among the DNMTs. This has increased the availability of biological information regarding this protein. In order to validate the reliability of the results generated by docking protocols, 3D structures and biological data for forty-five DNMTis were obtained from PubChem chemical library (<http://pubchem.ncbi.nlm.nih.gov/>), and their binding affinities and total scores were calculated with AutoDock Vina and Surflex-Dock following the same parameters described for NPs on DNMT1 (PDB code: 3SWR). The biological information consisted of the half maximal inhibitory concentration (μM , IC_{50}) values for DNMT1 activity, as reported for these chemicals in PubChem BioAssay (AID: 602386, Dose response confirmation of DNMT1 inhibitors in a Fluorescent Molecular Beacon assay). Correlation analysis to establish the relationships between binding scores on DNMT1, generated by AutoDock Vina and Surflex-Dock, and experimental biological data (LogIC_{50}) [122, 243] for DNMTis were calculated using STATISTICA 8.0 software [48].

5.4.5. Selection of Promissory NPs as DNMTis by Cluster Analysis

A molecular diversity *k*-means cluster analysis for selected NPs and well-known inhibitors, active and inactive include in training and test sets, was made based on 28 MDs (including the six calculated for screening) with STATISTICA 8.0 software [48]. The number of members in each cluster and the standard deviation of the variables in the cluster (kept as low as possible) were taken into account, to have an acceptable statistical quality of data partitions into the clusters. The values of the standard deviation between and within clusters, the respective Fisher ratio and their *p*-level of significance, were also examined. In the final selection of molecular descriptors vector the unsupervised filters in IMMAN software [52, 65] and the Fisher ratio in cluster analysis were taken into consideration. The final selected MDs included molecular weight, sum of the electronegativities (Se), sum of the polarizabilities (Sp), hydrogen (nH), carbon (nC), oxygen (nO), ALOGP, Neoplastic-80, among others, have been useful in the identification of anti-cancer drugs [66-68].

5.4.6 Searching of Information for Selected NPs (Assertions from Literature)

The selection of promissory NPs was performed utilizing, as a last filter, their available biological information. That is, an exhaustive searching of biological data reported for promissory NPs was performed using several search engines including; GoPubMed (<http://www.gpubmed.com>), PubReMiner (<http://bioinfo.amc.uva.nl/human-genetics/pubreminer/>), PubGraph (<http://datamining.cs.ucla.edu/pubgraph/>), among others.

5.4.7. Virtual Screening of NPs from NatProd Collection

The searching of new NPs as DNMTi was conducted in three stages: i) selection of actives NPs against DNMTs by LDA-based QSAR model (**Eq. 1**, see below) from 800 NPs contained in NatProd Collection (www.msdiscovery.com/natprod.html). These compounds were optimized under the same parameters utilized for the 47 compounds included in the training and test sets. Subsequently, only six MDs required (SIC2, Mor13m, GATS5m, SHP2, ZM2V, H-047) were calculated for these NPs using DRAGON 5.5 program. These MDs calculated for 800 NPs were evaluated by the classifier; ii) Molecular docking using AutoDock Vina and Surflex-Dock protocols for NPs classified as active by the LDA-based QSAR model on two DNMT structures (3SWR and 2QRV); iii) cluster analysis was carried out for selected NPs taking as reference training and test sets compounds (both actives and inactives) and searching for biological information from literature. Finally, six NPs were selected with new scaffolds as virtual DNMTi hits. That ensemble protocol is shown in Figure 5.3.

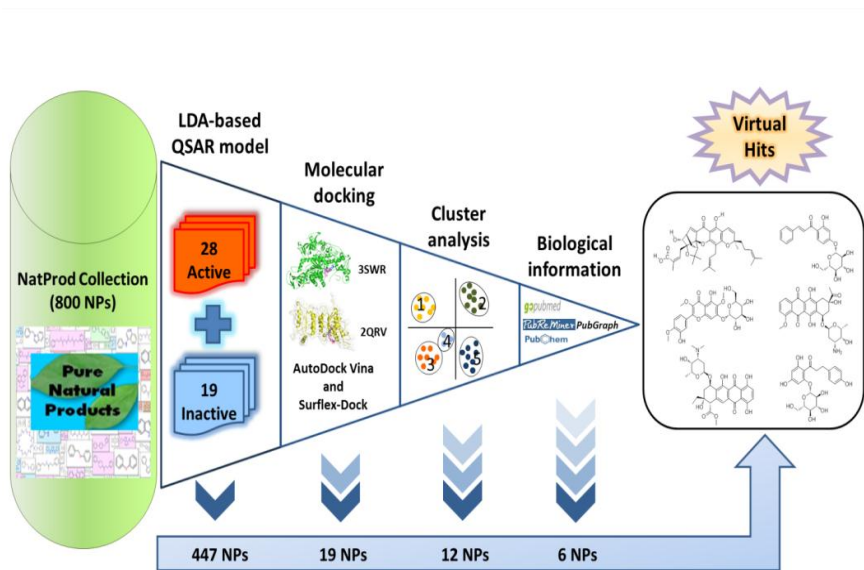


Figure 5.3. Pipeline of virtual screening for DNMTis discovery.

5.5. RESULTS AND DISCUSSION

5.5.1. LDA-based QSAR Model for identification of DNMTis

In order to perform a fast and reliable identification of NPs as DNMTis, a QSAR model was built (Eq. 1) utilizing six DRAGON's molecular descriptors (MDs) [47]. QSAR model with LDA-statistical parameters are show below:

$$\text{Class} = 56.44 \times \text{SIC2} + -9.66 \times \text{Mor13m} + 10.94 \times \text{GATS5m} + 130.55 \times \text{SHP2} + 0.05 \times \text{ZM2V} + 0.67 \times \text{H-047} - 135.41 \quad \text{..... (Eq. 1)}$$

$$N = 47, \text{Wilks' } \lambda = 0.204, D^2 = 15.17, F(6.25) = 16.262, p < 0.00001$$

The accuracy values (Q_{total}) of Eq. 1 for the training set was 96.9%, with a sensitivity and specificity of 94.7% and 100%, respectively, and the Matthews correlation coefficient (**C**) value obtained was 0.94 (see Table 5.2). In addition to this, similar values were obtained for test set, carrying out statistical parameters for accuracy of 93.3%, sensitivity of 88.9 %, specificity of 100%, and **C** value of 0.87. Moreover, both training and test sets presented a false positive rate of 0.0 %. Finally, statistical parameters obtained for this classifier are comparable with LDA-based

QSAR computational studies focused in drug discovery [49, 69, 70], showing the reliability of the QSAR to the virtual discovery of active compounds against DNMTs.

Table 5.2. Prediction performance of LDA-based QSAR model for classifying molecules as active or inactive against DNMTs.

	Actives	Inactives	N_{total}	C^a	Q_{total}^b (%)	Sensitivity rate (%)	Specificity (%)	False positive rate (%)
Training set^c								
Actives	18	1	19					
Inactives	0	13	13	0.94	96.9	94.7	100.0	0.0
N_{total}	18	14	32					
Test Set^d								
Actives	8	1	9					
Inactives	0	6	6	0.87	93.3	88.9	100.0	0.0
$N_{total}^{[e]}$	8	7	15					

^a Matthews correlation coefficient, ^b accuracy value, ^c 32 compounds (19 actives and 13 inactives against DNMTs), ^d 15 compounds (9 actives and 6 inactives against DNMTs), ^e number of compounds.

5.5.2. Application of LDA-based QSAR Model for Discovery of NPs as DNMTis

The NatProd Collection database comprises a diverse group of NPs constituted in 75% by alkaloids, flavonoids, sterols, triterpenes, diterpenes, sesquiterpenes, benzophenones, chalcones, stilbenes, limonoids, quassinoids, chromones, coumarins; and the remainder 25% encompasses quinones, quinonemethides, benzofurans, benzopyrans, rotenoids, xanthones, carbohydrates, benzotropolones, depsides, and depsidones. Virtual screening studies have also been conducted using this database to search for NPs as inhibitors of proteins related to inflammatory processes, ulcerative colitis and cancer, such as Interleukin 6 (IL-6) [71] and mitogen-activated protein kinase Phosphatase-1, demonstrating its applicability in natural-based drugs discovery.

LDA-based QSAR model was performed for discriminating of active/inactive molecules as DNMTis from 800 NPs from NatProd Collection previously optimized by molecular mechanics. In total, 447 compounds contained in the NPs collection were classified as active against DNMTs with $\Delta P\%$ greater than 50% with potential activity.

5.5.3. Searching of Promissory NPs as DNMTis by Molecular Docking Methods

Molecular docking validation performed by re-docked of sinefungin and SAH on their complex with DNMTs (3SWR and 2QRV, respectively), revealed an optimal reproduction of the predicted poses compared with experimental binding mode for these ligands (co-crystallized ligand), with satisfactory results with both AutoDock Vina and Surflex-Dock protocols.

For illustrative purposes, the best poses obtained for each DNMT-ligand complexes with utilized molecular docking protocols are shown in Figure 5.4, showing the best binding pose obtained according to experimental co-crystallized ligand. RMSD values.

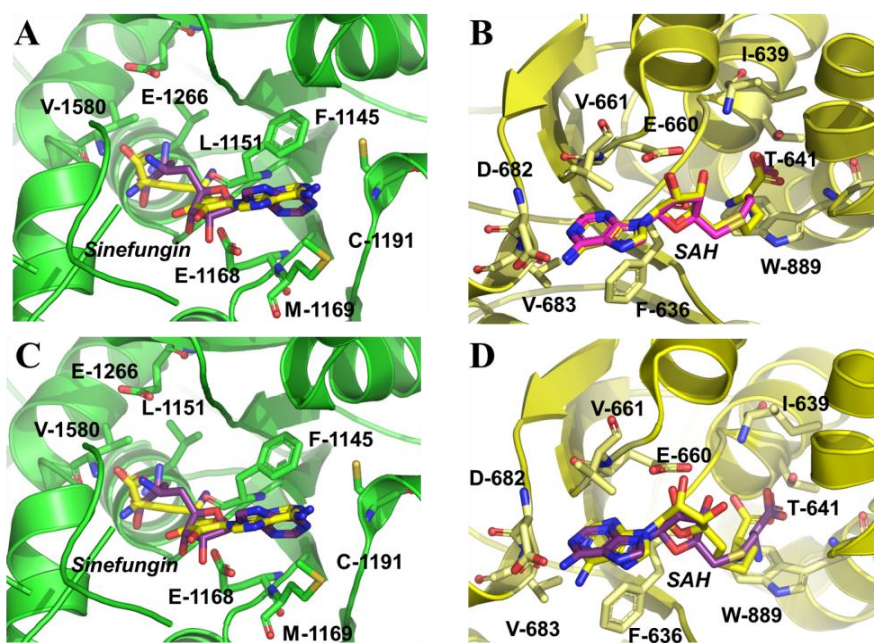


Figure 5.4. Molecular superposition between predicted (yellow) and co-crystallized pose (purple) for sinefungin (3SWR) and SAH (2QRV) with AutoDock Vina (A,B) and Surflex-Dock (C,D) protocols, showing interacting residues on experimental complexes with DNMTs.

The best conformation of pose replication expressed as the root mean standard deviation (RMSD) was 0.4997 Å. This value was obtained with AutoDock Vina for the 2QRV-SAHA complex, where the RMSD value for 3SWR-sinefungin was 0.8756 Å. In the case of Surflex-Dock, the best pose for sinefungin on 3SWR binding site presented a RMSD value of 1.9170 Å, and SAH presented a RMSD value of 1.1934

Å on 2QRV binding site. Obtained results were in agreement with similar studies conducted for this purpose. Medina-Franco et al. 2014, reported a RMSD value for sinefungin on 3SWR binding site of 0.547 Å using Glide XP program [9, 45]. These results showed the capability of using molecular docking protocols to reproduce the co-crystalized conformation of sinefungin and SAH on their experimental complexes with DNMTs.

5.5.4. Molecular docking results using AutoDock Vina and Surflex-Dock

Molecular docking of NPs on human DNMT1 and DNMT3A were preceded by pose validation using a re-docking co-crystalized ligand approach. A total of 447 compounds predicted as active against DNMTs by the LDA-based QSAR model were evaluated by molecular docking with DNMT1 (3SWR) and DNMT3A (2QRV). Finally, 67 NPs were selected according to the obtained affinity values (kcal/mol) [54] selecting those NPs with values less than -9.0 kcal/mol for 3SWR and less than -7.0 kcal/mol for 2QRV. These cut-off values were established according to the results obtained by molecular docking for the compounds used in the training and test sets on 3SWR and 2QRV structures.

In order to optimize the selection of compounds, 67 NPs selected by affinity values criteria with AutoDock Vina were subsequently evaluated with Surflex-Dock (SYBYL-X 2.0) as a third filter. The selection criteria for NPs was a Total score value greater than 6.0 (-log(Kd)) for both DNMT structures used, selecting the best 19 NPs as promising DNMTis, as observed in Table 5.3, which also show affinity values obtained with AutoDock Vina for these compounds.

Table 5.3. Compounds selected from NatProd collection as DNMT inhibitors using QSAR and molecular docking criteria.

Compound	Class ^a	$\Delta P\%$ ^b	3SWR kcal/mol AV ^c	2QRV kcal/mol AV	3SWR- log(Kd) ^d TS ^e	2QRV log(Kd) TS
Pectolarin	35.10	100.00	-10.4	-7.8	6.1	9.1
Daunorubicin	15.39	100.00	-9.3	-8.2	7.6	7.4
Derrubone	14.82	100.00	-9.1	-8.1	7.5	6.6
9,10-dihydro-12-hydroxygambogic acid	14.33	100.00	-9.5	-7.2	12.5	12.1
Digoxin	13.83	100.00	-11.4	-8.6	6.6	7.3
Pomiferin	13.76	100.00	-9.6	-9.1	7.5	6.4
Dihydromunduletone	13.33	100.00	-9.8	-7.3	7.0	8.1
Iridin	12.63	100.00	-9.4	-7.0	7.9	7.9
Phloridzin	11.03	100.00	-9.1	-8.3	9.2	8.5

Folicacid	8.42	99.96	-9.9	-8.0	8.7	8.1
Naringin	8.17	100.00	-9.8	-8.6	7.6	6.7
Centaurein	8.08	100.00	-9.7	-7.4	8.0	7.6

Table 5.3. Continued

Amygdalin	7.78	99.99	-9.2	-8.7	9.6	8.1
Pyrrromycin	6.79	100.00	-9.2	-7.4	8.9	9.8
4,2'- Dihydroxychalcone glucoside	5.94	99.99	-9.7	-8.9	6.4	7.6
Reserpine	5.77	100.00	-9.2	-7.8	9.1	7.8
Dimethylgambogate	5.69	100.00	-9.2	-8.2	12.0	11.6
Berbamine	5.02	100.00	-9.4	-7.7	7.4	7.3
Paclitaxel	4.50	100.00	-9.6	-7.8	9.9	9.9

^a Class: Classification obtained with LDA-based QSAR model, ^b $\Delta P\%:[P(\text{Active}) - P(\text{Inactive})] \times 100$, ^c AV: Affinity using AutoDock Vina, ^d logarithm negative of dissociation constant. ^e Total score using Surflex-Dock.

Several studies focused in DNMTs discovery have been developed using protein-ligand docking approaches. Yoo et al. (2012) reported aurintricarboxylic acid (ATA) as a novel inhibitor of DNMT1 and DNMT3A, employing the Glide program [9] to explain also the relevant implications in DNMTs inhibition [72]. Medina-Franco et al. (2014), conducted a structure-based rationalization of the activity of SW155246 and their structural analogues with human DNMT1 using the same program [45]. Although a number of studies for the discovery of DNMTs have been supported by methods of molecular docking, this report is the first where two different docking protocols, AutoDock Vina and Surflex-Dock are used to determine the interaction feasibility between compounds and DNMTs, applying the diversity of criteria for selection of NPs as new DNMTs.

5.5.5. Molecular docking validation with DNMTs biological data

The relationship between calculated binding scores (AutoDock Vina and Total score) and IC_{50} values (μM) could be taken as a measure of the likeliness of a particular compound to behave as a DNMTi. A group of forty-five DNMT1 inhibitors (AID: 602386) were docked to DNMT1 (PDB code: 3SWR), and their respective binding affinity and total score values were calculated. The relationship between the biological activity ($\log IC_{50}$) and the binding scores for these inhibitors on DNMT1 are shown in Figure 5.5. The correlation analysis indicated the inhibition of DNMT1 activity follows a highly dependence with calculated binding scores for these compounds ($r = 0.83$, p value < 0.0001 ; for binding affinity vs $\log IC_{50}$, $r = 0.65$, p value

<0.0001; for Total score vs $\log IC_{50}$), with correlation coefficients comparable to those reported in other studies for these validations [60, 56, 59, 73] as shown in Figure 5.5A and Figure 5.5B. These relationships were mostly linear in nature. The data revealed that NPs with affinity values lower than -9.0 kcal/mol and Total score values greater than 6.0 are likely to have IC_{50} values in the range of 4 to 25 μM , which suggest them as good candidates for DNMTs inhibition.

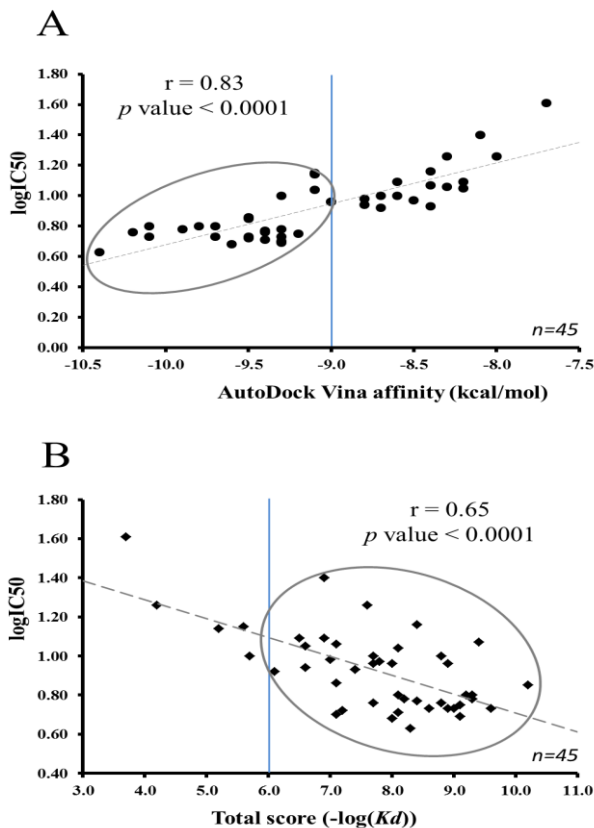


Figure 5.5. Correlation between binding affinities calculated by AutoDock Vina (A) and Total score by Surflex-Dock (B) and their half maximal inhibitory concentration for forty-five DNMT1 inhibitors; μM ($\log IC_{50}$). Circles show molecules with affinity values lower than -9.0 kcal/mol and Total score values greater than 6.0 . Regression lines were added for illustrative purposes.

5.6. Final Selection of NPs as New DNMTs by Cluster Analysis, Contact Patterns and Biological Information Reported So Far

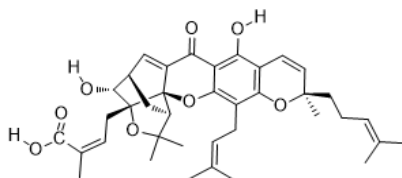
5.6.1 Cluster Analysis 19 NPs selected

Molecular diversity analysis by *k*-mean clustering for calculated 28 MDs of 19 NPs selected, and training and test set compounds; showed better clustering for compounds with *k* value = 11. Below are described the clusters containing the NPs selected: *Cluster 1*; comprised of dihydromunduletone, phloridzin, derrubone, pomiferin and 4,2'-Dihydroxychalcone 4-glucoside were placed in the same cluster with the active compounds ATA, EGCG and NCS97317 with centroid distance values between 0.31 to 0.51; *Cluster 7*: comprised of active compounds SGI-110, laccaic acid, pectolarin, amygdalin, iridin, centaurein, daunorubicin, pyrromycin, naringin grouped with the centroid distance values between 0.19 to 0.63; suggesting their probability as DNMTs. Interesting results were obtained from *Cluster 11* comprised of 9,10-dihydro-12-hydroxygambogic acid, digoxin, reserpine, berbamine, paclitaxel, and dimethyl gambogate. In this case, some NPs were not structurally similar to well-known DNMTs, suggesting that these compounds could become in new scaffold for cancer therapies. Folic acid was grouped in *Cluster 2* with the active compounds aza-Adomet, adoHcy, chlorogenic acid and sinefungin with centroid distance value of 0.46. Considering the representativeness of each cluster, 12 NPs were selected from the last analysis; these NPs were: phloridzin, pomiferin, 2',4'-dihydroxychalcone 4-glucoside, centaurein, daunorubicin, pyrromycin, 9,10-dihydro-12-hydroxygambogic acid, digoxin, reserpine, paclitaxel, folic acid and amygdalin.

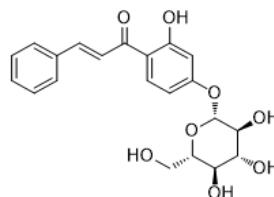
5.6.2. Contact Patterns at Distances Less Than 4 Å

A chemical environment analysis for these 12 selected NPs on the DNMTs binding site was conducted by counting and identifying the nearest-neighbor residues for each compound in order to determinate contact patterns at distances less than 4 Å on DNMTs structures (3SWR and 2QRV), and then comparing contact residues of selected NPs against those observed for known DNMTs, such as RG-108, sinefungin, SGI-110 and ATA (contacts for inactive compounds were also considered). Residues involved in the inhibition mechanism of DNMT1 and DNMT 3A [72, 74], such as, Phe-1145, Glu-1168, Glu-1169, Cys-1191, Glu-1266 and Val-1580 showed distances of less than 4 Å with selected NPs on 3SWR binding site. Furthermore, for 2QRV relevant residues were Phe-636, Ile-639, Glu-660, Val-661 and Asp-682, being these residues of interest in the searching for new DNMTs.

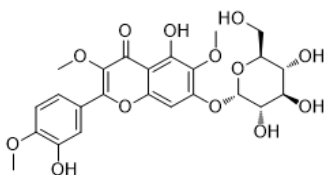
Finally, six NPs were selected as new and promising DNMTis (Figure 5.6); which are structurally different to those DNMT is reported in the literature.



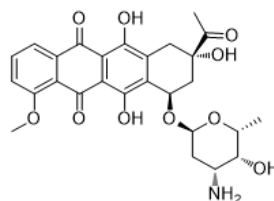
9,10-Dihydro-12-hydroxygambogic acid



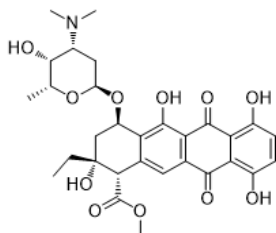
2',4'-Dihydroxychalcone 4'-glucoside



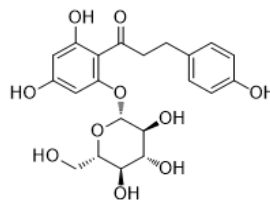
Centaurin



Daunorubicin



Pyrromycin



Phloridzin

Figure 5.6. Six NPs selected as promissory DNMTis.

5.6.3. Biological Information of Selected NPs

Exhaustive searching of biological information for selected NPs was conducted. A summary of the most relevant information for each of these compounds is presented below.

Phloridzin is a dietary natural product specifically found in apples with well-known beneficial biological effects [75]. It has been used as a pharmaceutical and research tool for physiology for over 150 years. This compound has been related to inhibition of the sodium-glucose symporters [76], and commonly applied to the treatment of diseases such as diabetes [77], obesity [78], stress [79], inflammation [80], polycystic kidney disease [81], and cancer [82].

2',4'-Dihydroxychalcone 4'-glucoside is isolated from *Adhatoda vasica* flowers [83]. This chemical contains very little biological information in the literature; however, its aglycone 2', 4'-Dihydroxychalcone and its derivatives have been implicated in pharmacological properties including, antimicrobial [84], antidepressant [85], and antineoplastic effects [86, 87].

Centaurein, a flavonoid isolated from *Bidens pilosa*, has been associated with immunomodulatory [88], antifungal [89], and anti-oxidant properties [90]. The role of centaurein in IFN-gamma regulation has been reported by inducing activity of NFAT and NFkB enhancers in Jurkat cells [91].

Daunorubicin, an anthracycline produced by *Streptomyces peucetius* [92], has been extensively used for the treatment of acute promyelocytic leukemia by acting through epigenetic inactivation of genes in the INK4/CDK/RB cell cycle pathway [93, 94], and other cancer therapies [95, 96], as well as against unwanted intraocular proliferation [97]. However, its anticancer effects have been related to inhibition of DNA topoisomerase II [98].

Pyrrromycin is also an anthracycline produced by *Streptomyces* [99] and its action modes has been mostly related to DNA topoisomerase II inhibition. This NP has shown several pharmacological activities, including antibiotic [100] and antitumor effects [101]. Also, this compound has been identified as an up-regulator of the ATP-binding cassette transporter A1 (ABCA1), a membrane transporter that directly contributes to high-density lipoprotein (HDL) biogenesis [102].

Finally, 9,10-dihydro-12-hydroxygambogic acid is a derivative of gambogic acid, found in *Garcinia hurburyi* tree [103]. Gambogic acid analogs have been proposed as caspases activators and apoptosis inducers [104]. Besides, it has been related to growth inhibition of distinct cancer cell lines, including hepatoma, breast, gastric, lung carcinoma, and also T-cell lymphoma cells [105]. Although it has been related with histone acetyltransferases (HAT) inhibitory properties, its anticancer mechanism is not clearly understood [106].

The discovery of inhibitors of DNMT1 is under permanent attention. A well-known bioassay, which uses a novel non-radioactive high-throughput process, has been employed to assay ligands as human DNMT1 inhibitors. The data are the most comprehensive worldwide (359521 compounds) and the results are publicly available at PubChem (<http://pubchem.ncbi.nlm.nih.gov/>) and ChEMBL (www.ebi.ac.uk/chembl/) databases, under the title: uHTS identification of DNMT1 inhibitors in a Fluorescent Molecular Beacon assay [Primary Screening] (AID: 588458). NPs digoxin, pomiferin, folic acid, paclitaxel, naringin, and amygdalin were classified as inactive for DNMT1 in this assay, and they were not included in the final

group of selected NPs. However, classical DNMTis inhibitors, such as curcumin [33], genistein [107], caffeic acid and chlorogenic acid [40], among others, were also reported as inactive in that experimental assay. Although fluorescence-based high-throughput screening (HTS) has been proposed as an economical, rapid and robust technique [108], these false inactives could be explained considering factors such as low solubility of evaluated compounds and interference by stray excitation light, which may underestimate activities and reduce HTS-hit rates [109].

5.6.4. Binding Mode Analysis for NPs on DNMTs Active Site

The binding pose for two selected NPs with the best affinity value (2',4'-dihydroxychalcone 4'-glucoside) and the total score (9,10-dihydro-12-hydroxygambogic acid) were analyzed by characterizing the interactions on DNMTs binding site, as predicted using LigandScout 3.1 software [63]. This software uses simplified pharmacophores based on Molecular Operating Environment (MOE) to detect the number and nature of interactions existing between ligand-residue on the protein binding site. The binding mode of 9,10-dihydro-12-hydroxygambogic acid and 2',4'-dihydroxychalcone 4'-glucoside on DNMT1 and DNMT3A binding sites are shown in Figure 5.7A and Figure 5.8A, respectively.

Interacting residues for 9,10-dihydro-12-hydroxygambogic acid binding site on DNMT1 determined by LigandScout program are shown in 3D (Figure 5.7b) and 2D (Figure 5.7c) views. Glu-1168 and Gln-1127 presented H-bond interaction with hydroxyl and carboxyl group of 9,10-dihydro-12-hydroxygambogic acid, and hydrophobic interactions were observed for amino acids Phe-648, Met-1169 and Leu-1247 (Figure 5.7c). On the other hand, 2',4'-dihydroxychalcone 4'-glucoside forms H-bonds through the hydroxyl groups present in the glycoside with the backbone of Phe-1145 and Ala-699, and the side chain of Glu-1266 in the ENV motif, which is a target of most DNMTis (motif IV: E/Glu-1266, N/Asn-1267, V/Val-1268). This last residue is an important residue because it participates directly in the mechanism of C5 cytosine methylation by stabilizing the substrate [197]. The residues Met-1169, Leu-1247, Ile-1167, and Phe-1145 showed hydrophobic interactions for this compound (Figure 5.7d and Figure 5.7e). Of interest, Met-1169 and Phe-1145, like Glu-1266 and Glu-1168, are present as interacting residues in the crystallographic structure of DNMT1-sinefungin complex (PDB code: 3SWR).

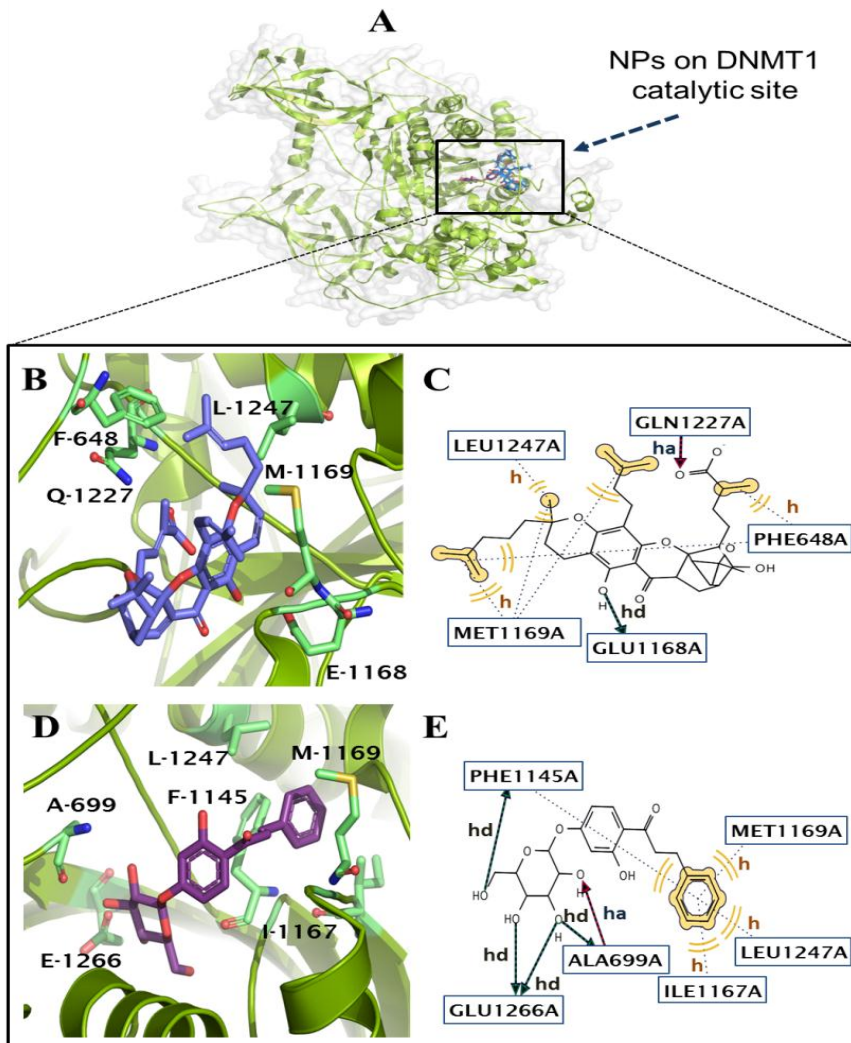


Figure 5.7. DNMT1-NPs (9,10-dihydro-12-hydroxygamboic acid and 2',4'-dihydroxychalcone 4'-glucoside) complexes. The catalytic site is shown in (A). Interacting residues for the best pose of 9,10-dihydro-12-hydroxygamboic acid (3D (B) and 2D (C) views) and 2',4'-dihydroxychalcone 4'-glucoside (3D (D) and 2D (E) views) on DNMT1 binding site as predicted by LigandScout 3.1. Interaction types: h=hydrophobic, ha = H-bond acceptor, hd = H-bond donor.

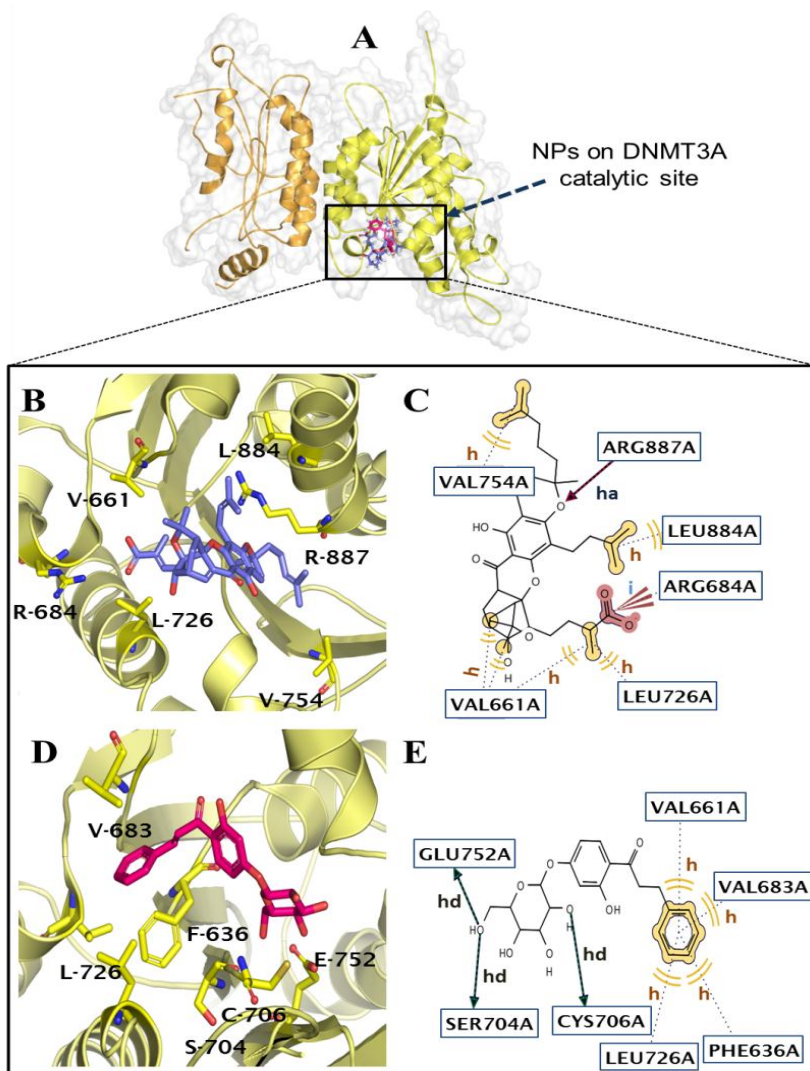


Figure 5.8. DNMT3A-NPs (9,10-dihydro-12-hydroxygamboic acid and 2',4'-dihydroxychalcone 4'-glucoside) complex. The complex is shown in (A). Interacting residues for the best pose of 9,10-dihydro-12-hydroxygamboic acid (3D (B) and 2D (C) views) and 2',4'-dihydroxychalcone 4'-glucoside (3D (B) and 2D (C) views) on DNMT3A binding site as predicted by LigandScout 3.1. Interactions type: i = negative ionizable, h= hydrophobic, ha = H-bond acceptor, hd = H-bond donor.

The best conformation for 9,10-dihydro-12-hydroxygambogic acid on DNMT3A binding site (Figure 5.8B and Figure 5.8C) forms a H-bond with Arg-887, and an ionizable negative interaction with the side-chain of Arg-684 through the carboxyl group. However, only hydrophobic interactions are observed with Val-661, Leu-726, Val-754 and Leu-884. The interactions with Arg-684 and Arg-887 residues have been reported for the inhibitor SGI-1027 on DNMT3A binding site [72]. The best conformations for 2',4'-dihydroxychalcone-4'-glucoside on DNMT3A binding site (Figure 5.8d and Figure 5.8e) showed H-bonds with the side-chain of Ser-704, Cys-706, Glu-752 through the hydroxyl groups of the glycoside fragment. For Phe-636, Val-661, Val-683 and Leu-726 residues only hydrophobic interactions were observed. It is important to highlight that the interaction with Phe-636 on DNMT3A binding site has been reported for known DNMTis, SGI-1027 RG108 and procainamide-conjugate (CBC12) [72]. Also, Phe-636 and Val-683 have been reported for the crystallographic DNMT3A-SAH complex (PDB code: 2QRV).

Binding mode analysis of NPs on DNMTs reveals that compounds such as 9,10-dihydro-12-hydroxygambogic acid and 2',4'-dihydroxychalcone 4'-glucoside have important interactions on DNMT1 and DNMT3A binding sites, according to reports based on the crystallographic structures of inhibitors with DNMT1 (PDB: 3SWR) and DNMT3A (PDB: 2QRV), as well as from molecular docking studies with known DNMTis [43, 45, 72]. These results suggest the potential application of these NPs in anticancer therapies through the reduction of DNMTs activity.

It is clear that some compounds reported here are clinical drugs, such as daunorubicin; which have pharmacokinetic and toxicological profiles as well as a well-known synthetic path. However, to date, these selected NPs have not been reported as DNMTis. Computational approaches proposed here may allow to make repurposing of these NPs in epigenetic studies. Furthermore, these compounds are structurally different from the well-known DNMTis reported so far, opening a new window to the design of more potent and specific compounds in the treatment of cancer and related diseases.

5.7. CONCLUSIONS

Proper identification of a lead molecule is the most critical component of the drug discovery process. To this purpose, this report has shown how computational approaches like QSAR, and molecular docking procedures, combined with statistical techniques analysis could be used as tools to ensure high hit rates expected in the discovery of new cancer drugs. LDA-based QSAR model of active/inactive molecules used in this virtual screening, showed satisfactory results, with an accuracy of 93%, molecular docking results using AutoDock Vina and Surflex-Dock, combined with *k*-

means analysis cluster, with $k=11$, and contact patterns of interacting residues up to 4 Å, suggest that several new structural chemotypes NPs (9,10-dihydro-12-hydroxygambogic acid, phloridzin, 2',4'- dihydrochalcone 4'-glucoside, daunorubicin, pyrromycin and centaurin) can be potential DNMTis. It is also suggested that the therapeutic effect of NPs could be achieved not only by inhibition of DNMT1 but also of DNMT3A. A major perspective of this study is the experimental validation of the consensus hits, and in addition to this, the multistep strategy used here can be implemented to screen other larger natural products databases. Our results also reinforce the notion that compounds with inhibitory DNMT activity can be found in natural sources, including dietary products. The methodology proposed in this study is an innovative approach for targeted identification of novel and selective inhibitors of DNMTs as a first step prior to *in vitro* and *in vivo* evaluations useful in the search of anticancer drugs from NPs.

5.8. REFERENCES

- [1] Ren, J., Singh, B.N., Huang, Q., Li, Z., Gao, Y., Mishra, P., et al. DNA hypermethylation as a chemotherapy target. *Cell Signal*. 2011, 23, 1082-93.
- [2] Vogt, A., Tamewitz, A., J Skoko, RP Sikorski, Giuliano, K., Lazo, J. The Benzo[c]phenanthridine Alkaloid, Sanguinarine, Is a Selective, Cell-active Inhibitor of Mitogen-activated Protein Kinase Phosphatase-1. *J Biol Chem* 2005, 280, 19078.
- [3] Venza, M., Visalli, M., Catalano, T., Fortunato, C., Oteri, R., Teti, D., et al. Impact of DNA methyltransferases on the epigenetic regulation of tumor necrosis factor-related apoptosis-inducing ligand (TRAIL) receptor expression in malignant melanoma. *Biochem Biophys Res Commun*. 2013, 441, 743-50.
- [4] Fernandez, A.F., Huidobro, C., Fraga, M.F. De novo DNA methyltransferases: oncogenes, tumor suppressors, or both? *Trends Genet*. 2012, 28, 474-9.
- [5] Sun, X., He, Y., Huang, C., Ma, T.-T., Li, J. The epigenetic feedback loop between DNA methylation and microRNAs in fibrotic disease with an emphasis on DNA methyltransferases. *Cell Signal*. 2013, 25, 1870-6.
- [6] Santi, D.V., Garrett, C.E., Barr, P.J. On the mechanism of inhibition of DNA-cytosine methyltransferases by cytosine analogs. *Cell*. 1983, 33, 9-10.
- [7] Taylor, S.M., Jones, P.A. Mechanism of action of eukaryotic DNA methyltransferase: Use of 5-azacytosine-containing DNA. *J Mol Biol*. 1982, 162, 679-92.
- [8] Yoder, J.A., Soman, N.S., Verdine, G.L., Bestor, T.H. DNA (cytosine-5)-methyltransferases in mouse cells and tissues. studies with a mechanism-based probe. *J Mol Biol*. 1997, 270, 385-95.
- [9] Yoo, J., Kim, J.H., Robertson, K.D., Medina-Franco, J.L. Molecular Modeling of Inhibitors of Human DNA Methyltransferase with a Crystal Structure: Discovery of a Novel DNMT1 Inhibitor. In: *Advances in Protein Chemistry and Structural Biology*, Christo, C., Tatyana, K.-C. Eds., Academic Press, 2012, Vol. Volume 87, pp. 219-47.

[10] Okano, M., Bell, D.W., Haber, D.A., Li, E. DNA Methyltransferases Dnmt3a and Dnmt3b Are Essential for De Novo Methylation and Mammalian Development. *Cell*. 1999, 99, 247-57.

[11] Li, J.-Y., Pu, M.-T., Hirasawa, R., Li, B.-Z., Huang, Y.-N., Zeng, R., et al. Synergistic Function of DNA Methyltransferases Dnmt3a and Dnmt3b in the Methylation of Oct4 and Nanog. *Mol Cell Biol*. 2007, 27, 8748-59.

[12] Dhawan, D., Ramos-Vara, J.A., Hahn, N.M., Waddell, J., Olbricht, G.R., Zheng, R., et al. DNMT1: An emerging target in the treatment of invasive urinary bladder cancer. *Urol Oncol*. 2013, 31, 1761-9.

[13] Cheng, P., Chen, H., Zhang, R.-P., Liu, S.-r., Zhou-Cun, A. Polymorphism in DNMT1 may modify the susceptibility to oligospermia. *Reprod Biomed Online*. 2014, 28, 644-9.

[14] Bian, E.-B., Huang, C., Wang, H., Chen, X.-X., Zhang, L., Lv, X.-W., et al. Repression of Smad7 mediated by DNMT1 determines hepatic stellate cell activation and liver fibrosis in rats. *Toxicol Lett*. 2014, 224, 175-85.

[15] Castellano, S., Kuck, D., Sala, M., Novellino, E., Lyko, F., Sbardella, G. Constrained Analogues of Procaine as Novel Small Molecule Inhibitors of DNA Methyltransferase-1. *J Med Chem*. 2008, 51, 2321-5.

[16] Asgatay, S., Champion, C., Marloie, G., Drujon, T., Senamaud-Beaufort, C., Ceccaldi, A., et al. Synthesis and Evaluation of Analogues of N-Phthaloyl-L-tryptophan (RG108) as Inhibitors of DNA Methyltransferase 1. *J Med Chem*. 2013, 57, 421-34.

[17] Suzuki, T., Tanaka, R., Hamada, S., Nakagawa, H., Miyata, N. Design, synthesis, inhibitory activity, and binding mode study of novel DNA methyltransferase 1 inhibitors. *Bioorg Med Chem Lett*. 2010, 20, 1124-7.

[18] Valente, S., Liu, Y., Schnekenburger, M., Zwergel, C., Cosconati, S., Gros, C., et al. Selective Non-nucleoside Inhibitors of Human DNA Methyltransferases Active in Cancer Including in Cancer Stem Cells. *J Med Chem*. 2014, 57, 701-13.

[19] Van De Voorde, L., Speeckaert, R., Van Gestel, D., Bracke, M., De Neve, W., Delanghe, J., et al. DNA methylation-based biomarkers in serum of patients with breast cancer. *Mutat Res Rev Mutat Res*. 2012, 751, 304-25.

[20] Mai, A. Targeting Epigenetics in Drug Discovery. *ChemMedChem*. 2014, 9, 415-7.

[21] Lyko, F., Brown, R. DNA Methyltransferase Inhibitors and the Development of Epigenetic Cancer Therapies. *J Natl Cancer Inst*. 2005, 97, 1498-506.

[22] Billam, M., Sobolewski, M., Davidson, N. Effects of a novel DNA methyltransferase inhibitor zebularine on human breast cancer cells. *Breast Cancer Res Treat*. 2010, 120, 581-92.

[23] Gray, S., Baird, A., O'Kelly, F., Nikolaidis, G., Almgren, M., Meunier, A., et al. Gemcitabine reactivates epigenetically silenced genes and functions as a DNA methyltransferase inhibitor. *Int J Mol Med*. 2012, 30, 1505-11.

[24] Fandy, T.E., Jiemi, A., Thakar, M., Rhoden, P., Suarez, L., Gore, S.D. Decitabine Induces Delayed Reactive Oxygen Species (ROS) Accumulation in Leukemia Cells and Induces the Expression of ROS Generating Enzymes. *Clin Cancer Res*. 2014, 20, 1249-58.

[25] Quintas-Cardama, A., Santos, F.P.S., Garcia-Manero, G. Therapy with azanucleosides for myelodysplastic syndromes. *Nat Rev Clin Oncol*. 2010, 7, 433-44.

[26] Méndez-Lucio, O., Tran, J., Medina-Franco, J.L., Meurice, N., Muller, M. Toward Drug Repurposing in Epigenetics: Olsalazine as a Hypomethylating Compound Active in a Cellular Context. *ChemMedChem*. 2014, 9, 560-5.

[27] Brueckner, B., García Boy, R., Siedlecki, P., Musch, T., Kliem, H.C., Zielenkiewicz, P., et al. Epigenetic Reactivation of Tumor Suppressor Genes by a Novel Small-Molecule Inhibitor of Human DNA Methyltransferases. *Cancer Res*. 2005, 65, 6305-11.

[28] Datta, J., Ghoshal, K., Denny, W.A., Gamage, S.A., Brooke, D.G., Phiasivongsa, P., et al. A New Class of Quinoline-Based DNA Hypomethylating Agents Reactivates Tumor Suppressor Genes by Blocking DNA Methyltransferase 1 Activity and Inducing Its Degradation. *Cancer Res*. 2009, 69, 4277-85.

[29] Rilova, E., Erdmann, A., Gros, C., Masson, V., Aussagues, Y., Poughon-Cassabois, V., et al. Design, Synthesis and Biological Evaluation of 4-Amino-N-(4-aminophenyl)benzamide Analogues of Quinoline-Based SGI-1027 as Inhibitors of DNA Methylation. *ChemMedChem*. 2014, 9, 590-601.

[30] Sharma, S., Kelly, T.K., Jones, P.A. Epigenetics in cancer. *Carcinogenesis*. 2010, 31, 27-36.

[31] Medina-Franco, J.L., López-Vallejo, F., Kuck, D., Lyko, F. Natural products as DNA methyltransferase inhibitors: a computer-aided discovery approach. *Mol Divers*. 2011, 15, 293-304.

[32] Cragg, G.M., Newman, D.J., Snader, K.M. Natural Products in Drug Discovery and Development. *J Nat Prod*. 1997, 60, 52-60.

[33] Medina-Franco, J.L. ADVANCES IN COMPUTATIONAL APPROACHES FOR DRUG DISCOVERY BASED ON NATURAL PRODUCTS. *Rev. Latinoamer. Quím*. 2013, 41, 95-110.

[34] Liu, Z., Xie, Z., Jones, W., Pavlovicz, R.E., Liu, S., Yu, J., et al. Curcumin is a potent DNA hypomethylation agent. *Bioorg Med Chem Lett*. 2009, 19, 706-9.

[35] Vaid, M., Prasad, R., Singh, T., Jones, V., Katiyar, S.K. Grape seed proanthocyanidins reactivate silenced tumor suppressor genes in human skin cancer cells by targeting epigenetic regulators. *Toxicol Appl Pharmacol*. 2012, 263, 122-30.

[36] Fang, M.Z., Wang, Y., Ai, N., Hou, Z., Sun, Y., Lu, H., et al. Tea Polyphenol (-)-Epigallocatechin-3-Gallate Inhibits DNA Methyltransferase and Reactivates Methylation-Silenced Genes in Cancer Cell Lines. *Cancer Res*. 2003, 63, 7563-70.

[37] Xie, Q., Bai, Q., Zou, L.-Y., Zhang, Q.-Y., Zhou, Y., Chang, H., et al. Genistein inhibits DNA methylation and increases expression of tumor suppressor genes in human breast cancer cells. *Genes Chromosomes Cancer*. 2014, 53, 422-31.

[38] García, J., Franci, G., Pereira, R., Benedetti, R., Nebbioso, A., Rodríguez-Barrios, F., et al. Epigenetic profiling of the antitumor natural product psammaphin A and its analogues. *Bioorg Med Chem*. 2011, 19, 3637-49.

[39] Agarwal, S., Amin, K., Jagadeesh, S., Baishay, G., Rao, P., Barua, N., et al. Mahanine restores RASSF1A expression by down-regulating DNMT1 and DNMT3B in prostate cancer cells. *Mol Cancer*. 2013, 12, 99.

[40] Lee, W.J., Zhu, B.T. Inhibition of DNA methylation by caffeic acid and chlorogenic acid, two common catechol-containing coffee polyphenols. *Carcinogenesis*. 2006, 27, 269-77.

[41] Fagan, R.L., Cryderman, D.E., Kopelovich, L., Wallrath, L.L., Brenner, C. Laccic Acid A Is a Direct, DNA-competitive Inhibitor of DNA Methyltransferase 1. *J Biol Chem.* 2013, 288, 23858-67.

[42] Siedlecki, P., Boy, R.G., Musch, T., Brueckner, B., Suhai, S., Lyko, F., et al. Discovery of Two Novel, Small-Molecule Inhibitors of DNA Methylation. *J Med Chem.* 2005, 49, 678-83.

[43] Medina-Franco, J., Yoo, J. Docking of a novel DNA methyltransferase inhibitor identified from high-throughput screening: insights to unveil inhibitors in chemical databases. *Mol Divers.* 2013, 17, 337-44.

[44] Singh, N., Dueñas-González, A., Lyko, F., Medina-Franco, J.L. Molecular Modeling and Molecular Dynamics Studies of Hydralazine with Human DNA Methyltransferase 1. *ChemMedChem.* 2009, 4, 792-9.

[45] Medina-Franco, J., Méndez-Lucio, O., Yoo, J. Rationalization of Activity Cliffs of a Sulfonamide Inhibitor of DNA Methyltransferases with Induced-Fit Docking. *Int J Mol Sci.* 2014, 15, 3253-61.

[46] Tripos. Sybyl X. In: 1699S Hanley Rd, St. Louis, MO, 2005.

[47] Mauri, A., Consonni, V., Pavan, M., Todeschini, R. DRAGON software: An easy approach to molecular descriptor calculations. *Match-Commun Math Co.* 2006, 56, 237-48.

[48] StatSoft. Statistica 8.0.360 In: Tulsa, OK, 2007.

[49] Meneses-Marcel, A., Marrero-Ponce, Y., Machado-Tugores, Y., Montero-Torres, A., Pereira, D.M., Escario, J.A., et al. A linear discrimination analysis based virtual screening of trichomonacidal lead-like compounds: Outcomes of in silico studies supported by experimental results. *Bioorg Med Chem Lett.* 2005, 15, 3838-43.

[50] J W Godden, F L Stahura, Bajorath, J. Variability of Molecular Descriptors in Compound Databases Revealed by Shannon Entropy Calculations. *J Chem Inf Comput Sci.* 2000, 40, 796-800.

[51] Godden, J.W., Bajorath, J. Chemical Descriptors with Distinct Levels of Information Content and Varying Sensitivity to Differences between Selected Compound Databases Identified by SE-DSE Analysis. *J Chem Inf Comput Sci.* 2002, 42, 87-93.

[52] Barigye, S.J., Pino Urias, R.W., Marrero-Ponce, Y. IMMAN (Information Theory based Chemometric Analysis). CAMD-BIR Unit, Santa Clara 2013.

[53] Barigye, S.J., Marrero-Ponce, Y., Martínez López, Y., Artilés Martínez, L.M., Pino-Urias, R.W., Martínez Santiago, O., et al. Relations Frequency Hypermatrices in Mutual, Conditional and Joint Entropy-Based Information Indices. *J. Comput. Chem.* 2013, 34, 259-74.

[54] Trott, O., Olson, A.J. AutoDock Vina: Improving the speed and accuracy of docking with a new scoring function, efficient optimization, and multithreading. *J Comput Chem.* 2010, 31, 455-61.

[55] Tuccinardi, T., Poli, G., Romboli, V., Giordano, A., Martinelli, A. Extensive consensus docking evaluation for ligand pose prediction and virtual screening studies. *J. Chem. Inf. Model.* 2014, 54, 2980-6.

[56] Carrasco, M.P., Gut, J., Rodrigues, T., Ribeiro, M.H.L., Lopes, F., Rosenthal, P.J., et al. Exploring the Molecular Basis of Qbc1 Complex Inhibitors Activity to Find Novel Antimalarials Hits. *Mol Inform.* 2013, 32, 659-70.

[57] Jain, A. Surflex-Dock 2.1: Robust performance from ligand energetic modeling, ring flexibility, and knowledge-based search. *J Comput Aided Mol Des.* 2007, 21, 281-306.

[58] Arnatt, C.K., Zhang, Y. G Protein-Coupled Estrogen Receptor (GPER) Agonist Dual Binding Mode Analyses Toward Understanding of Its Activation Mechanism: A Comparative Homology Modeling Approach. *Mol Inform.* 2013, 32, 647-58.

[59] Maldonado-Rojas, W., Olivero-Verbel, J. Food-Related Compounds That Modulate Expression of Inducible Nitric Oxide Synthase May Act as Its Inhibitors. *Molecules.* 2012, 17, 8118-35.

[60] Maldonado-Rojas, W., Olivero-Verbel, J. Potential interaction of natural dietary bioactive compounds with COX-2. *J Mol Graph Model.* 2011, 30, 157-66.

[61] DeLano, W.L. The PyMOL Molecular Graphics System. LLC, D.S. Ed., San Carlos, CA, USA, 1998–2003.

[62] Nguyen, E.D., Norn, C., Frimurer, T.M., Meiler, J. Assessment and challenges of ligand docking into comparative models of G-protein coupled receptors. *PloS one.* 2013, 8, e67302.

[63] Wolber, G., Langer, T. LigandScout: 3-D Pharmacophores Derived from Protein-Bound Ligands and Their Use as Virtual Screening Filters. *J Chem Inf Model.* 2004, 45, 160-9.

[64] Vuorinen, A., Nashev, L.G., Odermatt, A., Rollinger, J.M., Schuster, D. Pharmacophore Model Refinement for 11 β -Hydroxysteroid Dehydrogenase Inhibitors: Search for Modulators of Intracellular Glucocorticoid Concentrations. *Mol Inform.* 2014, 33, 15-25.

[65] Barigye, S.J., Pino Urias, R.W., Marrero-Ponce, Y., et al. IMMAN (Information Theory based Chemometric Analysis). CAMD-BIR Unit, Santa Clara 2013.

[66] Portugal, J. Evaluation of molecular descriptors for antitumor drugs with respect to noncovalent binding to DNA and antiproliferative activity. *BMC Pharmacol.* 2009, 9, 11.

[67] Shi, L.M., Fan, Y., Myers, T.G., O'Connor, P.M., Paull, K.D., Friend, S.H., et al. Mining the NCI Anticancer Drug Discovery Databases: Genetic Function Approximation for the QSAR Study of Anticancer Ellipticine Analogues. *J Chem Inf Comput Sci.* 1998, 38, 189-99.

[68] Zhang, S., Wei, L., Bastow, K., Zheng, W., Brossi, A., Lee, K.-H., et al. Antitumor Agents 252. Application of validated QSAR models to database mining: discovery of novel tylophorine derivatives as potential anticancer agents. *J Comput Aided Mol Des.* 2007, 21, 97-112.

[69] Montero-Torres, A., García-Sánchez, R.N., Marrero-Ponce, Y., Machado-Tugores, Y., Nogal-Ruiz, J.J., Martínez-Fernández, A.R., et al. Non-stochastic quadratic fingerprints and LDA-based QSAR models in hit and lead generation through virtual screening: theoretical and experimental assessment of a promising method for the discovery of new antimalarial compounds. *Eur J Med Chem.* 2006, 41, 483-93.

[70] Casañola-Martin, G.M., Marrero-Ponce, Y., Khan, M.T.H., Khan, S.B., Torrens, F., Pérez-Jiménez, F., et al. Bond-Based 2D Quadratic Fingerprints in QSAR Studies: Virtual and In vitro Tyrosinase Inhibitory Activity Elucidation. *Chem Biol Drug Des.* 2010, 76, 538-45.

[71] Galvez-Llompарт, M., Recio Iglesias, M., Gálvez, J., García-Domenech, R., DOI. Novel potential agents for ulcerative colitis by molecular topology: suppression of IL-6 production in Caco-2 and RAW 264.7 cell lines. *Mol Divers.* 2013, 17, 573–93.

[72] Yoo, J., Choi, S., Medina-Franco, J.L. Molecular modeling studies of the novel inhibitors of DNA methyltransferases SGI-1027 and CBC12: Implications for the mechanism of inhibition of DNMTs. *PloS one.* 2013, 8, e62152.

[73] Hare, A.A., Leng, L., Gandavadi, S., Du, X., Cournia, Z., Bucala, R., et al. Optimization of *N*-benzyl-benzoxazol-2-ones as receptor antagonists of macrophage migration inhibitory factor (MIF). *Bioorg Med Chem Lett.* 2010, 20, 5811-4.

[74] Jia, D., Jurkowska, R.Z., Zhang, X., Jeltsch, A., Cheng, X. Structure of Dnmt3a bound to Dnmt3L suggests a model for de novo DNA methylation. *Nature.* 2007, 449, 248-51.

[75] Nair, S., Ziaullah, Z., Rupasinghe, H.P.V. Phloridzin fatty acid esters induce apoptosis and alters gene expression in human liver cancer cells (261.2). *FASEB J.* 2014, 28.

[76] Ehrenkranz, J.R., Lewis, N.G., Ronald Kahn, C., Roth, J. Phlorizin: a review. *Diabetes Metab Res Rev.* 2005, 21, 31-8.

[77] Zhao, H., Yakar, S., Gavriloа, O., Sun, H., Zhang, Y., Kim, H., et al. Phloridzin improves hyperglycemia but not hepatic insulin resistance in a transgenic mouse model of type 2 diabetes. *Diabetes.* 2004, 53, 2901-9.

[78] Najafian, M., Jahromi, M.Z., Nowrooznejhad, M.J., Khajeaian, P., Kargar, M.M., Sadeghi, M., et al. Phloridzin reduces blood glucose levels and improves lipids metabolism in streptozotocin-induced diabetic rats. *Mol Biol Rep.* 2012, 39, 5299-306.

[79] Wang, G.-E., Li, Y.-F., Wu, Y.-P., Tsoi, B., Zhang, S.-J., Cao, L.-F., et al. Phloridzin improves lipoprotein lipase activity in stress-loaded mice via AMPK phosphorylation. *Int J Food Sci Nutr.* 2014, 0, 1-7.

[80] Huang, W.C., Chang, W.T., Wu, S.J., Xu, P.Y., Ting, N.C., Liou, C.J. Phloretin and phlorizin promote lipolysis and inhibit inflammation in mouse 3T3-L1 cells and in macrophage-adipocyte co-cultures. *Mol Nutr Food Res.* 2013, 57, 1803-13.

[81] Wang, X., Zhang, S., Liu, Y., Spichtig, D., Kapoor, S., Koepsell, H., et al. Targeting of sodium–glucose cotransporters with phlorizin inhibits polycystic kidney disease progression in Han: SPRD rats. *Kidney Int.* 2013.

[82] Leveen, H.H., Leveen, R.F., LeVeen, E.G. Inhibiting glucose transport. Google Patents, 1989.

[83] Bhartiya, H.P., Gupta, P.C. A chalcone glycoside from the flowers of *Adhatoda vasica*. *Phytochemistry.* 1982, 21, 247.

[84] Alvarez, M., Debattista, N., Pappano, N. Antimicrobial activity and synergism of some substituted flavonoids. *Folia Microbiol (Praha).* 2008, 53, 23-8.

[85] Guan, L.-P., Zhao, D.-H., Chang, Y., Wen, Z.-S., Tang, L.-M., Huang, F.-F. Synthesis of 2, 4-dihydroxychalcone derivatives as potential antidepressant effect. *Drug Res (Stuttg).* 2013, 63, 46-51.

[86] Xie, C., Sun, Y., Pan, C.-Y., Tang, L.-M., Guan, L.-P. 2, 4-Dihydroxychalcone derivatives as novel potent cell division cycle 25B phosphatase inhibitors and protein tyrosine phosphatase 1B inhibitors. *Pharmazie*. 2014, 69, 257-62.

[87] Yang, G.-M., Yan, R., Wang, Z.-X., Zhang, F.-F., Pan, Y., Cai, B.-C. Antitumor effects of two extracts from *Oxytropis falcata* on hepatocellular carcinoma in vitro and in vivo. *Chin J Nat Med*. 2013, 11, 519-24.

[88] Soidrou, S.H., Bousta, D., Lachkar, M., Hassane, S.O., El Youbi-Hamsas, A., El Mansouri, L., et al. Immunomodulatory Activity of Phenolic Fraction from *Piper Borbonense* and *Cassytha Filiformis* Growing in Comoros Islands. In: *Chemistry: The Key to our Sustainable Future*, Springer, 2014, pp. 105-12.

[89] Policegoudra, R., Chattopadhyay, P., Aradhya, S., Shivaswamy, R., Singh, L., Veer, V. Inhibitory effect of *Tridax procumbens* against human skin pathogens. *J Herb Med*. 2014, 4, 83-8.

[90] Bartolome, A.P., Villaseñor, I.M., Yang, W.-C. *Bidens pilosa* L.(Asteraceae): Botanical properties, traditional uses, phytochemistry, and pharmacology. *Evid Based Complement Alternat Med*. 2013, 2013.

[91] Chang, S.-L., Chiang, Y.-M., Chang, C.L.-T., Yeh, H.-H., Shyur, L.-F., Kuo, Y.-H., et al. Flavonoids, centaurein and centaureidin, from *Bidens pilosa*, stimulate IFN- γ expression. *J Ethnopharmacol*. 2007, 112, 232-6.

[92] Stutzman-Engwall, K.J., Otten, S., Hutchinson, C.R. Regulation of secondary metabolism in *Streptomyces* spp. and overproduction of daunorubicin in *Streptomyces peucetius*. *J Bacteriol*. 1992, 174, 144-54.

[93] Adès, L., Chevret, S., Raffoux, E., Guerci-Bresler, A., Pigneux, A., Vey, N., et al. Long-term follow-up of European APL 2000 trial, evaluating the role of cytarabine combined with ATRA and Daunorubicin in the treatment of nonelderly APL patients. *Am J Hematol*. 2013, 88, 556-9.

[94] Chim, C.S., Wong, A.S.Y., Kwong, Y.L. Epigenetic inactivation of INK4/CDK/RB cell cycle pathway in acute leukemias. *Annals of Hematology*. 2003, 82, 738-42.

[95] Schreier, V.N., Pethő, L., Orbán, E., Marquardt, A., Petre, B.A., Mező, G., et al. Protein Expression Profile of HT-29 Human Colon Cancer Cells after Treatment with a Cytotoxic Daunorubicin-GnRH-III Derivative Bioconjugate. *PloS one*. 2014, 9, e94041.

[96] Zanette, R.A., Kontoyiannis, D.P. Pre-exposure of *Candida* species to cytarabine and daunorubicin does not affect their in vitro antifungal susceptibility and virulence in flies. *Virulence*. 2013, 4, 344.

[97] Chhablani, J., Nieto, A., Hou, H., Wu, E.C., Freeman, W.R., Sailor, M.J., et al. Oxidized porous silicon particles covalently grafted with daunorubicin as a sustained intraocular drug delivery system. *Invest Ophthalmol Vis Sci*. 2013, 54, 1268-79.

[98] Hasinoff, B.B., Yalowich, J.C., Ling, Y., Buss, J.L. The effect of dexrazoxane (ICRF-187) on doxorubicin- and daunorubicin-mediated growth inhibition of Chinese hamster ovary cells. *Anticancer Drugs*. 1996, 7, 558-67.

[99] Igina, E., Tulemisova, K., Golubchikov, V., Nikitina, E. Comparison of antibiotic complexes formed by cultures of *Streptomyces griseoruber*. *Antibiot Khimioter*. 1989, 34, 13-6.

[100] Oki, T. New anthracycline antibiotics. *Jpn J Antibiot.* 1977, 30, 70-84.

[101] Nettleton Jr, D.E., Balitz, D.M., Doyle, T.W., Bradner, W.T., Johnson, D.L., O'Herron, F.A., et al. Antitumor agents from bohemiacid complex, III. The isolation of marcellomycin, musettamycin, rudolphomycin, mimimycin, collinemycin, alcindromycin, and bohemamine. *J Nat Prod.* 1980, 43, 242-58.

[102] Gao, J., Xu, Y., Yang, Y., Yang, Y., Zheng, Z., Jiang, W., et al. Identification of upregulators of human ATP-binding cassette transporter A1 via high-throughput screening of a synthetic and natural compound library. *J Biomol Screen.* 2008.

[103] Zhang, H.-Z., Kasibhatla, S., Wang, Y., Herich, J., Guastella, J., Tseng, B., et al. Discovery, characterization and SAR of gambogic acid as a potent apoptosis inducer by a HTS assay. *Bioorg Med Chem.* 2004, 12, 309-17.

[104] Cai, S.X., Drewe, J.A., Kasibhatla, S., Tseng, B., Wang, Y., Zhang, H.Z. Gambogic acid, analogs and derivatives as activators of caspases and inducers of apoptosis. *Google Patents*, 2002.

[105] Li, R., Chen, Y., Zeng, L.-l., Shu, W.-x., Zhao, F., Wen, L., et al. Gambogic acid induces G0/G1 arrest and apoptosis involving inhibition of SRC-3 and inactivation of Akt pathway in K562 leukemia cells. *Toxicology.* 2009, 262, 98-105.

[106] Furdas, S.D., Kannan, S., Sippl, W., Jung, M. Small Molecule Inhibitors of Histone Acetyltransferases as Epigenetic Tools and Drug Candidates. *Arch Pharm (Weinheim).* 2012, 345, 7-21.

[107] Li, Y., Tollefsbol, T.O. Impact on DNA methylation in cancer prevention and therapy by bioactive dietary components. *Curr Med Chem.* 2010, 17, 2141.

[108] Ye, Y., Stivers, J.T. Fluorescence-based high-throughput assay for human DNA (cytosine-5)-methyltransferase 1. *Anal Biochem.* 2010, 401, 168-72.

[109] Di, L., Kerns, E.H. Biological assay challenges from compound solubility: strategies for bioassay optimization. *Drug Discov Today.* 2006, 11, 446-51.

Chapter 6



CHAPTER 6. ANTICANCER ACTIVITY OF NATURAL DNA METHYLTRANSFERASE INHIBITORS AND INTERACTION WITH HUMAN SERUM ALBUMIN

6.1. ABSTRACT

Human DNA methyltransferases (DNMTs) have been proposed as important targets in epigenetic therapy. The overexpression levels of these DNMTs are reportedly in several cancers including colon, breast, prostate, liver, skin and leukemia. Therefore, the searching for DNA methyltransferase inhibitors (DNMTis) has become an alternative for cancer treatment. Virtual screening protocol showed that natural products (NPs) gambogic acid, phloridzin and digoxin have the potential to interact with DNMTs [296]. In this work, anti-methylating activity of three natural compounds (gambogic acid, phloridzin and digoxin), identified as potential inhibitors of DNMT1, were evaluated using the C-5 DNA methylase (M.SssI) and digestion with restriction enzyme (Bsh1236I), with a 465 bp fragment from human p16Ink4a promoter region. Additionally, these compounds were evaluated as antineoplastic agents in human breast adenocarcinoma (MCF-7), and human colon adenocarcinoma (HT-29) cell lines utilizing the MTT assay after 72 h exposure. The results showed that gambogic acid showed the most potent inhibitory properties on DNMT1 activity. However, digoxin was most effective toward HT-29 ($IC_{50} = 86 \pm 2$ nM) compared with gambogic acid ($IC_{50} = 2.9 \pm 0.2$ μ M) and phloridzin ($IC_{50} > 450$ μ M). MTT assays also showed to digoxin with a higher cytotoxic activity against MCF-7 cells ($IC_{50} = 63 \pm 1$ nM) followed by gambogic acid ($IC_{50} = 3.5 \pm 0.1$ μ M). Phloridzin did not elicit cytotoxic activity against MCF-7 or HT-29. These natural

products (gambogic acid, and digoxin) also could interact with human serum albumin (HSA), according to fluorescence spectroscopy, circular dichroism (CD), UV-Vis and molecular modeling. These data suggest that gambogic acid and digoxin could be potential anticancer drugs and serve as scaffold for designing new and more potent molecules via DNMTs inhibition for cancer therapies.

6.2. INTRODUCTION

In many normal cellular processes it is involved in epigenetic consisting essentially of DNA methylation [2, 3]. Whereas our cells all have the same DNA, but our bodies contain many different types of cells: neurons, liver cells, pancreatic cells, inflammatory cells, and others. This fact explain because the cells, tissues and organs are different. Mainly because there are genes that are "active" or expressed, as well as others that are "inactive" or inhibited [4, 5]. Epigenetic silencing being known as a mechanism to disable genes, thereby contribute to processes of differential expression. This process may also explain, in part, why the twins (with the same genetic characteristics) are not phenotypically identical. That is why epigenetics is important for embryonic development, X chromosome inactivation in female mammals [6, 7], supporting the importance of regulating gene expression by epigenetic changes.

DNA methylation regulates gene expression in mammalian development [8]. However, hypermethylation of the promoter regions play an important role in the development of cancer by transcriptional silencing of genes regulating cell normal development, such as tumor suppressor genes [9, 10]. DNA methylation is catalyzed by DNA methyltransferases (DNMTs) [11,12]. These enzymes are responsible of transferring a methyl group from S-adenosyl-L-methionine (SAM) to carbon-5 of cytosine in DNA [13, 14]. Three types of DNMTs have been identified, DNMT3 (DNMT3A and DNMT3B) related with *de novo* DNA methylation [15, 16], and DNMT1, the most abundant and active, related with maintenance of DNA methylation patterns, such as shown in Figure 6.1 [17, 18]. DNMT1 has been reported with an important role in carcinogenesis [19, 20] and related with hypermethylation of promoter of tumor suppressor genes [21, 22]. Currently, DNMT1 are important targets in cancer therapies, with remarkable interest in searching of new and more potent specific inhibitors of DNMT1 [14, 23].

DNMTs inhibitors have been classified as nucleosides (azacitidine, decitabine and zebularine) [24-26] and non-nucleoside (sinefungin, RG-108 and SGI-1027, SW155246, SID49645275, among others) [27-30]. However, only two of them, azacitidine and decitabine, have been approved as drugs for the treatment of myeloplastic syndromes [31], although side effects have been reported [32, 33].

Natural compounds such as, epigallocatechin-3-gallate (EGCG), curcumin, genistein, psammaplina A, laccic acid, have been proposed as inhibitors of DNMT1 [1, 34, 35]. However, these exhibit a weak inhibitory activity. Computational methods have served for searching of new DNMT1 inhibitors. Recently, natural compounds have been re-taken as a promising source of new and selective compounds against cancer [1, 24].

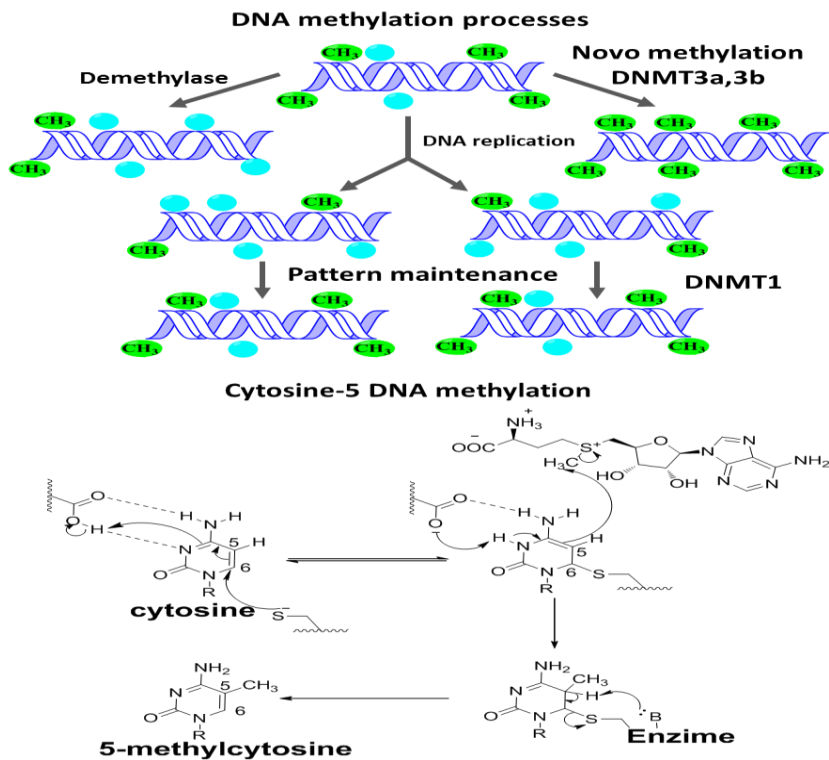


Figure 6.1. Proposed catalytic mechanism for DNA methylation by DNMTs.

In this work the anti-methylating activity of three natural compounds (gambogic acid, phloridzin and digoxin), identified as potential inhibitors of DNMT1, was evaluated by virtual screening [1], using the C-5 DNA methylase (M.SssI) and digestion with restriction enzyme (Bsh1236I), with a 465 bp fragment from human p16^{ink4a} promoter region [36]. Furthermore its antineoplastic activity was evaluated with human cancer cells HT-29 and MCF-7. Additionally, the interaction of these compounds with human albumin was studied by spectroscopic methods (circular dichroism, UV-VIS, and quenching of fluorescence) and computational methods of molecular protein-ligand docking.

6.3. MATERIALS AND METHODS

6.3.1. Molecular Modelling of Interaction of NPs with human DNMT1

The crystal structure of DNMT1 (PDB: 3SWR) was used for the docking studies. The water molecules were removed and the protein structure was minimized with the Powell method with Kollman United/All Atom force field and the Amber charges. Finally, the protein structure was prepared for the docking runs performed with Surflex-Dock from SYBYL X-2.0 package [1]. 3D structures of gambogic acid, digoxin and phloridzin were optimized using DFT with B3LYP 6-31-G basis set with Gaussian 09 program, and the final structure was saved as Mol2 format [37]. Docking calculation were performed by flexible docking algorithm with default settings and using the protocol on co-crystallized ligand sinefungin, threshold 0.1 and bloat 10. The poses with the most higher Total score (-logkd) values were saved for identifying of the main interacting residues in the binding site HAS-gambogic acid by LigandScout 3.0 program [38].

6.3.2. In vitro Evaluation of the Inhibitory Activity against DNMT1 of Promising Natural Compounds.

The inhibitory activity against DNMT1 of natural compounds, gambogic acid, phloridzin and digoxin was evaluated using the methylation assay [230], the substrate DNA for the in vitro was a 465 bp fragment from the promoter region of the human p16^{ink4a} gene obtained for PCR, using DNA extracted from human blood, and the primers, Forward: 5'-ACGCCTTTGCTGGCAGCGGG-3' Reverse: 5'-GCCAGTCAGCCGAAGGCTCCATG-3'. The methylation reaction contained 950 to 1000 ng substrate DNA and 1 μ L of M.SssI methylase (CpG Methyl transferase, Thermo Fisher Scientific, #EM0821) in a final volume of 20 μ L. Evaluated natural compounds were added to final concentrations of 5 to 2000 μ mol/L, respectively. Methylation reactions were performed at 37 °C for 1 hours. After completion, the reaction was inactivated at 65°C for 15 minutes and the DNA was purified using the

Thermo Scientific GeneJET PCR Purification Kit (Thermo Fisher Scientific, #K0701). The DNA was eluted with 20 μL of elution buffer to increase the concentration, and subsequently digested for 1 hour at 37 $^{\circ}\text{C}$ with the restriction enzyme Bsh1236I (BstUI, Thermo Fisher Scientific, #ER0922). The reaction products were analyzed by electrophoresis on 1.2% Tris-borate EDTA agarose gels.

6.3.3. Evaluation of antitumor activity of natural compounds in MCF-7 and HT-29 cells.

Evaluation of the anticarcinogenic properties of natural compounds was performed by the MTT reduction assays to 72 hours with breast cancer (MCF-7) and colon (HT-29) cell lines, both of human origin.

Breast (MCF-7) and colon (HT-29) cancer cells.

HT-29 cells were cultured in Dulbecco's modified medium (DMEM) Eagle supplemented 10% fetal bovine serum, penicillin (100 U/mL), streptomycin (10 $\mu\text{g}/\text{mL}$) and 0.2 mM sodium pyruvate. At the same time the cell line MCF-7 was grown in Eagle's minimum essential medium (EMEM), supplemented with 10% fetal bovine serum. All cell cultures (HT-29 and MCF-7) were incubated in an atmosphere with 5% CO_2 and 100% relative humidity at 37 $^{\circ}\text{C}$. Maintenance of cell lines was established by weekly passes and changing the culture medium twice a week [39].

HT-29 and MCF-7 cell viability by MTT assay.

Cells were pre-incubated at a concentration of 1×10^6 cells/mL in culture medium for 2 hours at 37 $^{\circ}\text{C}$ and 5% CO_2 . They were then seeded at a concentration of 1×10^4 cells in 100 μL of culture medium and different concentrations (in order μM) the compound evaluated dissolved in solution of 5% DMSO were placed in microplates (tissue culture grade, 96 well, flat bottom) and incubated for 72 hours at 37 $^{\circ}\text{C}$ and 5% CO_2 . For each well were subsequently added 75 μL of MTT (for final concentration of 1 mg/mL in medium for each type of cells) and incubated for 2 hours at 37 $^{\circ}\text{C}$ and 5% CO_2 . Untreated cells (only 5% DMSO) were taken as negative control [40]. Controls and samples were made in lines of eight wells for each concentration and three replicates of each compound for cell line employed.

The spectrophotometric absorbance of the samples was measured using a microplate reader (ELx800 - BioTek). The wavelength for the absorbance of formazan product was set between 570 and 620 nm. The IC_{50} , defined as the concentration of compound required to inhibit cell growth to 50% was determined by plotting a graph of Log (concentration of evaluated compound) vs % inhibition of cell growth. A line drawn from the 50% value on the Y axis meets the curve and interpolates the X axis, whose value is the Log (molar concentration of the

compound) [39]. The antilog of this value gives the IC_{50} value. The percentage inhibition of the tested compounds against cell lines tested was calculated using the following formula:

$$\% \text{ Living cells} = ((As - Ab) / ((Ac - Ab)) \times 100$$

Where, **As** = absorbance of the sample **Ab** = absorbance of the blank (culture medium), and **Ac** = absorbance of the negative control (untreated cells).

% Inhibition = 100% living cells

6.3.4. Evaluation of the interaction of natural compounds human serum albumin (HSA) using UV-VIS, quenching of fluorescence and UV-CD

Natural compounds were also evaluated as ligands of human serum albumin (HSA), which is the most abundant protein and transporter drug of human blood. For this, different spectroscopic techniques were used such as ultraviolet-visible (UV-VIS), quenching of fluorescence and circular dichroism (UV-CD).

UV-VIS spectra for titration of HSA with natural compounds evaluated

UV-VIS UV-Vis spectra were recorded with a double beam Lambda Bio 20 Perkin Elmer spectrophotometer for certification of HSA with natural products (gambogic acid and digoxin), with a scan absorbance between 200 and 400 nm for all assays. The volume of HSA at a concentration of 2.5×10^{-5} M was 1 mL, and the concentration ranges of the compounds tested were between 0 and 16.4 μ M based on the final volume. Solutions of protein and ligands were prepared in buffer 10 mM phosphate, 20 mM NaCl at pH 7.4.

Quenching fluorescence spectra for titration of HSA with natural compounds evaluated

The interaction of HSA with natural compounds was also evaluated with fluorescence quenching spectroscopy. Titrations were performed HSA at a concentration of 2.5×10^{-5} M with concentrations for natural compounds between 0 and 16.4 μ M. Solutions of protein and ligands were prepared in buffer 10 mM phosphate, 20 mM NaCl at pH 7.4. Excitation wavelength was 280 nm and the emission spectra were obtained by scan between 285 to 400 nm using a Shimadzu RF-5301 PC spectrofluorophotometer equipped with a temperature controller with. Titrations were realized with three different temperatures (303, 310 and 317 K) [41]. The Van't Hoff equation, $\ln K = -\Delta H^0/RT + \Delta S^0/R$, was used to determine the thermodynamic parameters governing the HSA–natural products interactions.

Molecular docking for HSA-gambogic acid complex

The crystal structure of HSA (PDB: 4S1Y) was used for the docking studies. The water molecules were removed and the protein structure was minimized with the Powell method with Kollman United/All Atom force field and the Amber charges. Finally, the protein structure was prepared for the docking runs performed with Surflex–Dock from SYBYL X-2.0 package [1]. 3D structure of gambogic acid was optimized using DFT with B3LYP 631-G basis set with Gaussian 09 program, and the final structure was saved as Mol2 format [37]. Docking calculation employs an automatic flexible docking algorithm with default settings and using the protocol automatic, threshold 0.1 and bloat 10. The poses with the most higher Total score (-logkd) values were saved for identifying of the main interacting residues in the binding site HAS-gambogic acid by LigandScout 3.0 program [38].

UV-CD spectra for titration of HSA with gambogic acid

UV-CD spectral for titration of HSA with gambogic acid was performed, solutions of protein and ligand were prepared in buffer 10 mM phosphate, 20 mM NaCl at pH 7.4. Far UV spectra were obtained by scanning of wavelength between 190 nm to 250 nm, for concentrations of 0 to 1.25 μ M vs mean residue molar ellipticity at 209.6 nm and 222 nm using a Jasco, J-810 spectropolarimeter, equipped with a xenon lamp monochromatic linearly polarized and a temperature controller accessory. Six scans were accumulated within the spectral range of 195–250 nm, at a scan rate of 100 nm/min, a response time of 2 s, bandwidth of 2 nm, and pitch data of 0.1 nm. (+)-10-Camphorsulfonic acid was used for calibration of the spectropolarimeter following the manufacturer's instructions [42]. Data analysis were performed using the software supplied by the manufacturer, where only baseline correction at 245 nm and 250 nm for far UV CD were performed. The relationship between the concentration of acid gambogic and ellipticity for both wavelengths was studied for protein-ligand complex [39].

6.4. RESULTS AND DISCUSSION

6.4.1. Interaction of evaluated natural compound with DNMT1

Molecular docking protein ligand showed that gambogic acid (-logKd=11.6), digoxin (-logKd = 6.6) and phloridzin (-log Kd= 9.2) binding to hDNMT1 (PDB: 3SWR) on catalytic site (Figure 6.2). Main residues involved in the interaction were predicted by LigandScout 3.1, showing important residues for enzyme activity such

as Cys-1191 and Glu-1168 [43], among others. Additionally, these residues are presents in the interaction of DNMT1 with co-crystallized inhibitor sinefungin [1].

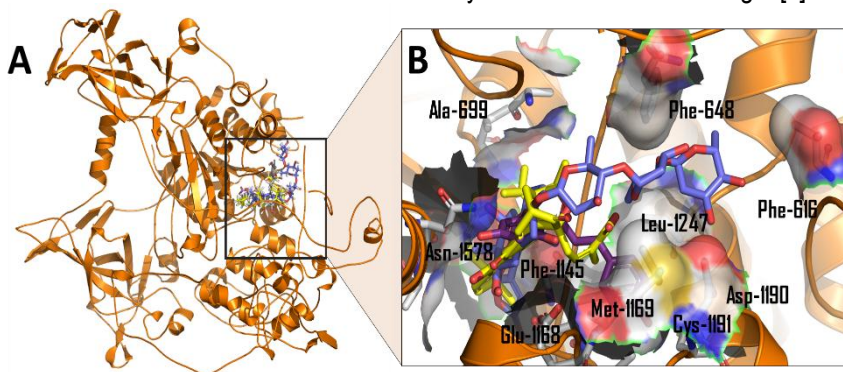


Figure 6.2. Human DNMT1-natural compounds complex binding site (A), and main residues involved in the interaction for gambogic acid (yellow), digoxin (blue) and phloridzin (purple) (B) predicted by LigandScout 3.1.

6.4.2. Inhibition of Purified Recombinant DNA Methyltransferase Activity by Evaluated Natural Compounds.

In vitro methylation assay was performed [36] (Figure 6.3) with previous optimization assays for working range for concentration of natural compounds and reaction time of M.SssI for human p16^{Ink4a} promoter region (Figure 6.3A) methylation and posterior digestion with Bsh1236I restriction enzyme were performed for establishing of the best conditions for assays. Several times were evaluated (15, 30, 60 and 120 minutes), showing that only 15 minutes are enough for methylation of 1 ng of human p16^{Ink4a} promoter region obtained by PCR (Figure 6.3B).

Treatments with gambogic acid (GA), digoxin (DG) at 500 μM , resulted in a detectable decrease in DNA methyltransferase activity, as visualized by the appearance of small Bsh1236I restriction fragments in the electrophoresis analysis. However, phloridzin (PZ) required a higher concentration about 2000 μM for present any inhibitory effect on DNA methylation (Figure 6.3C). Surprising, GA presented the most potent DNMT1 inhibition with appreciable inhibition in concentrations of 5 μM (Figure 6.3D), being these results better than those reported for the RG-108 inhibitor evaluated by this protocols [36].

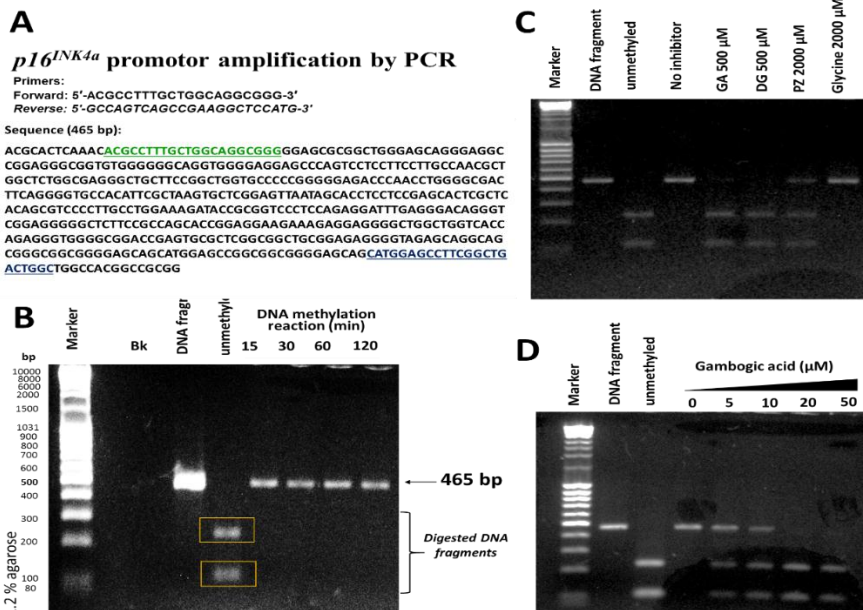


Figure 6.3. In vitro inhibition of DNA methylation for natural compounds. The substrate DNA for the in vitro methylation assay was a 465 bp fragment from human p16^{INK4a} promoter region obtained by PCR (A) Optimization of reaction time for DNA methylation by M.SssI and posterior digestion with Bsh1236I restriction enzyme by 1 hour (B). Treatment with gambogic acid (GA), digoxin (DG, at 500 μ M and phloridzin (PZ at 200 μ M) showed reduction of DNA methylation (B). Gambogic acid presented potent inhibitory activity even at treatment of 5 μ M (D).

6.4.3. Antineoplastic activity of natural compounds on MCF-7 and HT-29 cells.

The anti-proliferative activity of gambogic acid, digoxin and phloridzin was determined in breast cancer cells (HT-29) cell lines and colon cancer (MCF-7) using 3-(4,5-dimethylthiazol-2-yl)-2,5-diphenyltetrazolium bromide (MTT) assay for cell viability after 72 h exposure [99]. Control experiments were carried out in a medium 100% and 5% DMSO Medium. A graph of representative dose response of natural products gambogic and digoxin against HT-29 and MCF-7 is shown in Figure 6.4. However, phloridzin didn't show cytotoxic activity against MCF-7 or HT-29 cells at lower concentrations 75 μ M.

Results shown that digoxin, a cardiac glycosides commonly used therapy for rate control in atrial fibrillation [44] showed the most potent effects in both cell lines. The IC₅₀ values were 86 \pm 2 nM and 63 \pm 1 μ M for HT-29 and MCF-7 cells respectively. Gambogic acid also showed antiproliferative activity for HT-29 and MCF-7 cells (288 \pm

20 nM and $350 \pm 10 \mu\text{M}$ respectively). This obtained data support their reported antineoplastic activity [45, 46]. Several studies had reported that digoxin can reduce prostate cancer risk, as a drug for prostate cancer treatment [47, 48]. Gambogic acid also had been with activity against gastric cancer and glioblastoma [49, 50]. However, anticancer mechanism for these compounds are not yet all clear. According to the data suggests that digoxin and gambogic acid could have explained its activity via inhibition of DNMT1, which have been reported in higher levels in breast and colon cancer [51, 52].

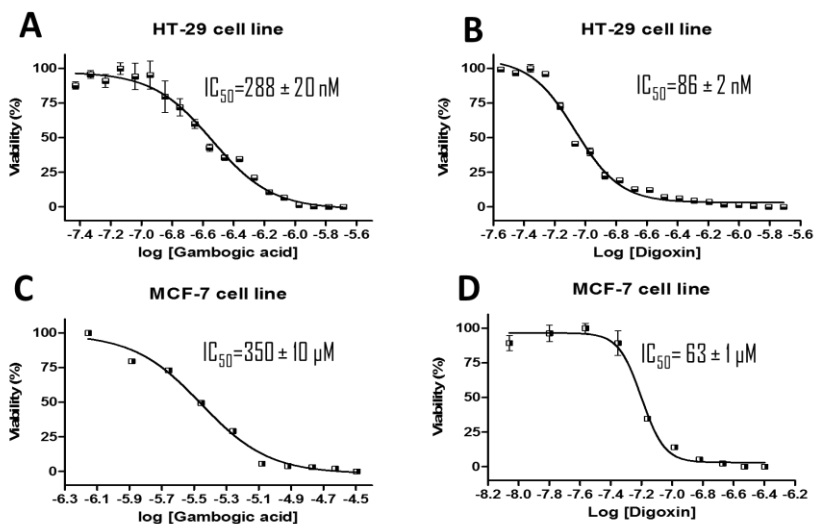


Figure 6.4. Cytotoxic properties of evaluated natural compounds. Dose-response curves of gambogic acid againsts HT-29 (A) and MCF-7 (C). Dose-response curves of digoxin into HT-29 (B) and MCF-7 (D). Phloridzin not presented cytotoxic activity for concentrations of 450 μM . The IC₅₀ values are shown.

6.4.4. Spectroscopic studies and molecular docking for interaction of natural compounds with HAS

Evaluation of HSA-natural compound interaction by UV-VIS

Titration of HSA with natural compounds evaluated, showed only for the HSA-gambogic acid complex increases absorbance values at 280 and 365 nm (Figure 6.5A), suggesting the protein ligand interaction. However, in the titration for digoxin, significant changes were not observed comparing with the initial spectrum of the protein (Figure 6.5B). The absorption spectrum for the compounds tested at the highest concentration titration (16.4 μM) showed that gambogic acid has absorption

peaks between 250 and 400 nm (Figure 6.5C), requiring the correction methods for calculations thermodynamic parameters with fluorescence quenching spectroscopy. For digoxin, absorption peaks were not presented in this area so that no correction methods will be required for fluorescence analysis [39].

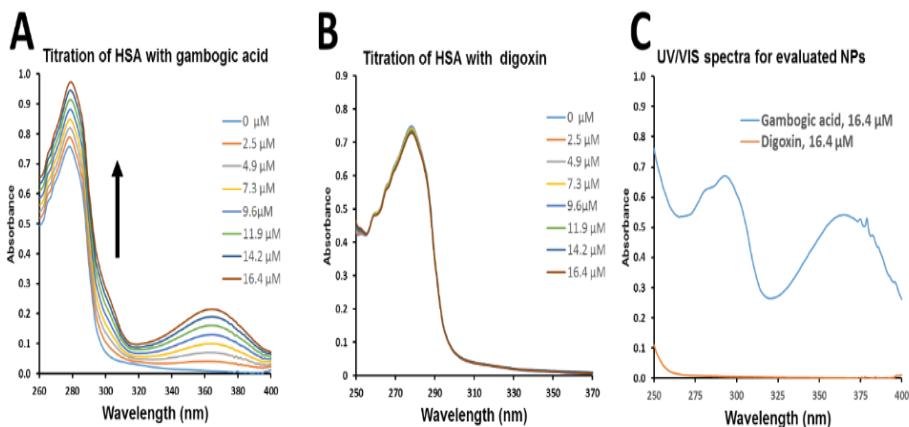


Figure 6.5. UV/VIS spectra for titration of HSA with NPs. The intensity of absorption directly increase with the concentration of gambogic acid for peaks in 280 and 365 nm (A). However, for digoxin not were observed significant variations (B), the used concentration of HSA for this assay was 2.5×10^{-5} M.

Analysis of HSA-natural compound interaction using fluoresce quenching

The analysis of the results was directed fluorescence results obtained with gambogic acid and digoxin. The thermodynamic parameters were calculated for titrations with HAS-gambogic acid (Figure 6.6A) and digoxin (Figure 6.6B) with temperatures of 30, 37 and 44 ° C (303, 310, and 317 K) for subsequent calculations of thermodynamic parameters. Due to the UV-VIS spectrum for gambogic acid, with absorption bands in the zone of fluorescence emission for HSA, a correction method was applied for quenching spectra HSA-gambogic acid for the inner filter effect using the formula $[F_{corr} = F_{obs} \text{antilog}(\text{Abs excitation} + \text{Abs emission})/2]$, F=Fluorescence, Abs=absorbance.

A decrease in fluorescence intensity at 360 nm, when excited at 280 nm, respectively, is attributed to changes in the environment of the protein fluorophores caused to the presence of natural compounds evaluated, probably for the interaction with Trp-214, the only tryptophan residue in human serum albumin [53, 54].

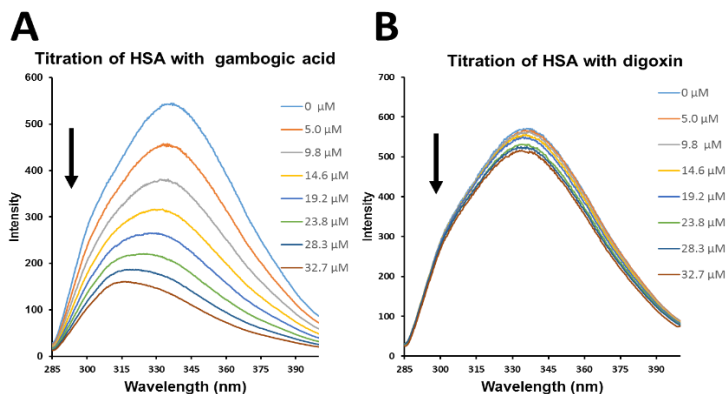


Figure 6.6. Fluorescence quenching spectra of titration of HSA with gambogic acid (A) and digoxin (B).

The fluorescence quenching mechanisms usually contain dynamic quenching and static quenching, which are caused by diffusion and ground-state complex formation respectively [55]. To elucidate the possible mechanism responsible for the quenching of HSA intrinsic fluorescence intensity, the Stern–Volmer plot was constructed for gambogic acid (Figure 6.7A) and digoxin (Figure 6.7B). Stern–Volmer quation (Eq.1) was used to analyze the data, where F_0 and F are the fluorescence intensities in the absence and presence of quencher respectively, K_q is the biomolecular quenching constant, τ_0 is the life time of the fluorescence in absence of quencher (for biopolymer is 10^{-8} s^{-1}), $[Q]$ is the concentration of quencher, and K_{sv} is the Stern–Volmer quenching constant [39].

$$\frac{F_0}{F} = 1 + K_{sv} [Q] = 1 + K_q \tau_0 [Q]$$

Eq. 1

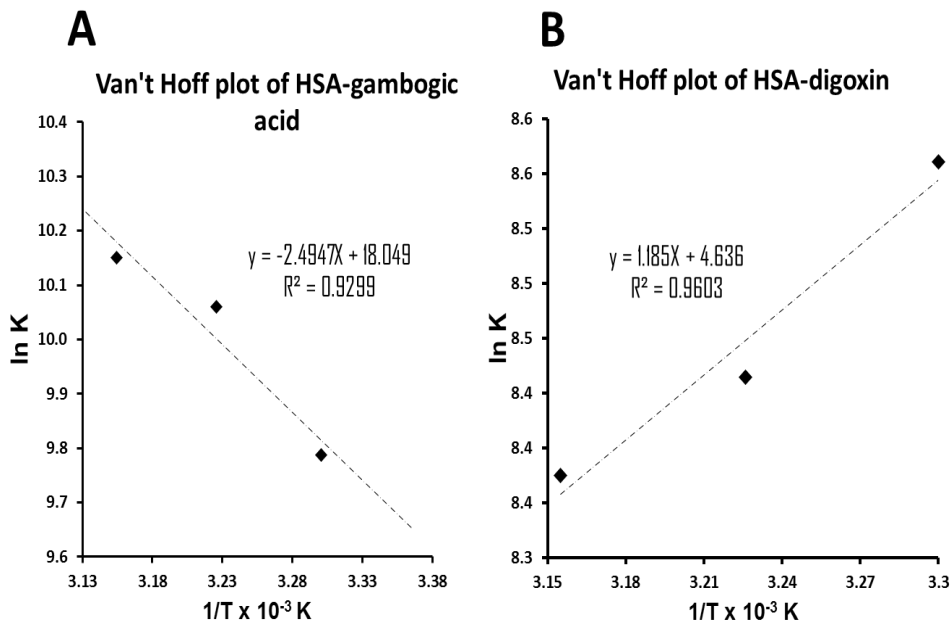


Figure 6.7. Van't Hoff plot for titrations of HSA with gambogic acid (A) and digoxin (B).

In principle, the static quenching constant decreases as the temperature is raised. A linear Stern–Volmer plot is indicative of a single quenching mechanism, either static or dynamic, in general titrations for HSA with natural compounds were linear [39]. However, major variations were observed for gambogic acid (Figure 6.6A). Different thermodynamic parameters as variations in enthalpy, entropy and free energy can be calculated starting from the Van't Hoff equation, (Table 1) and the equation for Gibbs free energy. $\Delta G^\circ = \Delta H^\circ - \Delta T\Delta S^\circ$, depending on the temperatures used in each of the HSA- natural compound titration (Table 6.1) [41].

Table 6.1. Thermodynamic parameters for HSA–natural compounds interactions.

Compound	Van't Hoff equation	m	b
Gambogic acid	$y = -2494.7X + 18.049$	-2494.7	18.049
Digoxin	$y = 1918.2X + 1.8732$	1918.2	1.8732

Compound	ΔH°	ΔS°	ΔG° (303K)	ΔG° (310K)	ΔG° (317K)
Gambogic acid	20.7	150.1	-24.7	-25.8	-26.8
Digoxin	-15.9	15.6	-20.7	-20.8	-20.9

m = slope of the graph, b = Intercept, ΔH° = enthalpy, ΔS° = Entropy, ΔG° = Gibbs Free Energy.

Based on the method proposed by Ross and Subramanian [56] for protein-ligand interactions can be used thermodynamic parameters ΔH° , ΔS° and ΔG° to describe intermolecular forces governing forces on the complex through the following propositions: $\Delta H^\circ > 0$ and $\Delta S^\circ > 0$ implies hydrophobic interactions; $\Delta H^\circ < 0$ and $\Delta S^\circ < 0$ suggests van der Waals and hydrogen bonding; $\Delta H^\circ \sim 0$ (slightly positive or negative) and $\Delta S^\circ > 0$ implies electrostatic and ionic interactions [39, 41].

According to the above, HSA-gambogic acid complex presents electrostatic and hydrophobic and ionic interactions. As for the HSA-digoxin complex features a combination of electrostatic type interactions and van type derWaals (dipole-dipole, dispersion, $\Delta H^\circ < 0$) and electrostatic and ionic interactions ($\Delta S^\circ > 0$). For digoxin, suggest interactions type van der Waals and electrostatics [56].

Evaluation of interaction HSA- natural compounds complex by molecular docking

The interaction of natural compounds (gambogic acid and digoxin) to HSA (PDB: 4S1Y) was performed using molecular docking protocols with Surflex-Dock from SYBYL-X 2.0 package [1]. Obtained Total scores (-Logkd) values shown that the best value was to the gambogic acid, with a total score of 9.4 (for digoxin -Logkd value was 6.5), supporting the data obtained for the thermodynamic parameters (Table 6.1). Additionally, binding sites were identified on HSA protein (Figure 6.8A) and the interacting residues were predicted by the LigandScout 3.1 program [38]. The main residues were Trp-214, Ala-191 (hydrophobic interactions), Ser-192, Lys-195 and Lys-436 (bond hydrogen acceptor), as is presented in Figure 6.8B. Trp-214 residue, located in the binding site with gambogic acid and digoxin, belong to HSA subdomain IIA, a binding site of the studied drugs [53].

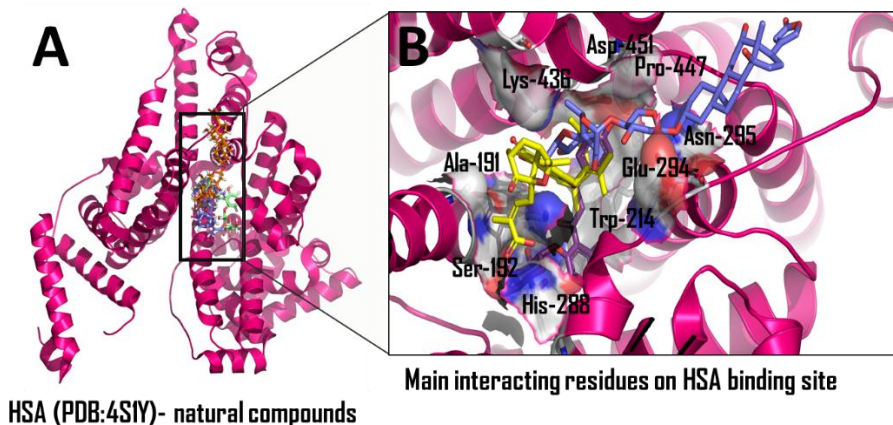


Figure 6.8. HSA-natural compounds complex binding site (A), and main residues involved in the interaction for gambogic acid (yellow) and digoxin (blue) (B) Predicted by LigandScout 3.1.

Studies of circular dichroism for HSA-gambogic acid interaction

Far UV CD studies were performed for titration of HSA with gambogic acid. CD spectra provides a wealth of information both the structural changes in HSA upon ligand titration when examining the far UV CD spectral region (190 to 250 nm) and the conformation and extent of the hydrophobic interaction by examining the near UV CD spectral region. Spectral data for HSA in the absence of gambogic acid are according to those previously published by in the far and near UV CD spectral range [57, 58]. A decrease for initial ellipticity of HSA is probably caused by changes on secondary structure (Figure 6.9A) probably due to the interaction with gambogic acid at concentrations greater than 0.32 mM at 209.6 nm (Figure 6.9B) and 222 nm (Figure 6.9C), docking calculations presented that gambogic acid can binding to subdomain IIA of human serum albumin, a site for drugs [53, 54]. The data suggest a direct relationship between the concentration of acid gambogic and ellipticity for both wavelengths (209.6 and 222.0 nm, indicating the interaction between HSA and gambogic acid.

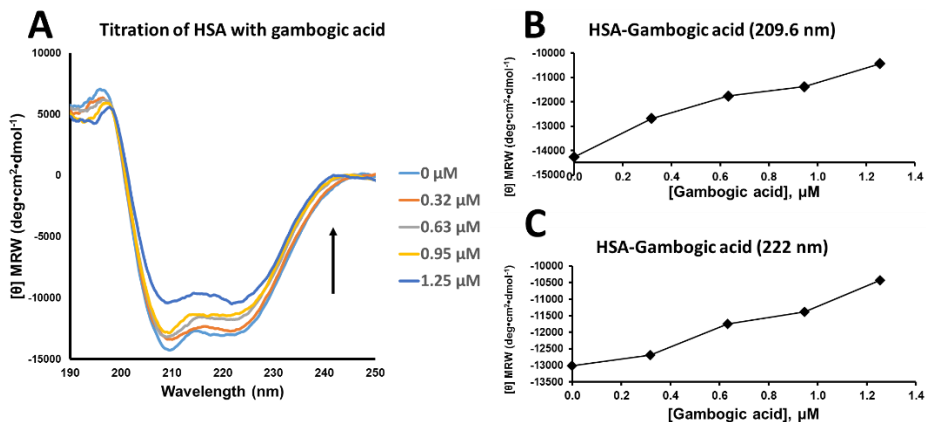


Figure 6.9. UV-CD Spectral overlay for titration of HSA with gambogic acid (A). Relationship for concentrations of gambogic acid (0 to 1.25 μM) vs mean residue molar ellipticity at 209.6 nm (B), and 222.0 nm (C).

6.5. CONCLUSIONS

The results suggest that acid gambogic, potent inhibitor of DNMT1 and digoxin have promising cytotoxic properties against cell lines HT-29 and MCF-7 at concentrations nM and μM respectively. Spectroscopic methods showed interaction between HSA and gambogic acid. Regarding thermodynamic parameters calculated, these suggest a static interaction for complex formation HSA- gambogic acid, methods of molecular docking support information obtained with values for ΔH° = enthalpy, ΔS° = entropy, ΔG° = Free energy Gibbs. The digoxin and gambogic acid could be a platform for the discovery of new anticancer compounds, with greater potency and selectivity by inhibiting DNA methyltransferases decreasing side effects.

6.6. REFERENCES

- [1] Maldonado-Rojas, W., Olivero-Verbel, J., Marrero-Ponce, Y. Computational fishing of new DNA methyltransferase inhibitors from natural products. *J Mol Graph Model*. 2015, 60, 43-54.
- [2] Razin, A., Riggs, A.D. DNA methylation and gene function. *Science*. 1980, 210, 604-10.
- [3] Li, E., Beard, C., Jaenisch, R. Role for DNA methylation in genomic imprinting. *Nature*. 1993, 366, 362-5.
- [4] Feil, R. Environmental and nutritional effects on the epigenetic regulation of genes. *Mutat Res Fundam Mol Mech Mut*. 2006, 600, 46-57.
- [5] Jaenisch, R., Bird, A. Epigenetic regulation of gene expression: how the genome integrates intrinsic and environmental signals. *Nat Genet*. 2003, 33, 245-54.

- [6] Simmons, D. Epigenetic influence and disease. *Nat Educ.* 2008, 1, 6.
- [7] Egger, G., Liang, G., Aparicio, A., Jones, P.A. Epigenetics in human disease and prospects for epigenetic therapy. *Nature.* 2004, 429, 457-63.
- [8] Jones, P.A., Takai, D. The role of DNA methylation in mammalian epigenetics. *Science.* 2001, 293, 1068-70.
- [9] Esteller, M., Corn, P.G., Baylin, S.B., Herman, J.G. A gene hypermethylation profile of human cancer. *Cancer Res.* 2001, 61, 3225-9.
- [10] Baylin, S.B. DNA methylation and gene silencing in cancer. *Nat Clin Pract Oncol.* 2005, 2, S4-S11.
- [11] Robertson, K.D., Uzvolgyi, E., Liang, G., Talmadge, C., Sumegi, J., Gonzales, F.A., et al. The human DNA methyltransferases (DNMTs) 1, 3a and 3b: coordinate mRNA expression in normal tissues and overexpression in tumors. *Nucleic Acids Res.* 1999, 27, 2291-8.
- [12] Gonzalo, S., Jaco, I., Fraga, M.F., Chen, T., Li, E., Esteller, M., et al. DNA methyltransferases control telomere length and telomere recombination in mammalian cells. *Nat Cell Biol.* 2006, 8, 416-24.
- [13] Santi, D.V., Garrett, C.E., Barr, P.J. On the mechanism of inhibition of DNA-cytosine methyltransferases by cytosine analogs. *Cell.* 1983, 33, 9-10.
- [14] Yoo, J., Kim, J.H., Robertson, K.D., Medina-Franco, J.L. Molecular modeling of inhibitors of human DNA methyltransferase with a crystal structure: discovery of a novel DNMT1 inhibitor. *Adv Prot Chem Struct Biol.* 2012, 87.
- [15] Okano, M., Bell, D.W., Haber, D.A., Li, E. DNA methyltransferases Dnmt3a and Dnmt3b are essential for de novo methylation and mammalian development. *Cell.* 1999, 99, 247-57.
- [16] Meilinger, D., Fellingner, K., Bultmann, S., Rothbauer, U., Bonapace, I.M., Klinkert, W.E., et al. Np95 interacts with de novo DNA methyltransferases, Dnmt3a and Dnmt3b, and mediates epigenetic silencing of the viral CMV promoter in embryonic stem cells. *EMBO reports.* 2009, 10, 1259-64.
- [17] Bird, A. DNA methylation patterns and epigenetic memory. *Gen Develop.* 2002, 16, 6-21.
- [18] Law, J.A., Jacobsen, S.E. Establishing, maintaining and modifying DNA methylation patterns in plants and animals. *Nat Rev Genet.* 2010, 11, 204-20.
- [19] Peng, D.-F., Kanai, Y., Sawada, M., Ushijima, S., Hiraoka, N., Kitazawa, S., et al. DNA methylation of multiple tumor-related genes in association with overexpression of DNA methyltransferase 1 (DNMT1) during multistage carcinogenesis of the pancreas. *Carcinogenesis.* 2006, 27, 1160-8.
- [20] Jones, P.A., Baylin, S.B. The fundamental role of epigenetic events in cancer. *Nat Rev Genet.* 2002, 3, 415-28.
- [21] Zhang, B., Hu, L., Zang, M., Wang, H., Zhao, W., Li, J., et al. *Helicobacter pylori* CagA induces tumor suppressor gene hypermethylation by upregulating DNMT1 via AKT-NFκB pathway in gastric cancer development. *Oncotarget.* 2016, 7, 9788-800.

[22] Si, X., Liu, Y., Lv, J., Ding, H., Zhang, X., Shao, L., et al. ER α propelled aberrant global DNA hypermethylation by activating the DNMT1 gene to enhance anticancer drug resistance in human breast cancer cells. *Oncotarget*. 2016.

[23] Zhong, B., Vatolin, S., Idippily, N.D., Lama, R., Alhadad, L.A., Reu, F.J., et al. Structural optimization of non-nucleoside DNA methyltransferase inhibitor as anti-cancer agent. *Bioorg Med Chem Lett*. 2016.

[24] Flotho, C., Claus, R., Batz, C., Schneider, M., Sandrock, I., Ihde, S., et al. The DNA methyltransferase inhibitors azacitidine, decitabine and zebularine exert differential effects on cancer gene expression in acute myeloid leukemia cells. *Leukemia*. 2009, 23, 1019-28.

[25] Yoo, C.B., Jones, P.A. Epigenetic therapy of cancer: past, present and future. *Nat Rev Drug Discov*. 2006, 5, 37-50.

[26] Gnyszka, A., JASTRZEBSKI, Z., Flis, S. DNA methyltransferase inhibitors and their emerging role in epigenetic therapy of cancer. *Anticancer Res*. 2013, 33, 2989-96.

[27] Stresemann, C., Brueckner, B., Musch, T., Stopper, H., Lyko, F. Functional diversity of DNA methyltransferase inhibitors in human cancer cell lines. *Cancer Res*. 2006, 66, 2794-800.

[28] Svedruzic, Z.e.M., Reich, N.O. DNA cytosine C5 methyltransferase Dnmt1: catalysis-dependent release of allosteric inhibition. *Biochemistry*. 2005, 44, 9472-85.

[29] Medina-Franco, J.L., Méndez-Lucio, O., Yoo, J. Rationalization of activity cliffs of a sulfonamide inhibitor of DNA methyltransferases with induced-fit docking. *Int J Mol Sci*. 2014, 15, 3253-61.

[30] Medina-Franco, J.L., Yoo, J. Docking of a novel DNA methyltransferase inhibitor identified from high-throughput screening: insights to unveil inhibitors in chemical databases. *Molec Divers*. 2013, 17, 337-44.

[31] Yang, X., Lay, F., Han, H., Jones, P.A. Targeting DNA methylation for epigenetic therapy. *Trends Pharmacol Sci*. 2010, 31, 536-46.

[32] Issa, J.-P.J., Garcia-Manero, G., Giles, F.J., Mannari, R., Thomas, D., Faderl, S., et al. Phase 1 study of low-dose prolonged exposure schedules of the hypomethylating agent 5-aza-2'-deoxycytidine (decitabine) in hematopoietic malignancies. *Blood*. 2004, 103, 1635-40.

[33] Silverman, L., Holland, J., Weinberg, R., Alter, B., Davis, R., Ellison, R., et al. Effects of treatment with 5-azacytidine on the in vivo and in vitro hematopoiesis in patients with myelodysplastic syndromes. *Leukemia*. 1993, 7, 21-9.

[34] Asgatay, S., Champion, C., Marloie, G., Drujon, T., Senamaud-Beaufort, C., Ceccaldi, A., et al. Synthesis and evaluation of analogues of N-phthaloyl-L-tryptophan (RG108) as inhibitors of DNA methyltransferase 1. *J Med Chem*. 2014, 57, 421-34.

[35] Medina-Franco, J.L., López-Vallejo, F., Kuck, D., Lyko, F. Natural products as DNA methyltransferase inhibitors: a computer-aided discovery approach. *Molec Divers*. 2011, 15, 293-304.

[36] Brueckner, B., Boy, R.G., Siedlecki, P., Musch, T., Kliem, H.C., Zielenkiewicz, P., et al. Epigenetic reactivation of tumor suppressor genes by a novel small-molecule inhibitor of human DNA methyltransferases. *Cancer Res*. 2005, 65, 6305-11.

[37] Maldonado-Rojas, W., Olivero-Verbel, J. Potential interaction of natural dietary bioactive compounds with COX-2. *J Mol Graph Model*. 2011, 30, 157-66.

[38] Wolber, G., Langer, T. LigandScout: 3-D pharmacophores derived from protein-bound ligands and their use as virtual screening filters. *J Chem Inf Model.* 2005, 45, 160-9.

[39] Narváez-Pita, X., Ortega-Zuniga, C., Acevedo-Morantes, C.Y., Pastrana, B., Olivero-Verbel, J., Maldonado-Rojas, W., et al. Water soluble molybdenocene complexes: Synthesis, cytotoxic activity and binding studies to ubiquitin by fluorescence spectroscopy, circular dichroism and molecular modeling. *J Inorg Biochem.* 2014, 132, 77-91.

[40] Vistica, D.T., Skehan, P., Scudiero, D., Monks, A., Pittman, A., Boyd, M.R. Tetrazolium-based assays for cellular viability: a critical examination of selected parameters affecting formazan production. *Cancer Res.* 1991, 51, 2515-20.

[41] Domínguez-García, M., Ortega-Zúñiga, C., Meléndez, E. New tungstenocenes containing 3-hydroxy-4-pyrone ligands: antiproliferative activity on HT-29 and MCF-7 cell lines and binding to human serum albumin studied by fluorescence spectroscopy and molecular modeling methods. *J Biol Inorg Chem.* 2013, 18, 195-209.

[42] Chen, G.C., Yang, J.T. Two-point calibration of circular dichrometer with d-10-camphorsulfonic acid. *Anal Lett.* 1977, 10, 1195-207.

[43] Chikan, N.A., Bhavaniprasad, V., Anbarasu, K., Shabir, N., Patel, T.N. From natural products to drugs for epimutation computer-aided drug design. *Appl Biochem Biotech.* 2013, 170, 164-75.

[44] Qureshi, W., Alirhayim, Z., Ahmed, A., Al-Mallah, M., AbdulAziz, K. Digoxin Use in Atrial Fibrillation Is Associated with Increased Risk of Mortality: A Systematic Review and Meta-Analysis of More than 200,000 Patients. *J Am Coll Cardiol.* 2015, 65.

[45] Kapoor, S. Digoxin and its Antineoplastic Properties: An Evolving Role in Oncology. *J Pediatr hematol Oncol.* 2014, 36, 666-7.

[46] Shi, X., Chen, X., Li, X., Lan, X., Zhao, C., Liu, S., et al. Gambogic acid induces apoptosis in imatinib-resistant chronic myeloid leukemia cells via inducing proteasome inhibition and caspase-dependent Bcr-Abl downregulation. *Clin Cancer Res.* 2014, 20, 151-63.

[47] Platz, E.A., Yegnasubramanian, S., Liu, J.O., Chong, C.R., Shim, J.S., Kenfield, S.A., et al. A novel two-stage, transdisciplinary study identifies digoxin as a possible drug for prostate cancer treatment. *Cancer Discov.* 2011, 1, 68-77.

[48] Yeh, J.-Y., Huang, W.J., Kan, S.-F., Wang, P.S. Inhibitory effects of digitalis on the proliferation of androgen dependent and independent prostate cancer cells. *J Urol.* 2001, 166, 1937-42.

[49] Liu, W., Guo, Q.-L., You, Q.-D., Zhao, L., Gu, H.-Y., Yuan, S.-T. Anticancer effect and apoptosis induction of gambogic acid in human gastric cancer line BGC-823. *World J Gastroenterol.* 2005, 11, 3655-9.

[50] Qiang, L., Yang, Y., You, Q.-D., Ma, Y.-J., Yang, L., Nie, F.-F., et al. Inhibition of glioblastoma growth and angiogenesis by gambogic acid: an in vitro and in vivo study. *Biochem Pharmacol.* 2008, 75, 1083-92.

[51] Girault, I., Tozlu, S., Lidereau, R., Bièche, I. Expression analysis of DNA methyltransferases 1, 3A, and 3B in sporadic breast carcinomas. *Clin Cancer Res.* 2003, 9, 4415-22.

[52] Jin, B., Yao, B., Li, J.-L., Fields, C.R., Delmas, A.L., Liu, C., et al. DNMT1 and DNMT3B modulate distinct polycomb-mediated histone modifications in colon cancer. *Cancer Res.* 2009, 69, 7412-21.

[53] Sułkowska, A. Interaction of drugs with bovine and human serum albumin. *J Mol Struct.* 2002, 614, 227-32.

[54] Tayeh, N., Rungassamy, T., Albani, J.R. Fluorescence spectral resolution of tryptophan residues in bovine and human serum albumins. *J Pharm Biomed Anal.* 2009, 50, 107-16.

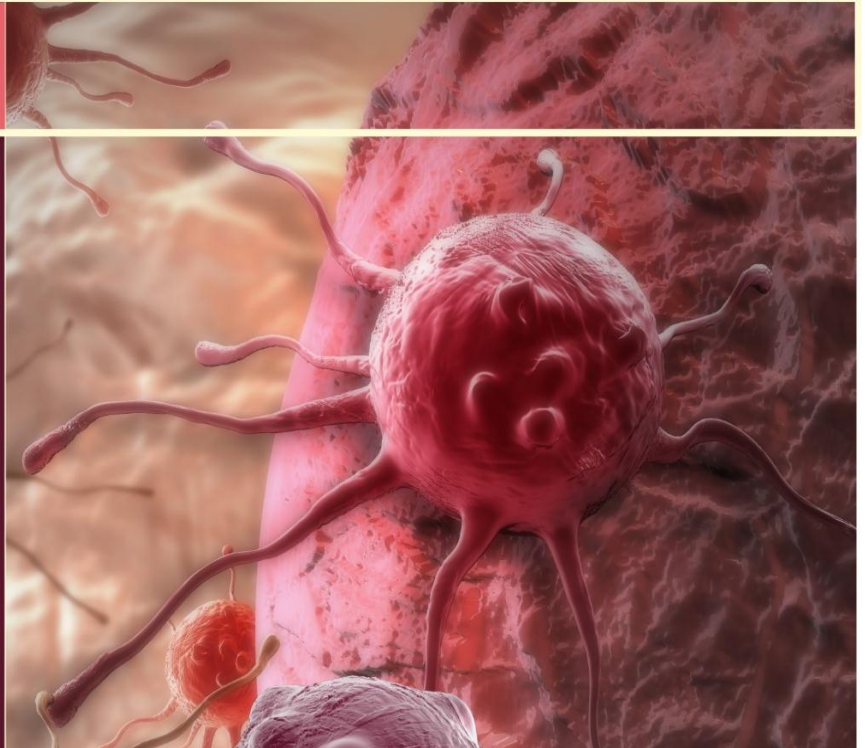
[55] Gao, Y., Shao, C., Ji, W., Xiao, M., Yi, F., Zhou, T., et al. Studies on the Binding Mechanism of VB 1 and VB 9 with Trypsin. *Am J Anal Chem.* 2013, 2013.

[56] Ross, P.D., Subramanian, S. Thermodynamics of protein association reactions: forces contributing to stability. *Biochemistry.* 1981, 20, 3096-102.

[57] Zsila, F. Circular dichroism spectroscopic detection of ligand binding induced subdomain IB specific structural adjustment of human serum albumin. *J Phys Chem B.* 2013, 117, 10798-806.

[58] Varshney, A., Ansari, Y., Zaidi, N., Ahmad, E., Badr, G., Alam, P., et al. Analysis of binding interaction between antibacterial ciprofloxacin and human serum albumin by spectroscopic techniques. *Cell Biochem Biophys.* 2014, 70, 93-101.

Chapter 7



CHAPTER 7. CONCLUSIONS AND FINAL REMARKS

Cancer is a disease caused by multiple factors, where most of these factors correspond to the toxicological effects of environmental contaminants such as UV radiation, heavy metals, endocrine disruptors, polycyclic aromatic hydrocarbons, among others. Currently, there is great global interest in the search for more effective cancer treatments to reduce the alarming number of annual deaths reported by this disease.

Natural compounds have been considered a valuable source for the discovery of more effective drugs with fewer adverse effects. In this thesis, was performed a rational searching to identify bioactive molecules capable to inhibit enzymatic activity of cancer target proteins, we found different promissory compounds with potential therapeutic properties. This multidisciplinary strategy, involving different methodologies combining computational approaches, molecular biology assays, spectroscopic methods and powerful statistical tools in order to ensure solid and reliable information. The results showed that naturally occurring compounds may have inhibitory effects on cancer-related protein, such as COX-2, iNOS and DNMTs, and modulate biochemical mechanisms governing in carcinogenic process. Obtained data for natural compounds evidence its potential applicability in the prevention and treatment of cancer.

Molecular docking protocols revealed that some natural compounds, such as curcumin (natural dye from turmeric) and all-*trans* retinoic acid (vitamin A derivative) can interact directly with the COX-2 enzyme, in addition to the known properties of transcription regulators for this protein. We found that curcumin has the ability to bind competitively and allosterically to COX-2 in the presence of potent inhibitor celecoxib

(synthetic inhibitor) increasing their inhibitory effect. Methods of molecular docking protein-ligand, also revealed that food-related compounds, silibinin (flavonolignan) and cyanidin-3-rutinoside (anthocyanin), also can exert a direct inhibitory action on iNOS enzyme, besides known regulation of inflammation-related genes.

Multistep strategy used, combined computational approaches statistical techniques analysis to ensure high hit rates expected in the discovery of new cancer drugs. LDA-based QSAR model showed satisfactory results suggest that several new natural chemotypes (9,10-dihydro-12-hydroxygambogic acid, phloridzin, 2',4'-dihydroxychalcone 4'-glucoside, daunorubicin, pyrromycin and centaurin) can be potential DNMT inhibitors. Also suggested that the potential therapeutic effect of natural compounds be achieved not only by inhibition of DNMT1 but also of DNMT3A. Finally, suggest our methodology as an innovative approach for targeted identification of novel and selective inhibitors of DNMTs as a first step prior to *in vitro* and *in vivo* evaluations useful in the search of anticancer drugs.

The *in vitro* evaluation of inhibitory activity of DNMTs for natural compounds gambogic acid, digoxin and phloridzin revealed that these compounds have activity against DNMT1 (M.Sssl). Gambogic acid was the most potent DNMT1 inhibitor (inhibitory effect to 5 μ M). Digoxin and gambogic acid presented promising cytotoxic properties against both HT-29 and MCF-7 with IC₅₀ values in nM and μ M range. Additionally, spectroscopic methods showed interaction between human serum albumin, drug transporter, with digoxin and gambogic acid. Thermodynamic parameters calculated, suggest static interaction for complex formation HSA-gambogic acid and HSA-digoxin. Methods of molecular docking support the experimental information obtained with values for ΔH° = enthalpy, ΔS° = entropy, ΔG° = free energy Gibbs. Our results revealed that natural compound digoxin and gambogic acid could be scaffold for the discovery of new anticancer compounds, with greater potency and selectivity by inhibiting DNA methyltransferases decreasing side effects.

Finally, another of the contributions made in this thesis was the contribution to construction of a data base with 2D and 3D promising molecules from Colombian biodiversity named Natural Compound Databank from Colombia (NCDC) the first database of natural compounds of Colombia, where users can find more It contains 2680 molecules, including information about the corresponding 2D and 3D structures, physicochemical properties (Figure 7.1). Medicinal plants have been used for years in daily life and to treat diseases all over the world. Colombia accounts for approximately 10% of the world's biodiversity and is home to about 50.000 species of plants. (http://190.27.248.60:8088/web_ncdc/index.php). This database is still under development and not available yet.

The figure displays four screenshots of the NCDC website. The top-left screenshot shows the homepage with a woman in a lab coat and the text 'Universidad de Cartagena'. The top-right screenshot is a 'WELCOME TO NCDC!' page with a molecular model and a description of the database. The bottom-left screenshot is titled 'REGISTERED PLANTS' and shows a grid of plant images with labels: Achiote, Aguacate, Ajeno, Aji, Ajo, Ajonjolí, Alazán, and Albahaca. The bottom-right screenshot is titled 'Registered Compounds' and shows a grid of chemical structures with labels: β -Cubebin, Abietic acid, Alantoin, Acaric, Actinogenin, and Aspic Acid.

Figure 7.1. Natural Compound Databank from Colombia (NCDC), some screenshot of database are visualized.

NCDC, is expected to be a useful tool for future research focused in discovery of compounds with promissory properties for prevention and treatment diseases, application in cosmetics and food industry.

GLOSSARY

Natural bioactive compound: extranutritional constituent (molecule) that typically occur in small quantities in foods. They are being intensively studied to evaluate their effects on health.

Cancer: is the name given to a set of related diseases. In all cancers, some of the body's cells begin to divide without stopping and spread to surrounding tissues.

Circular dichroism (CD): is the difference in the absorption of left-handed circularly polarized light and right-handed circularly polarized light and occurs when a molecule contains one or more chiral chromophores (light-absorbing groups). This technique is used to investigate the secondary structure of proteins.

Cytotoxic assay: Testing the effects of compounds on the viability of cells grown in culture is widely used as a predictor of potential toxic effects in whole animals. There are different assays, these have been widely used by the pharmaceutical industry to screen for cytotoxicity in compound libraries.

DNA methylation: Is a heritable epigenetic mark involving the covalent transfer of a methyl group to the C-5 position of the cytosine ring of DNA by DNA methyltransferases (DNMTs).

Docking: Computational tool that using several algorithms tries to predict the structure of the intermolecular complex, formed between two or more constituent molecules. Molecular docking generally applied to protein-ligand interactions.

Drug: In pharmacology, is defined as chemical substance used in the treatment, cure, prevention, or diagnosis of disease or used to otherwise enhance physical or mental well-being.

Drug discovery: Process through which potential new medicines are identified. It involves a wide range of scientific disciplines, including biology, chemistry and pharmacology.

Enzyme: are several complex proteins produced by cells and act as catalysts in specific biochemical reactions.

Enzyme inhibitors: are substances which alter the catalytic action of the enzyme and consequently slow down, or in some cases, stop catalysis. There are three common types of enzyme inhibition - competitive, non-competitive and substrate inhibition.

Ligand: is a substance that bind biomolecule and forms a complex to serve a biological purpose.

Molecular modelling: Molecular modelling encompasses all theoretical methods and computational techniques used to mimic and study the structure and behavior of molecules, ranging from small chemical systems to large biological molecules and material assemblies.

PCR-RFLP: It is a technique very frequently used in molecular studies, and is the combination of two basic methods in molecular biology. First a PCR amplification of the target gene is performed, and then digestion (or cut pieces) of the amplified product with restriction enzymes is carried out, to see the resulting fragments or restriction fragments of evaluated gene.

Posing: The process of determining whether a given conformation and orientation of a ligand fits the active site. This is usually a fuzzy procedure that returns many alternative results.

QSAR: Quantitative Structure Activity Relationship (QSAR) are regression or classification models used as reliable alternative in the food and pharmaceutical industry for the analysis of related compounds.

Scoring: During posing phase usually involves simple energy calculations (electrostatic, van der Waals, ligand steric, among others). Further re-scoring might attempt in order to estimate more accurately the free energy binding (ΔG , and therefore K_A) perhaps including properties such as entropy and solvation.

Spectroscopy: is the analysis of the interaction between matter and any portion of the electromagnetic spectrum. Traditionally, spectroscopy involved the visible spectrum of light, but x-ray, gamma, and UV spectroscopy also are valuable analytical techniques. Spectroscopy may involve any interaction between light and matter, including absorption, emission, scattering, etc.

Virtual screening: It is a computational technique uses computer-based methods to discover new ligands on the basis of biological structures widely used in drug discovery reducing time and costs.

ABBREVIATIONS

ABCA1	ATP-binding cassette transporter A1
AdoHcy-S	S-adenosyl-L-homocysteine
AdoMet	S-adenosyl-L-methionine
AID	Assay ID in PubChem Bioassay
AIDS	Acquired immune deficiency syndrome
AMT	2-amino-5,6-dihydro-6-methyl-4H-1,3-thiazine
AP-1	Activator protein-1
ATA	Aurintricarboxylic acid
AV	AutoDock Vina
BRCA1	Breast cancer 1
Bsh1236I	Restriction enzyme
CD	Circular dichroism
CID	PubChem chemical structure identifier
CSC	Cancer stem cells
COX-2	Cyclooxygenase-2
DMEM	Dulbecco's modified medium
DNMT	DNA methyltransferases
DNMTi	DNA methyltransferase inhibitor
EGCG	Epigallocatechin-3-gallate
EMEM	Eagle's minimum essential medium
eNOS	Endothelial nitric oxide synthase
ERKs	Extracellular signal-regulated kinases
FDA	Food and Drug Administration
ΔG	Gibbs free change
GATS5m	2D autocorrelation
GOLD	Global Operations Leadership Development
H-047	Atomic centered-fragment
ΔH	Enthalpy change
HDL	High-density lipoprotein
HSA	Human serum albumin
HTS	High-throughput screening
HT-29	Colorectal cancer cell lines
IC ₅₀	Experimental half maximal inhibitory concentration
iNOS	Inducible nitric oxide synthase
IMMAN	Information theory based chemometric analysis
JNK	c-Jun N-terminal
LDA	Linear Discriminant Analysis

L-NIL	L -Lysine ω -acetamide dihydrochloride
MAPK	Mitogen-activated protein kinase
MCF-7	Breast cancer cell lines
MGMT	O-6-methylguanine-DNA methyltransferase
MOE Molecular	Operating Environment
Mor13m	3D-moRSE descriptor
M.Sssl	DNA methylase
mM	milimolar concentration
MTT	3-(4,5-dimethylthiazol-2-yl)-2,5-diphenyltetrazolium bromide
NFAT	Nuclear factor of activated T cells
NF κ β	Nuclear factor kB
nNOS	Neuronal nitric oxide synthase
NPs	Natural products
nM	Nanomolar concentration
NO	Nitric oxide
p16 ^{ink4A}	Cyclin-dependent kinase inhibitor 2A
p38	Mitogen-activated protein kinases
PCR	Polymerase Chain Reaction
PDB	Protein data bank
QSAR	Quantitative structure activity relationship
μ M	Micromolar concentration
UV-VIS	Ultraviolet-Visible radiation
RFLP	Restriction Fragment Length Polymorphism
RMSD	Root mean square deviation
Δ S	Entropy change
SAM	S-adenosyl-L-methionine
SHP2	Randić molecular profile
SIC2	Information index
SOCS1	Suppressor of cytokine signaling 1
STAT-1	Signal transducers and activation of transcription-1
TFPI2	Tissue factor pathway inhibitor 2
WHO	World Health Organization
WIF1	WNT inhibitory factor 1
ZM2V	Topological descriptor